Spring 5-31-2002

Bi-axially loaded slender reinforced concrete columns subjected to sustained loads

Song Gu
New Jersey Institute of Technology

ABSTRACT

BI-AXIALLY LOADED SLENDER REINFORCED CONCRETE COLUMNS SUBJECTED TO SUSTAINED LOADS

by
Song Gu

A generalized analytical approach is presented in this research to predict the behavior both of slender and short reinforced concrete columns under sustained biaxial eccentric load.

The present analysis proposes equations established at a cross section of a reinforced concrete column by combining force equilibrium, constitutive law, and compatibility conditions. The strain and curvature of each section and the deflection of the column can then be obtained and resolved.

The established creep computation models, recommended separately by American Concrete Institute (ACI) 209R-92 and the Comite' Euro-International du Be'ton (CEB)-FIP 1990 Model Code have been used to calculate creep and shrinkage for a member under a constant elastic compressive concrete strain for a given period.

This present analysis also proposes a computerized method for time and strain adjustment. The Time and Strain Adjustment of Creep Method, combining a creep calculation with a constant elastic strain such as those mentioned above, the creep strain at each cross section can then be calculated, stored and adjusted to age of concrete, load changes and deflection modifications during each time increment phase.

In the conventional load-deflection analysis process, with projected transformations, a spatial deflection curve is resolved into a couple of planar curves

located separately in two orthogonal plans. Based on the force equilibrium equations of inner force at a column section, a set of three simultaneous non-linear differential equations are derived to establish the relationships between the planar curve functions with the eccentric load upon the top of column. Using the Green's Integral Formula, the strain and stress nonlinear functions and column section properties can be solely integrated into a few important coefficients of the differential equations. Thus, it makes the approach also suitable for columns with non-rectangular sections and any kinds of constitutive laws of materials.

The presented rational computer analysis results have been compared with the existing bi-axial and uniaxial experimental data, which are available in literature. They indicate that the results from the proposed analysis correlate with experimental data well.

BI-AXIALLY LOADED SLENDER REINFORCED CONCRETE COLUMNS SUBJECTED TO SUSTAINED LOADS

by
Song Gu

A Dissertation
Submitted to the Faculty of
New Jersey Institute of Technology
In Partial Fulfillment of the Requirements for the Degree of
Doctor of Philosophy in Civil Engineering

Department of Civil and Environmental Engineering

May 2002

APPROVAL PAGE

BI-AXIALLY LOADED SLENDER REINFORCED CONCRETE COLUMNS SUBJECTED TO SUSTAINED LOADS

Song Gu

Dr. C. T. Thomas Hsu, Dissertation Advisor — Date
Professor of Civil and Environmental Engineering, NJIT

Dr. Methi Wecharatana, Committee Member — Date
Professor of Civil and Environmental Engineering, NJIT

Dr. Dorairaja Raghu, Committee Member — Date
Professor of Civil and Environmental Engineering, NJIT

Professor Walter Konon, Committee Member — Date
Professor and Associate Chair of Department of Civil and Environmental Engineering, NJIT

Dr. Michael Y. Xing, Committee Member — Date
Associate of Thorton-Tomasetti Engineers, Newark, NJ

BIOGRAPHICAL SKETCH

Author: Song Gu

Degree: Doctor of Philosophy

Date: May 2002

Undergraduate and Graduate Education:

- Doctor of Philosophy in Civil Engineering
  New Jersey Institute of Technology, Newark, NJ, May 2002

- Master's Degree in Structural Engineering
  Tongji University, Shanghai, P. R. of China, June 1988

- Bachelor's Degree in Structural Engineering
  Tsinghua University, Beijing, P. R. of China, July 1985

Major: Civil Engineering

Publications:

Song Gu and C. T. Thomas Hsu (2002), "Computer Analysis of Reinforced Concrete Columns Subjected to Biaxial Sustained Loads" 15th ASCE Engineering Mechanics Conference, Columbia University, NY, June.

Song Gu, Bolong Zhu and Yuzhou Chen (1989), "Study on Aseismic Detailing of the Reinforced Concrete Frame Connections", Journal of Structural Engineers, No. 2, pp. 18-24, Shanghai, China (in Chinese).

This dissertation is dedicated to my whole family members both in United States and the People's Republic of China

ACKNOWLEDGEMENT

I wish to express my sincere gratitude to my Advisor, Professor C. T. Thomas Hsu, for his guidance, encouragement, and help throughout the course of this research.

Special thanks to my dissertation committee members, Professor Methi Wecharatana, Professor Dorairaja Raghu, Professor Walter Konon, and Dr. Michael Xing for their constructive evaluation and valuable suggestions. Thanks also to Professor Edward G. Dauenheimer, for his evaluation and suggestions in this study.

Appreciation is expressed to Mr. Russell Sage, PE and the company of NK Architects for their understanding and encouragement.

I wish to thank my friend, Dr. Xianglin Gu, for his suggestions and encouragement.

Also to thank my parents, Boqi Gu and Ziwen Qian, for their hopes, encouragement and assistance.

Finally, I wish to express my love to my wife Xun Chen and my children for their constant encouragement and understanding, throughout the course of this Ph.D. study.

TABLE OF CONTENTS

TABLE OF CONTENTS
(Continued)

TABLE OF CONTENTS
(Continued)

Chapter **Page**

TABLE OF CONTENTS
(Continued)

Chapter **Page**

LIST OF FIGURES

LIST OF FIGURES
(Continued)

LIST OF FIGURES
(Continued)

Figure **Page**

LIST OF TABLES

CHAPTER 1

INTRODUCTION

1.1 Research Background

The study of the behavior of slender reinforced concrete columns under sustained loads has experienced a history of nearly 50 years.

Ostlund (1957) from Norway is probably the earliest researcher in the world to study the strength capacity of slender reinforced concrete columns under sustained loads. He suggested using the reduced elastic modulus of concrete to estimate creep effects. This concept established the basic direction for the engineering approach afterwards.

From the1960s, many scholars in North America appeared to be interested in this research area. Mauch & Holley (1963) at M.I.T., performed theoretical analysis on creep buckling of reinforced concrete columns and their work became the first publication appeared in North American academic journals. Just at the same time, ACI Building Code (ACI Committee 318, 1963) required engineering consideration of creep effects on deflections of slender columns under sustained loads in some situations. This appeared the first reinforced concrete (RC) structures building code to specify such effects in engineering design. Eight years later, in the next generation version of ACI Building Code (ACI Committee 318, 1971), a formal design method for slender column under sustained loading was introduced.

Drysdale and Huggins (1971) at University of Toronto, Toronto, Canada, published their study on sustained bi-axial load on slender concrete columns. This is the first publication in this field to study the slender concrete columns subjected to bi-axial

bending moments and axial loads. Their experimental data of bi-axially loaded columns under sustained loads are still the only test results available in the literature at this time.

Recent advance in high strength concrete (HSC) structures has resulted in using smaller section sizes of columns. As the time dependent properties of HSC are different from those of normal strength concrete (NSC), Claeson & Gylltoft (2000) carried out their experiment on slender HSC column under sustained loads. In their analysis, the method provided by CEB-FIP Model Code was used.

According to literature research, the most active research period in this field happened during 1963-1971. During that period, there were more than 10 research papers being published in academic journals in North America and a formal design method, named as **Moment Magnifier Method** (MMM), was introduced into the ACI building code (1971). Today, this MMM is still being used in the latest ACI building code (1999).

The argument to MMM is that, the quantity of concrete time-dependent properties has not being considered, which means, the capacity of slender column strength is unchanged no matter how big creep and shrinkage are being developed. This is probably due to the consideration of simplicity and feasibility in using formulas. On the other hand, it has reflected the fact that, the concrete time-dependent properties are still not fully understood at this time. In addition, due to time factor, this type of analysis becomes four-dimensional analysis assuming that the columns are under bi-axial bending loads. For creep, the time effects are definitely not a linear. Thus, it was very difficult to perform such an analysis with a typical Personal Computer or even a Work Station in ten or twenty years ago, which would cost much time and require much storage.

Since 1971, more and more research results have been published on time-dependent properties of concrete. Many theories and analytical methods have been established and updated to describe the behavior of concrete creep and shrinkage. ACI Committee 209 and CEB-FIP have developed theoretical analysis models for concrete creep and shrinkage (ACI Committee 209, 1994, & CEB-FIP, 1993). Although these theories of concrete time-dependent properties are not perfect, they do provide powerful theoretical assistance to the study of behavior of long RC columns under sustained loads.

In recent years, the high-speed development of computer technology also makes it possible to overcome the storage and speed difficulties when tackling three or four-dimensional nonlinear structural problems.

In engineering practice, it has passed more than a century since the concrete material was invented. Thousands of skyscrapers in concrete structures have been built up all over the world. Among those concrete structures, a lot of them have been standing for more than 50 years. Some of them have stood for even more than 80 years, which are close to the end of concrete life duration. All these facts have raised a question that needs to be solved which is, what is really happening to the behavior of those slender columns inside those old buildings.

1.2 Objectives of Research

The objectives of this research are:

1. To establish a theoretical analysis model and algorithm in order to simulate the loading and deformation process of slender columns made of NSC/HSC under bi-axial sustained loads (uni-axial bending is treated as a special case of bi-axial

bending). Existing experimental data are to be used to verify the validity of analytical models developed.

2. To analyze important material and geometry variables that influence the behavior of slender columns under sustained loads with the established method.
3. To compare and evaluate the current design criteria with design examples.

1.3 Statement of Originality

A generalized theoretical approach is created to predict the behavior of slender reinforced concrete columns made of NSC/HSC under sustained bi-axial/uni-axial eccentric loads. This approach includes the following original points:

1. Applying Green's Integral Transformation to the three balanced force equations, the strain and stress relationship and column section properties are integrated into a few important coefficients of the differential equations. Thus, it makes the algorithm generalized to non-rectangular section columns and all kinds of constitutive functions.
2. Established a computerized method for the adjustment of creep increments due to the changes of elastic strain during the sustained loading duration. The method is named as Time and Strain Adjustment of Creep Method. It is utilized to work with a creep model for a constant elastic strain. The creep strain at each cross section can then be calculated, adjusted and stored at each time increment phase, load changes and deflection modifications.

3. Proposed a theoretical mechanism based on both test and analysis results to explain the behavior of stress and strain developments in slender R/C column buckling under sustained loading.

1.4 Outline of Research

Three equations are established at a column cross section by combining force equilibrium, constitutive law, and compatibility conditions. The strains and curvatures at each section of the column are resolved. Knowing boundary conditions and all curvatures at each cross section, the deflections at each section can be obtained by using numerical approximate methods.

In the instant load-deflection analysis process, with projected transformations, a spatial deflection curve is resolved into a couple of planar curves located separately in two orthogonal plans. Given coordinates of a point at a cross section, the axial strain can be calculated with curvatures of the two planar curves and the maximum concrete compression strain at a corner. Based on force equilibrium equations of inner force at a column section, a set of three simultaneous non-linear integral equations are derived to establish the relationships between the planar curve functions with the eccentric load upon the top of the column. Utilizing the Green's Integral Formula, the strain and stress nonlinear relationships and column section properties can be solely integrated into a few important coefficients of the equations. Thus, the approach is suitable for columns with non-rectangular sections and any kinds of constitutive laws of materials.

During the sustained loading process, creep and shrinkage strains have occurred and they are added and combined to the total strain and curvature of each section.

The present analysis proposes a computerized method to allow creep increment to be adjusted with increasing of time and variation of strain, the **Time and Strain Adjustment of Creep Method** (**TSACM**), combining the creep analisis models used for constant elastic strains, such as those regulated in American Concrete Institute (ACI) 209-92 and the Comite' Euro-International du Be'ton (CEB)-FIP 1990 Model Code. The creep strain at each cross section can be stored, calculated and adjusted and at each time increment phase, load changes and deflection modifications.

The present rational computer analysis results have been compared with the existing bi-axial and uniaxial experimental data available in the literature. It is indicated that the results from the proposed analysis correlate with experimental data well.

Some important material and geometry variables effects on the behavior of slender columns under sustained loads are analyzed. Results are compared with those per ACI 318-99 building code.

In this study, C Language is utilized to compose source code.

CHAPTER 2

LITERATURE REVIEW

2.1 Classification of Concrete Time-dependent Properties

Time-dependent properties of concrete have played an important part in the buckling of slender R/C columns under sustained loads. The time-dependent behavior of concrete members is normally classified as creep and shrinkage.

Creep is defined as the time-dependent increase of strain in hardened concrete subjected to sustained stress (ACI 209, 1994).

Shrinkage is defined as the decrease in concrete volume with time after hardening of concrete. That decrease is due to changes in the moisture content of the concrete and physical-chemical changes, which occur without stress attributable to actions external to the concrete (ACI 209, 1994). As the shrinkage is not related to loads, analysis results show that it is far less as important as creep to affect the behavior of slender columns (Mauch, 1966), which is to be confirmed in this study.

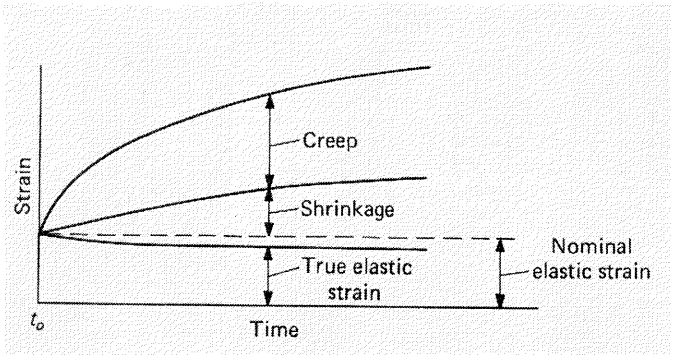

Figure 2.1 Changes in Strain of a Loaded and Drying Specimen (Wang and Salmon, 1992)

Figure 2.1 shows the relationships between elastic, creep and shrinkage strains subjected to sustained loading; t_0 is the time of application of load.

2.2 Mechanism of Concrete Creep and Shrinkage

2.2.1 Factors Affecting Creep and Shrinkage

Normally, creep of concrete is classified as two parts: basic creep and dry creep (ACI 209, 1994). Basic creep is also called real creep, which is developed under the condition of humidity equilibrium. This creep value is measured from the specimens under sealing. It is related to constant elastic stress and loading duration (Wang et al, 1985). Dry creep is the result of the exchange between the environment and tested specimen, which is increased with time (Wang et al, 1985).

Concrete creep is a complicated phenomenon due to a wide variety of factors affecting it. Those factors are normally recognized as (Han, 1996):

1. *Cement type and fineness of cement*:

Different types and fineness of cement result in different hydrated rates of cement paste. At the same concrete age, cement paste with different hydrated rates will achieve different proportions of the final strength (CEB-FIP, 1993). It has been concluded (Han, 1996) that the slower the strength is being developed, the larger the potential of creep strain will pose. This effect has been considered in CEB-FIP Model 90 (1993), for both calculations of creep and shrinkage. In that model, types of cement are classified as SL, slowing hardening cement, N or R, normal or rapid hardening cement, and RS, rapid hardening high strength cements. Refer to Appendix B for more details about cement classification in CEB-FIP Model 90.

2. *Aggregates grading and the property of admixtures*:

Normal weight aggregates, stone and sands, exhibit extremely negligible creep comparing to cement paste. Thus, good grading aggregates effectively resist the creep

tendency of cement paste due to stress redistribution inside of concrete admixture. The main factors of the resistance are the amount of coarse aggregate and the modulus of elasticity of the aggregate (Han, 1996). ACI-209R-92 (1994) includes this factor by introducing fine aggregate percentage correction factor γ_{ψ}. The larger the fine aggregate percentage is, the larger the creep will be. Refer to Appendix A for more details about correction factor γ_{ψ}.

3. *Water cement ratio*:

Cement content does not influence concrete creep, but water cement ratio does (Wang and Salmon, 1992). It is due to the fact that increase water cement ratio that also will increase free water in concrete admixture. This may firstly increase the amount of the micro cracks developed in concrete during the hydrated process; secondly decrease the cement paste strength, which turns out increasing the possibility of stress redistribution from cement paste to aggregates under sustained loading, thus increases concrete creep (Han, 1996). Since water cement ratio affects concrete slump value, ACI-209R-92 introduces the creep correction factor of slump γ_s to include water cement ratio effect on creep. Refer to Appendix A for calculation of correction factor γ_s.

4. *Curing humidity and temperature*:

Relative humidity and temperature are the two important factors for concrete curing. Obviously, better curing will achieve better quality of concrete products, which means higher density and less micro cracks, therefore less creep. Thus, a certain level of relative humidity and temperature are helpful to curb the development of concrete creep. On the other hand, a long duration of high level relative humidity (such as 100%) environment for curing process before loading, may also store a lot free water inside of

concrete, which turns out enhancing creep (Han, 1996). Steamed curing is better than the moist for concrete to curb development of creep. This has been reflected in the ACI-209-92R Model calculation. Refer to Appendix A for detailed calculation.

5. *Age of concrete at loading*:

The older the age of concrete means the longer the hydrated process endued, thus less creep potential to develop. Both ACI and CEB-FIP models have included this effect.

6. *Relative humidity and temperature after loading*:

After the loading, higher relative humidity and a certain level of temperature are effective to decelerate the loss of free water from admixture and promote the developing hydrated process of concrete. Thus, less creep would develop. Both ACI and CEB-FIP models have included this effect.

7. *Concrete stress/strength level*:

It is generally accepted that until a stress level, the concrete creep is proportional to elastic compressive stress (Wang and Salmon, 1992). Above that level, significant internal micro-cracks happen and extend widely, thus accelerate creep (Han, 1996). Under a certain level of concrete compressive stress level, about 40% of ultimate strength, both ACI and CEB introduce linear product models. Above that level, CEB uses a nonlinear exponent function to consider high stress effect. See Appendix B for detailed calculation.

8. *Dimension effect*:

Theoretically, dimension effect could be zero if no dry contraction (dry creep) happens (Wang et al, 1985). In another words, if a specimen is sealed in 100% relative humidity environment from curing until the end of loading, then the specimen size should

have no effects on concrete creep. In practical situations, due to different relative humidity conditions, that effect does exist, and sometimes very large (Wang et al, 1985). The ratio of volume/surface areas is used to estimate a dimension effect on creep (ACI 209, 1994). The larger the value is, the slower and the less loss of free water will be in the admixture, thus, the less creep could happen (Han, 1996).

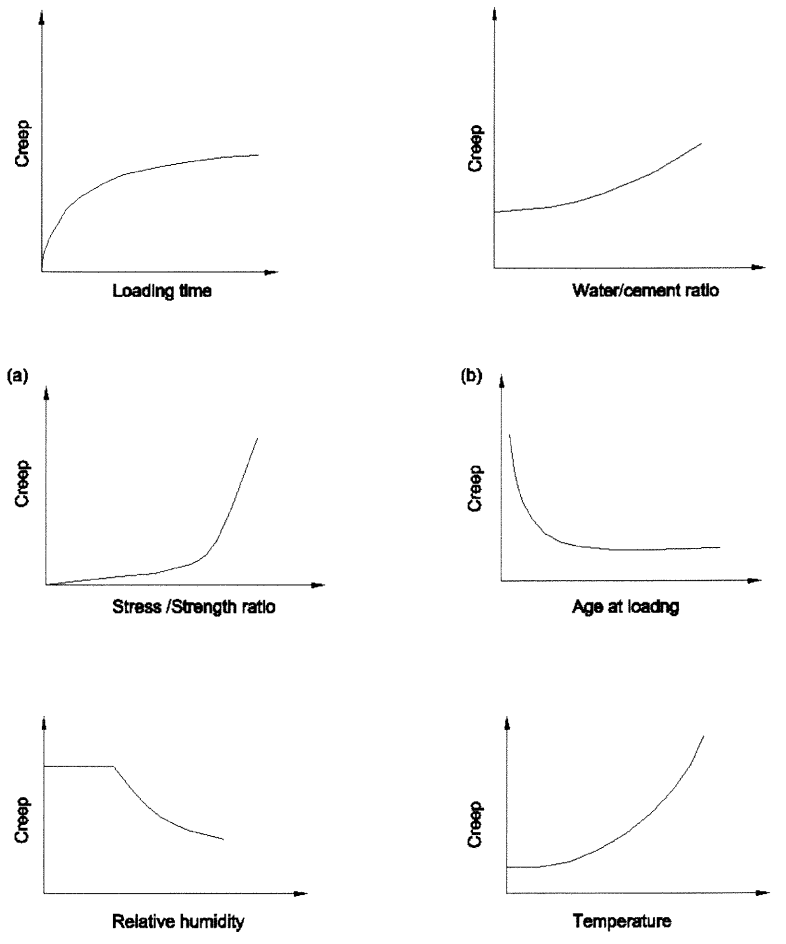

Figure 2.2 Relationships between Creep and Various Factors Which Influence Creep

The relationships between creep and various factors, which influence creep, are shown in Figure 2.2 (Han, 1996). Generally, those factors are primarily related to

moisture loss, which influence creep, have been found to influence shrinkage as well (Wang and Salmon, 1992).

Although creep and shrinkage are two different chemical and physical processes of concrete, but development of each process relates the other one closely. For example, shrinkage produces micro cracks, which might contribute more creep to happen. On the other hand, under the external loading pores inside the concrete become smaller, thus resulting a slow down of the transport of free water to the environment. Therefore, the development of shrinkage could be slower.

2.2.2 Mechanism of Concrete Creep

1. *Viscous Flow Theory*

In this theory, cement paste is assumed as to be a high viscous fluid, which increases viscosity with time as development of chemical changes continues. When concrete is loaded, the viscous paste is flowing under compressive stress. The movement will gradually transfer the stress on cement paste to the aggregate. The rate of creep will progressively reduced as the stress redistribution ends. However, viscous flow theory cannot explain the phenomena of volume changes within the creep process. Further more, the theory also assumes proportionality between stress/strain and rate of stress over rate of strain. It is suitable for concrete compressive stress is in the range of 30 to 50% of the strength. That stress upper limitation is believed due to the development of micro cracks. Nevertheless, the viscous flow theory can be used to describe mechanism of creep with some observations (Neville, Dilger and Brooks, 1983) (Han, 1996).

2. *Plastic Flow Theory*

The plastic flow theory is similar to the one that explains the mechanism of metal creep. It suggests that creep of concrete is caused by a plastic flow called crystalline, i.e. a slipping along planes within a crystal lattice. The plastic flow is a result of a slip in a plan of maximum shear stress. The water inside concrete is assumed to act as lubricant thus makes flow easier. One of the shortcomings of this theory is, for metals at room temperatures, the plastic flow occurs only when the applied stress equals or exceeds the yield point. While in the case of concrete, there is no such a yield point. Additionally, the theory cannot explain volume changes either. However, at very high stress level, the theory seems explaining concrete creep better (Han, 1996).

3. *Seepage Theory*

In this theory, the creep of concrete is explained as seepage of gel water under pressure. The gel water inside of concrete admixture is in a state of equilibrium under vapor pressure. When an external load is applied to the concrete, the pressure is changed and equilibrium broken. The gel water is reorganized to obtain the new equilibrium. It affects the colloidal stresses and van der Waals force. A new equilibrium is reached by seepage of gel water inside the cement gel. It is obvious that the density (porous) of the cement paste has a strong effect on the seepage. One of challenges to this theory is how to explain the remained creep in the unloading process. According to the theory, after removal of the external load, due to reducing of pressure of gel water, the original equilibrium would re-establish. The result of creep recover test cannot support this point. One basic argument about the seepage theory is that, if the gel water is slowly squeezed out of the pores and the capillary water evaporates, a considerable weightless could be

happened during the creep process. Nevertheless, this could not be proved by experiment either (Neville, Dilger and Brooks, 1983) (Han, 1996).

4. *Micro-cracking Theory*

The development of micro-cracks associated with creep has been confirmed by results from acoustic measurement. It is estimated that micro cracking is taking 10 to 25% of the total creep deformation in concrete. The extent of the development of micro cracking being due to creep depends on existing micro-cracks prior to loading. At high stress level, micro cracking contributes considerably to concrete creep (Han, 1996).

Due to its complicity, even though quite a few research results have been achieved on concrete creep, to clarify the mechanism of concrete creep is still very difficult. As being described by Illston et al. (1979): " The physical and chemical happenings that are associated with creep are on a molecular scale, and there is no convincing direct evidence of what actually goes on; so the explanation of creep has, perforce, consisted of interpreting engineering level observations in terms of likely physical and chemical phenomena." It is generally agreed none of the mechanisms proposed up to date can explain all of observed facts.

2.2.3 Mechanism of Concrete Shrinkage

Shrinkage of concrete is classified as plastic shrinkage, chemical shrinkage and drying shrinkage (Gilbert, 2001).

Plastic shrinkage, which happens in the wet concrete, may result in significant cracking during a setting process. This cracking occurs due to capillary tension in pore water. Since the bond between plastic concrete and reinforcement has not yet developed,

the steel is ineffective in controlling such cracks. This problem may be severe in the case of low water content and existing silica fume concrete. Thus, high strength concretes are prone to plastic shrinkage (Gilbert, 2001).

Drying shrinkage is caused primarily by the loss of water during the drying process. Chemical (or endogenous) shrinkage results from various chemical reactions within the cement paste and includes hydration shrinkage, which is related to the degree of hydration of the binder in a sealed specimen (Gilbert, 2001).

Concrete shrinkage strain is usually considered as the sum of drying and chemical shrinkage components (Gilbert, 2001).

2.2.4 Different Properties of Creep and Shrinkage between NSC and HSC

HSC is not only characterized by superior engineering properties such as higher compressive strength, elastic modulus and density, but also by remarkably different material physical properties such as more discontinuous and closed pore structure, smaller pore sizes, and a more uniform pore distribution. This , among others, is a result of addition of silica fume or the like. Those differences in the microstructure cause changes in properties like creep and shrinkage. (Han, 1996)

It has been found that creep is much lower in HSC than NSC, especially under the drying conditions. The ratio of sustained loading strength to short-term strength is also higher in HSC than NSC. Results from experiments have confirmed that the mount of cracks including those related at initial state is much less in HSC. Consequently, smaller inelastic deformations and higher creep-stress linearity limits have also been observed (Han,1996). In CEB-FIP Model 90, concrete strength has been considered in calculating

the creep and shrinkage coefficients (Refer to Appendix B for more details). The higher is the strength, the smaller are the values of those coefficients.

2.3 Analytical Models to Predict Creep and Shrinkage

There are three types of models which have been developed to predict concrete creep and shrinkage. One method is a material science approach. In that approach, the models are developed on theories about microstructure of concrete material. As pointed out by Wittmann (1982), the models are very complicated in presentation and therefore very difficult for use in practical engineering. Another method is to formulate empirical linear models on basis of test data. Although it still suffers some basic theoretical weakness, it is a more accrurate method in most practical situations. Particularly, it is much easier to be adopted in engineering application. The third approach is to create a nonlinear creep model based on rheology theory (Shen, 1992), (Walraven and Shen, 1993). Compared with microstructure model, it has avoided using the complicacity of micro-structural theory and exponent presentation. However, most parameters in the formula are still needed to be determined from the experiments.

2.3.1 ACI 209R-92 Models

1. *Creep Model*

A general empirical method, developed by Branson (1971), which has been accepted by ACI-209, gives a creep coefficient equation under loading ages of 7 days for moist cured concrete and 1-3 days for steam cured concrete:

$$v_t = \frac{creep\ strain}{initial\ elastic\ strain} \tag{2.1a}$$

$$v_u = \frac{v_u t^{0.6}}{(10 + t^{0.6})} \tag{2.1b}$$

where t is the duration of loading (days) and v_u is the ultimate creep coefficient.

$$v_u = 2.35\gamma_c \tag{2.2}$$

$$\gamma_c = \gamma_{la}\gamma_\lambda\gamma_{at}\gamma_s\gamma_\psi\gamma_a \tag{2.3}$$

γ_c denotes the product of the applicable correction factors defined in Eq. (2.3)

γ_{la} denotes the correction factor for loading age

γ_λ denotes the correction factor for ambient relative humidity

γ_{at} denotes the correction factor for average thickness of member other than 6 inch

γ_s denotes the correction factor for slump

γ_ψ denotes the correction factor for fine aggregate percentage

γ_a denotes the correction factor for air content

See Appendix A for calculations of the factors. In this research, since all test data collected do not provide air content information. An assumption of 6% is made for the creep estimation of all concrete specimens.

Figure 2.3 shows typical creep variation with duration of loading (Wang and Salmon, 1992).

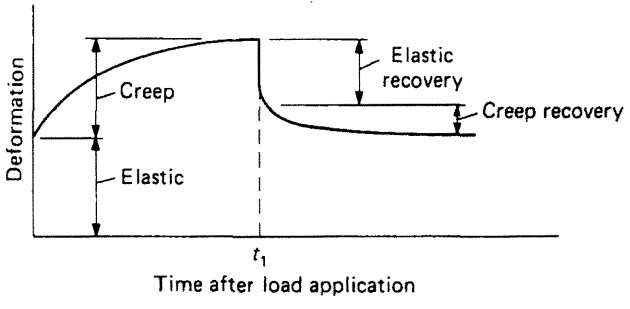

Figure 2.3 Typical Relationships between Deformations of Elastic, Creep and the Recoveries

2. *Shrinkage Model*

Shrinkage after age 7 days for moist cured concrete is given by:

$$(\varepsilon_{sh})_h = \frac{t}{(35+t)} (\varepsilon_{sh})_u \tag{2.4}$$

where t is the time after shrinkage is considered, and $(\varepsilon_{sh})_u$ is the ultimate shrinkage strain.

Shrinkage after age 1-3 days for steam-cured concrete is given by:

$$(\varepsilon_{sh})_h = \frac{t}{(55+t)} (\varepsilon_{sh})_u \tag{2.5}$$

In absence of specific shrinkage data for local aggregates and conditions, the average values suggested for $(\varepsilon_{sh})_u$ are:

$$(\varepsilon_{sh})_u = 780\ \gamma_{sh} x 10^6 \text{ in./in., (m/m)} \tag{2.6}$$

$$\gamma_{sh} = \gamma_{cp}\gamma_{\lambda}\gamma_{at}\gamma_{s}\gamma_{\psi}\gamma_{c}\gamma_{a} \tag{2.7}$$

where,

γ_{sh} denotes the product of the applicable correction factors defined in Eq. (2.7)

γ_{cp} denotes the correction factor for initial moist curing

γ_c denotes the correction factor for cement content

See Appendix A for calculations of factors $\gamma_{cp}, \gamma_{\lambda}, \gamma_{at}, \gamma_s, \gamma_{\psi}, \gamma_c$, and γ_a.

Figure 2.4 shows a typical shrinkage strain variation with time after moist curing (Wang and Salmon, 1992).

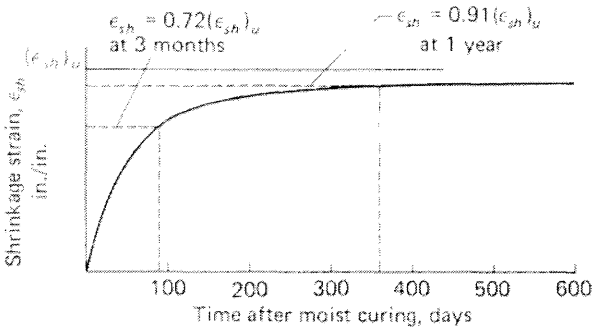

Figure 2.4 Standard Shrinkage Strain Variation with Time after Moist Curing

3. *Concrete compressive strength versus time*

$$(f_c')_t = \frac{t}{a + \beta t}(f_c')_{28} \tag{2.8}$$

where, a in days and β are constants, $(f_c')_{28}$=28-day strength and t in days is the age of concrete. The values of a and β are related to the type of cement used and the type of curing employed. Typical values recommended are given in Table 2.2.1 of ACI 209R-92 (ACI Committee 209, 1994).

2.3.2 Models of CEB-FIP Model Code 1990

1. *Creep Model*:

When stress σ_c <0.4$f_{cm}(t_0)$, the creep is assumed to be linearly related to the stress. For constant stress applied at time t_0 this leads to:

$$\varepsilon_{cc}(t,t_0) = \frac{\sigma_c(t_0)}{E_{ci}}\phi(t,t_0) \tag{2.9}$$

where,

$f_{cm}(t_0)$ is the mean concrete compressive strength at an age of days t_0

E_{ci} is the modulus of elasticity at the age of 28 days

$\phi(t,t_0)$ is the creep coefficient. It may be calculated from:

$$\phi(t,t_0) = \phi_0 \beta_c(t-t_0) \tag{2.10}$$

ϕ_0 is the notional creep coefficient, refer to Appendix B for more information.

$\beta_c(t-t_0)$ is the function to describe the development of creep with time after loading (see Appendix B for more information)

t is t he age of concrete at the moment considered (in days)

t_0 is the age of concrete at loading (in days)

For a stress level in the range of $0.4f_{cm}(t_0) < \sigma_c < 0.6f_{cm}(t_0)$ the non-linearity of creep may be taken into account using the following Equations:

$$\phi_{0,k} = \phi_0 \exp[\alpha_\sigma(k_\sigma - 0.4)] \tag{2.11}$$

where,

$\phi_{0,k}$ is the non-linear notional creep coefficient, which replaces ϕ_0 in Eq. (2.10)

k_σ is the stress/strength ratio $\quad k_\sigma = \sigma_c / f_{cm}(t_0)$ (2.12)

$$\alpha_\sigma = 1.5 \tag{2.13}$$

2. *Development of strength with time*

For a mean temperature of 20°C and curing in accordance with ISO 2736/2, the relative compressive strength of concrete at various ages $f_{cm}(t)$ may be estimated from Equations (2.14):

$$f_{cm}(t) = \beta_{cc}(t) f_{cm} \tag{2.14}$$

where,

$$\beta_{cc}(t) = \exp\{s[1 - (\frac{28}{t/t_1})^{1/2}]\} \tag{2.15}$$

f_{cm} is the mean compressive strength of concrete at an age of 28 days

$f_{cm}(t)$ is the mean compressive strength of concrete at an age of t days

$\beta_{cc}(t)$ is a coefficient, which depends on the age of concrete t days

s is a coefficient which depends on the type of cement: s=0.20 for rapid hardening high strength cements RS, 0.25 for normal and rapid hardening cements N and R, and 0.38 for slowly hardening cements SL.

t_1 equals1 day

3. *Strength under sustained loads*

The combined effect of sustained stresses and of continued hydration is given by Equations (2.16) and (2.17)

$$f_{cm,sus}(t,t_0) = f_{cm}\beta_{cc}(t)\beta_{c,us}(t,t_0) \tag{2.16}$$

with

$$\beta_{c,sus}(t,t_0) = 0.96 - 0.12\{\ln[72(\frac{t-t_0}{t_1})]\}^{1/4} \tag{2.17}$$

where,

$f_{cm,sus}(t,t_0)$ is the mean compressive strength of concrete at time t when subjected to a high-sustained compressive stress at an age at loading $t_0<t$

$\beta_{c,sus}(t,t_0)$ is a coefficient which depends on the time under high sustained loads t-t_0 (days). The coefficient describes the decrease of strength with time under load and is defined for (t-t_0)>0.015days (=20 min)

4. *Shrinkage Model*

The total shrinkage strain $\varepsilon_{cs}(t,t_0)$ may be calculated from:

$$\varepsilon_{cs}(t,t_0) = \varepsilon_{cs0}\beta_s(t\text{-}t_s) \tag{2.18}$$

ε_{cs0} is the notional shrinkage coefficient

β_s *is* the coefficient to describe shrinkage with time

t is the age of concrete (days)

t_s is the age of concrete (days) at the beginning of shrinkage

Refer to Appendix B for more details of calculations.

2.3.3 Non-linear Model for Creep

According to Walraven and Shen (1993), the nonlinear model contains two nonlinear springs and a non-linear dashpot (see Figure 2.5).

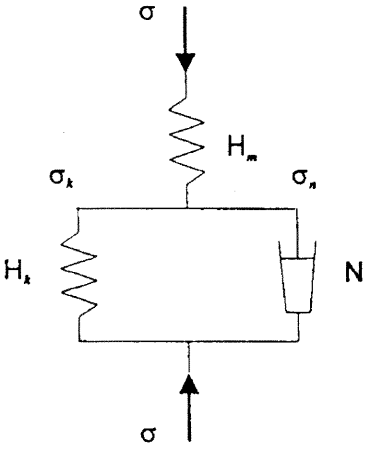

Figure 2.5 A Non-linear Model for Concrete Consisting of Two Springs and One Dashpot [after Shen (1993)]

A general constitutive equation can be derived in the following:

$$\int_0^t \omega \, dt = \int_{\theta_k(t_0)}^{\theta_k(t)} \frac{1+(c_k-2).\theta_k}{\zeta - 2.\xi.\theta_k + \mu\theta_k^2} d\theta_k \qquad (2.18)$$

where,

ω is the creep rate factor

c_k is the nonlinearity factor for spring H_k

θ_k is the strain level, in. H_k i.e. $\varepsilon_k/\varepsilon_{ku}$

ε_{ku} is the ultimate strain of spring H_k

$$\mu_k = 1+(c_k-2).\lambda \tag{2.19}$$

$$\xi = [c_k-(c_k-2).\zeta+ \lambda] \tag{2.20}$$

$$\zeta = \alpha_m(t_0) + \lambda\ \theta_k(t_0) \tag{2.21}$$

α_m is the stress level, i.e. σ_m/f_m

λ=0, for creep

t_0 is the concrete age at loading

The characteristics of the spring H can be described in the following:

For loading: $$\alpha_m = f_m(\theta_m) = \frac{(c_m\theta - \theta_m^2)}{1+(c_m-2).\theta_m} \tag{2.22}$$

For unloading and reloading: $$\alpha_m = f_m(\theta_m) = \alpha_m^* + c_{um}.\Delta\ \theta_k \tag{2.23}$$

where,

c_m is the nonlinearity factor for spring H_m

θ_m is the strain level, in. H_m i.e. $\varepsilon_m/\varepsilon_{mu}$

c_{um} is the material factor for unloading

ε_{mu} is the ultimate strain of spring H_m

α_m^* is the highest stress level in the history

2.3.4 Micro-structure Model for Creep

Wittmann et al. (1982) used the activation energy approach to describe the creep of concrete. It is assumed that the movement of solid particles is responsible for the creep of concrete.

$$\varepsilon_{cr} = \left(\frac{A_1}{t^{m_e}}\right)\left(A_2.e^{-\frac{Q_0}{RT}}\right)\left[A_3.\sinh\left(\frac{V_a}{R.T.\sigma}\right)\right] \quad (2.24)$$

where,

ε_{cr} is the creep of concrete

A_1, A_2 and A_3 are constants

V_a is activation volume

Q_0 is a constant

R is gas constant

T is absolute temperature

σ is the applied stress

m_e is a constant

t is the concrete age

2.4 Studies on Slender RC Column Buckling under Sustained Loads

2.4.1 Effects of Creep and Shrinkage on Strength of RC Column

Except for non-eccentrically loaded columns, any occurrence of creep will increase geometrically the bending curvature of a section in a column, because the higher compressive strain yields the higher creep strain. As a result, the increasing of bending curvatures of column sections yields the increasing of the lateral deflection of the column, which in turn increases the axial load's eccentricities to column sections thus affecting the internal concrete and reinforcing steel strains and stresses. Although the development of creep may help redistribute part of concrete compression stress to steel reinforcing in compression zone, concrete creep might still decrease the buckling capacity of slender columns.

As it is not caused by concrete stress changes, shrinkage will tend to relax the concrete compression stress and redistribute the force difference to longitudinal reinforcement. That is, to increase the compressive stress in steel reinforcement previously in compression, and /or to decrease the tensile stress in steel reinforcement previously in tension. As a result the moment curvature of a section decreases, this, in general, is beneficial to the increase of buckling strength of the slender columns.

2.4.2 Experimental Studies

From the mid 1950s, academic researchers started to pay attention to studying the slender RC columns under sustained axial loads. During 1960 through 1970, the research and experiments in this field became very active. Breen and Green (1969) from University of Texas investigated behavior of restrained and unrestrained reinforced concrete columns under sustained loads in their Ph.D. programs. Goyal (1971) from Scotland, performed study of (pinned) slender columns under sustained loads. Lately, Gilbert and Mickleborough (1993) studied the creep effects in slender reinforced and pre-stressed concrete columns. When HSC is widely used in engineering practice, some researchers began their focus on the experiments with the R/C column made of HSC (Claeson, 2000). Until now, most test data are still from the specimens made of NSC.

Drysdale et al. (1971) published their research on sustained bi-axial load on slender concrete columns. This is the only published paper that has focused on the experiments in bi-axially loaded slender RC columns under sustained loads. Due to the loading equipment and other conditions limits, the scales of test specimens are about 1:5 ~ 1:2; the sustained load durations are less than 3 years; all specimens are pinned top and

bottom and loaded eccentrically and symmetrically. Per ACI-129-R92 model, concrete could have reached 87% of the total creep strain in 3 years. Per CEB-FIP 90 model, that number becomes 77~90%. Thus, most of creep has developed in that period, which means, the 3 year experimental results should have reflected the real creep process from this point of view. Refer to Chapter 4 for more discussions of the experimental results.

2.4.3 Theoretical Analysis

Ostlund (1957) suggested the **Reduced Modulus of Elasticity** (**RME**) to estimate the effect of creep on buckling load of RC column. According to Ostlund, the reduced modulus of elasticity of concrete E_r can be obtained from the following formula:

$$E_r = \frac{E}{(1+\alpha.E)} \tag{2.21}$$

$$\alpha = \frac{\varphi_0}{a} \tag{2.22}$$

where,

α denotes liquidity constant in the creep law for the method of superposition

φ_0 denotes liquidity constant in the creep law for the rate of creep method

a denotes time constant in creep law

E denotes concrete elastic modulus

Ostlund's study opened the theoretical analysis in this field. The advantage of the method is its simplicity and easy to be applied in engineering. In fact, this concept has provided the basic direction for the ACI-318 Building Codes since 1971.

The difficulty with this approach is that the value of E/E_r is not directly known and varies in a large arrange. In ACI-318, $(1+\beta_d)$ is used instead of $(1+\alpha E)$ to get the

reduced *EI* value. It has neglected the value variations of concrete creep. In particular, the reduced modulus approach could not be used reliably to determine the resistance of a column to a long- duration (dead) load, followed by an additional (live) load. (Mauch, 1966)

Bresler and Selna (1964) proposed a powerful method for creep buckling of RC slender column analysis. It is called the **Relaxation Procedure**. In this method, during a time interval, the strain distribution is initially held unchanged. Under the situation, if the creep and shrinkage components change, the elastic components of total strain must also change by the same amount in the opposite direction. The internal force equilibrium could not be kept unless both a change of axial force ΔN and a change of bending moment ΔM are applied to this section. The strain state is thawed (relaxed) after the changes of internal forces being applied to the section. This approach is accurate for the material that is linear elastic at short-term.

That is, at section i,

$$\Delta\varepsilon_{0i}=\frac{B.\Delta M_i + I.\Delta N_i}{E_c\left(A.I - B^2\right)} \tag{2.23}$$

$$\Delta\kappa_i = \frac{A.\Delta M_i + B.\Delta N_i}{E_c\left(A.I - B^2\right)} \tag{2.24}$$

where,

$\Delta\varepsilon_{0i}$ is the change in strain of the top fiber

$\Delta\kappa_i$ is the change in curvature of the section

$A=\int dA$ is the area of the transformed section

$B=\int y dA$ is the first moment of the transformed area about the top surface of the section

I is the secondary moment of the transformed area about the top surface of the section

E_c is the concrete elastic modulus

ΔM_i is the change of bending moment

ΔN_i is the change of axial force

Bazant et al. (1972) proposed the **Age-adjusted Effective Modulus Method (AEMM)** to model the effects of creep.

$$E''(t,t_0) = \frac{E(t_0)}{1+\chi(t,t_0)\phi(t,t_0)} \tag{2.25}$$

where,

$E''(t,t_0)$ is the age-adjusted effective modulus

$E(t_0)$ is the instantaneous elastic modulus in time t_0

$\phi(t,t_0)$ is the increment of the time-dependent concrete creep coefficient associated with the time interval and load increment under consideration

$\chi(t,t_0)$ is the aging coefficient for concrete during the same interval

Combining Bazant's AEMM and Relaxation Procedure proposed by Bresler and Selna (1964). Gilbert et al. (1993) proposed a non-linear procedure for the time-dependent analysis of reinforced and pre-stressed concrete columns under uni-axial sustained eccentric compression. In their method, both material and geometric non-linearites are taken into account in an iterative computer-based solution procedure, in which, for short-term analysis, stress-strain relation for concrete is bi-linear with crack point in between. Individual cross-sections are analyzed using the age-adjusted effective modulus method to include the effects of creep and shrinkage. In which,

$$\Delta\varepsilon_{0i}=\frac{B_e.\Delta M_i + I_e.\Delta N_i}{E''(t,t_0)(A_e I_e - B_e^2)} \tag{2.26}$$

$$\Delta\kappa_i = \frac{A_e.\Delta M_i + B_e.\Delta N_i}{E''(t,t_0)(A_e I_e - B_e^2)} \tag{2.27}$$

where,

$\Delta\varepsilon_{0i}$ is the change in strain of the top fiber

$\Delta\kappa_i$ is the change in curvature of the section

A_e is the effective area of the transformed section

B_e is the first moment of the effective transformed area about the top surface of the section

I_e is the secondary moment of the effective transformed area about the top surface of the section

ΔM_i is change of bending moment

ΔN_i is change of axial force

Dividing the time scale into several increments, the gradual development of time-dependent cracking can be traced as the lateral deflection of the column and the internal secondary moments increase with time due to creep. In the numerical analysis part, the variation of curvature along the member is assumed to be parabolic. That is:

$$\delta = \frac{L^2(k_A + 10k_C + k_B)}{96} \tag{2.28}$$

where,

δ is the lateral deflection of column at mid-height

k_A is the curvature of top section

κ_B is the curvature of bottom section

κ_C is the curvature at mid-height section

L the length of column

Claeson et al. (2000) presented the analysis of slender HSC columns under uni-axial sustained eccentric loads by using CEB-FIP 90 Model Code (1993). The analysis used a moment-curvature approach. The calculations were based on a cross-sectional analysis. The second order effects were taken into account by assuming a sine curve deflection shape. In addition, the confining effect of the stirrups was carried out. Creep of the concrete was taken into account using the Equation (2.8) from CEB-FIP.

The modulus of elasticity for concrete was not assumed to increase with respect to time. The experiment pointed out that, HSC columns exhibited fewer tendencies to creep and could sustain the axial load without much increase in deformation for a longer period. They also exhibited less nonlinear creep.

For the RC slender columns under sustained bi-axial bending loads, Drysdale et al presented an analysis method in 1971. To describe two-dimensional distribution of strain on sections, cross section was divided into a grid. Using the symmetric feature for loading at top of a pinned column, only half was analyzed. The half column was divided into four segments. The distributions of strain on sections were assumed first manually and then corrected by computerized iteration process controlled by three internal force equilibrium equations at each section and the moment eccentricity at the end of column. For creep prediction, a nonlinear creep model was used and the **Modified Superposition Method for Creep Prediction** was adapted to this computerized analysis.

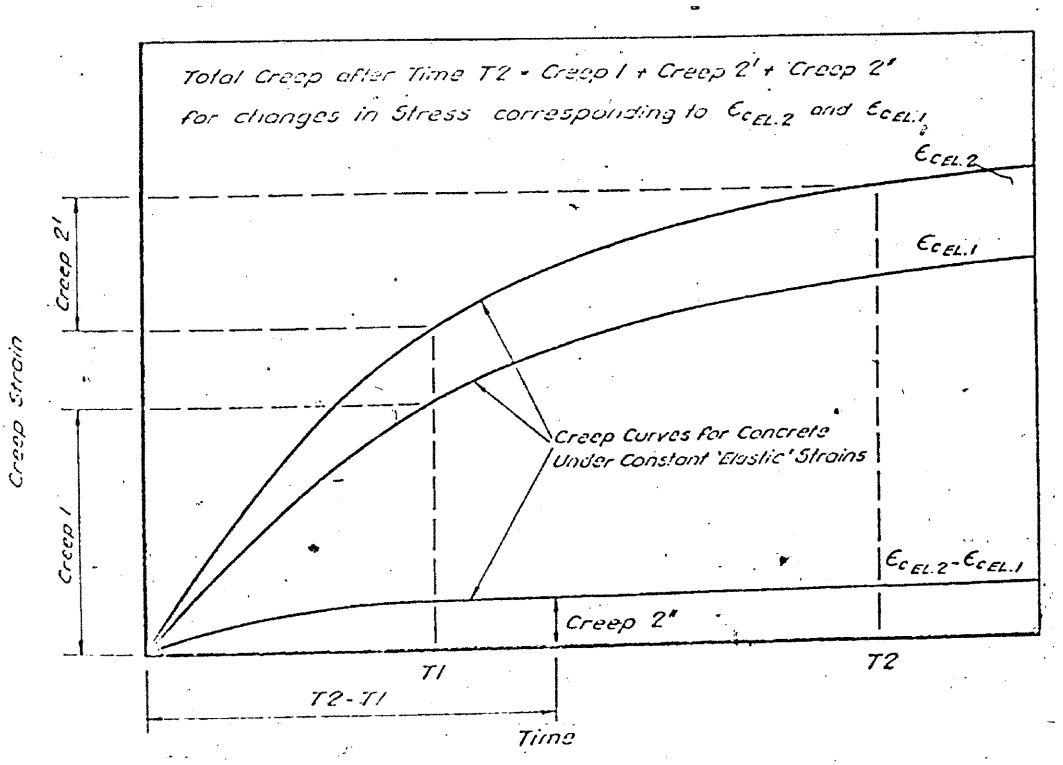

Figure 2.6 Modified Superposition Method for Calculating Concrete Creep (Drysdale, 1967)

From Figure 2.6 the total creep at t_2 equals:

$$creep(t_2)=creep_1+creep\ _2'+creep\ _2'' \tag{2.29}$$

where,

$creep_1$: creep strain under initial constant elastic strain $_{EL,1}$ during time t_0 to t_1

$creep_2'$: creep strain under initial constant elastic strain $_{EL,2}$ during time t_1 to t_2

$creep_2''$: creep strain difference between lines of $\varepsilon_{c\,EL,1}$ and $\varepsilon_{c\,EL,2}$ during time t_0 to t_2-t_1

$\varepsilon_{c\,EL,1}$: creep strain line under constant stress σ_1

$\varepsilon_{c\,EL,2}$: creep strain line under constant stress σ_2

Obviously, the shortcoming of this method is that the concrete creep will be over estimated when stress is decreasing, which frequently occurs at early phase of sustained loading.

Mauch (1965) also performed theoretical study on RC slender column creep buckling based on rheology theory, which resulted in a very complicated mathematic formula. According to his research, slender column reductions in carrying capacity due to creep were 40 to 50 percent for columns with a slenderness of L/D=25 to 40, where L is the length of column and D is the diameter of column. Smaller reductions occurred for shorter columns.

2.5 Engineering Approach Specified by Engineering Design Codes

In 1963, ACI made substantial modifications to the design procedures applicable to slender columns, including the effects of sustained loads in some cases. The Code required that for a certain type of restrained column with L/D>30, an analysis taking into account the effect of additional deflections on moment was required. The Code retained the use of a long column reduction factor. The reduction factor was expressed as a linear function of the slenderness ratio and applied equally to load and moment (ACI-318, 1963).

In 1971, ACI introduced the Moment Magnifier Design Method for design of slender columns under both short term and sustained loads. The design method has been adopted till today.

1. *ACI 318-99 Provisions*:

In ACI 318-99 Building Code, the effect of sustained load on slender column is considered in calculation of Stiffness Parameter *EI*, which is taken as following:

If $0.2E_cI_g > E_sI_s$ $$EI = \frac{0.4E_cI_g}{1+\beta_d} \quad (2.30a)$$

else, $$EI = \frac{0.2E_cI_g + E_sI_s}{1+\beta_d} \quad (2.30b)$$

where,

E_c denotes concrete modulus of elasticity

I_g denotes gross moment of inertia of concrete section

β_d denotes proportion of the factored axial load that is considered sustained

$$\beta_d = \frac{\text{factored sustained axial load}}{\text{factored total axial load}}$$

E_s denotes steel modulus of elasticity

I_s denotes gross moment of inertia of reinforcement

The value of *EI* is needed for calculating the Euler buckling load P_c of a column, which affects the strength of a RC slender column.

$$P_c = \frac{\pi^2 EI}{(kL_u)^2} \quad (2.31)$$

where,

kL_u is the effective length of column

In case of a braced slender column, the design moment M_{max} is:

$$M_{max} = \delta_b . M_{2b} \quad (2.32a)$$

or $$M_{max} = \delta_b . M_m \quad (2.32b)$$

where,

M_{2b} is the larger end moment acting on the member

M_{1b} is the smaller end moment acting on the member

That is: $|M_{2b}| > |M_{1b}|$

M_{2b}/ M_{1b} positive for single curvature

M_m is primary bending moment due to transverse loading

$$\delta_b = \frac{C_m}{1 - \frac{P_u}{\phi P_c}} \tag{2.33}$$

C_m is a factor in Moment Magnifier for braced Frames

Transverse loading: $C_m = 1.0$ (2.34)

End moments only:

$$C_m = 0.6 + 0.4\frac{M_{1b}}{M_{2b}} \geq 0.4 \tag{2.35}$$

where,

P_u is a factored axial force

Here the effect of the sustained load directly reflects on the value of β_d. β_d is a component of the column section stiffness parameter *EI*. *EI* affects the Euler buckling capacity of column P_c, which influences the value of magnifier δ_b.

MacGregor et al (1970) indicated the reason to choose β_d, (R_m noted at that time) for creep consideration:" This factor has been chosen to give the correct trend when compared to analysis and tests (Green, 1966) of columns under sustained loads".

Obviously, there are two problems about the Moment Magnifier Method. First, it is not based on any theories of concrete time-dependent behavior. Second, it needs to analyze more test data results to improve the method.

2. *CEB-FIP Model Code 1990*:

In CEB-FIP 90, the creep effects have been introduced as the creep eccentricity e_c

$$e_c = (e_0 + e_a)\left[\exp\left(\frac{\varphi(t,t_0)}{\frac{N_E}{N_{sg}} - 1}\right) - 1\right] \tag{2.36}$$

where,

e_0 denotes the first order eccentricity

e_a denotes the additional eccentricity introduced by the effects of geometrical imperfections

N_{sg} denotes the axial force in the element, under the quasi-permanent combination of actions

N_E denotes the critical Euler-load of the column.

In this model, the creep coefficient $\phi(t,t_0)$ (see Eq.(2.9)) has been included, which reflects the quantity level of creep influence.

2.6 Summary

1. *Results of Previous Studies*

a). Creep decreases the carrying capacity of slender reinforced concrete columns.

b). HSC columns exhibit fewer tendencies to creep and can sustain the axial load and exhibit less nonlinear creep.

2. *Unsolved problems*

a). There are no experimental test data available for bi-axial bending slender HSC columns. Only one experimental work is known for NSC columns under biaxial sustained loads.

b). Due to the conditional limit, the experimental longest duration of sustained loads is less than 3 years, which means a possible 15-20% creep effects have not been studied.

c). In theoretical analysis, the calculation of creep due to stress changes has not been thoroughly studied.

d). Most analysis research were performed in 1960s, the models for creep and shrinkage are needed to be updated.

e). Unlike CEB-FIP 90 Models, the design method in the ACI building codes is not established on the studies of concrete creep and shrinkage. Consequently, the current ACI building code is based on the results on concrete slender columns under sustained loads around 1970.

CHAPTER 3

PROPOSED ANALYTICAL APPROACH

A new numerical method is developed to study the behavior of bi-axially loaded slender RC columns, made of NSC/HSC, under sustained loads. In this approach, both material non-linearity (concrete) and geometry non-linearity are considered. Latest concrete time-dependent models are adopted. It is also a generalized method in terms of loading history, column supports, material (concrete) stress-strain behavior and shapes of column sections (unchanged through length of column). Except for basic dimension, loading history, support condition, and material properties, no further manually initial input data are needed.

3.1 Analysis Strategies

As it is a bi-axial bending problem, all forces, (axial force, moments and stresses) and deformation variables (strains, curvatures, and deflections) are projected to XZ and YZ planes separately. For example, the curvatures on a section ϕ are divided into ϕ_x, and ϕ_y respectively.

The solution process is based on an iteration method:

1. The columns are divided into a number of segments. At start end of each segment, a cross section is recorded to present the segment on which three simultaneous differential equations of internal force equilibrium are established.
2. For the short-term loading process, the concrete maximum compressive strain ε_{ce} and two orthogonal projected curvatures ϕ_x and ϕ_y of a section can be solved from

the three simultaneous differential equations on a cross section. The initial iteration data is obtained from linear elastic analysis.

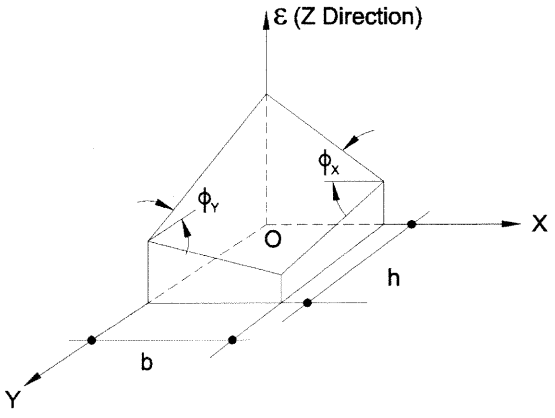

Figure 3.1 Projected Curvatures of ϕ_x and ϕ_y

3. Knowing the curvatures of all segments, the deflection line of the column can be obtained accurate enough with a numerical method.
4. To include the effects of second order deflection, a second round of iteration is performed. The control of the iteration is the error allowance between the two consecutive rounds of maximum deflection of the column.
5. For sustained load duration, the loading period is divided into a series tiny time intervals. At each interval, the creep and shrinkage strain components are calculated by concrete creep and shrinkage theoretical models and adjusted according to the **TSACM**, the method generated herein. The key point is that, **TSACM** is able to adjust creep under the situation while concrete elastic stress is decreasing, which is a typical phenomenon for reinforced concrete column creep buckling. Concrete strength and modulus of elasticity are age adjusted at each time interval.

3.2 Analysis Assumptions

The following basic assumptions are made for the analysis:

1. Linear distribution of strain across the section is valid.
2. Concrete is treated as continuous uniformed medium.
3. No tensile stress is considered for concrete.
4. Bond between concrete and reinforcement is perfect.
5. Under sustained loading, the age and /or stress adjusted concrete stress-strain equation of short term is valid for describing the elastic stress-strain changes.

3.3 Solution Procedures

3.3.1 Basic Equations

1. *Equilibrium Equations*

According to the co-ordinate system shown in Figure 3.2, the force and moments equilibrium equations on a cross section are:

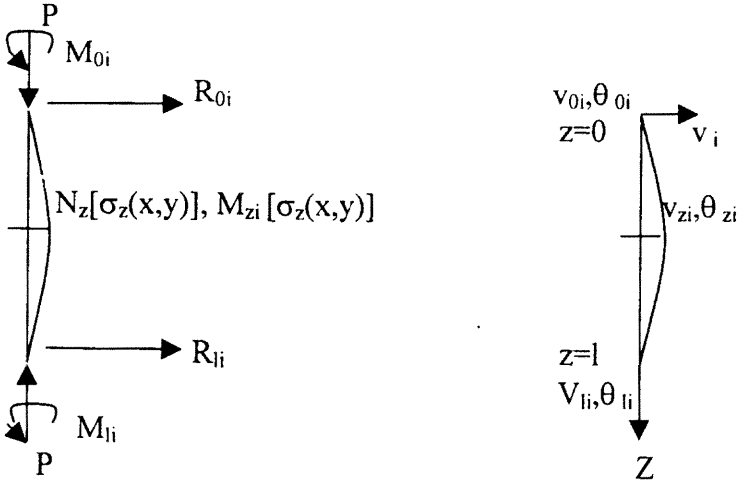

Figure 3.2 System of Global Forces and Deflections

$$\Sigma \mathbf{F}_z = 0 \tag{3.1}$$

$$\Sigma \mathbf{M}_x=0 \tag{3.2}$$

$$\Sigma \mathbf{M}_y=0 \tag{3.3}$$

Substitute symbols of external and internal forces of into the above equations, thus:

$$P- N_z[\sigma_z(x,y)]=0 \tag{3.4}$$

$$M_{0x}+P.u(z)- M_x[\sigma_z(x,y)]- R_{0x}.z=0 \tag{3.5}$$

$$M_{0y}+P.v(z)- M_y[\sigma_z(x,y)]- R_{0y}.z=0 \tag{3.6}$$

where,

P denotes axial load

M_{0y} denotes Moment at top of column rotating over y axis

M_{0x} denotes Moment at top of column rotating over -x axis

$N_z[\sigma_z(x,y)]$ denotes stress resultant along z axis

$M_y[\sigma_z(x,y)]$ denotes stress moment resultant rotating over y axis

$M_x[\sigma_z(x,y)]$ denotes stress moment resultant rotating over-x axis

$u(z)$ denotes deflection at the center of the section projected along x axis

$v(z)$ denotes deflection at the center of the section projected along y axis

$\sigma_z(x,y)$ denotes concrete compressive stress at point (x,y,z)

x, y, z denote global coordinates

2. *Constitutive laws*:

Since tension in concrete is neglected, only compression is considered. For both NSC and HSC, the Modified Hognestad Formula (Park, et al, 1975) (Kent, et al., 1971) is applied:

when $\varepsilon \leq \varepsilon$ $$\sigma_c = f_c'[2(\frac{\varepsilon}{\varepsilon_0})- (\frac{\varepsilon}{\varepsilon_0})^2] \tag{3.7}$$

when $\varepsilon_0 < \varepsilon \leq \varepsilon_u$ $\sigma_c = f_c' [1-Z(\varepsilon - \varepsilon_0)]$ (3.8)

where,

$$Z = \frac{0.5}{\varepsilon_{50} + \varepsilon_{50h} - \varepsilon_0} \quad (3.9)$$

$$\varepsilon_{50u} = \frac{3 + \varepsilon_0 f_c'}{f_c' - 1000} \quad (3.10)$$

$$\varepsilon_{50h} = 0.75 \rho_s \sqrt{\frac{b''}{s_h}} \quad (3.11)$$

σ_c is the concrete compressive stress

ε is the concrete compressive strain

f_c' is the concrete cylinder strength

ε_0 is the concrete strain refers to maximum strength, take 0.002

ε_u is the concrete ultimate strain, use 0.003

ε_{50}, ε_{50u} and ε_{50h}, refer to Figure 3.3 for physical meanings

b'' is the width of confined core measured to outside of hoops

s_h is the spacing of hoops

ρ_s is the reinforcement ratio

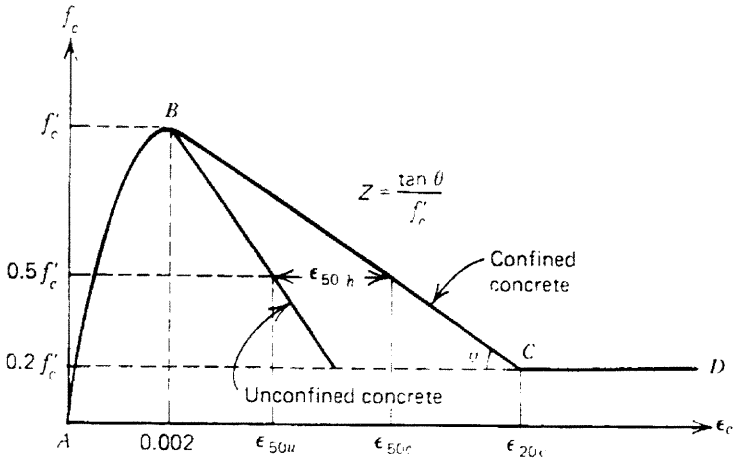

Figure 3.3 Concrete Compressive Stress-strain Relationships (Park and Paulay, 1975)

4. *Stress and Strain relationship of steel reinforcement*:

Select bi-linear model with a flat portion corresponding to the yield point.

If $\varepsilon_s < \frac{f_y}{E_s}$: $\sigma_s = \varepsilon_s . E_s$ (3.12)

else $\varepsilon_s \geq \frac{f_y}{E_s}$: $\sigma_s = f_y$ (3.13)

where,

σ_s is the stress in steel reinforcement

ε_s is the strain in steel reinforcement

E_s is the modulus of steel

f_y is the steel yield point

4. *Compatibility Equations*:

$$\varepsilon = \varepsilon_{ec0} - \phi_x . x - \phi_y . y \quad (3.14)$$

$$\phi_x = -u''(z) \quad (3.15)$$

$$\phi_y = -v''(z) \quad (3.16)$$

where,

ε is the strain of a point (x,y,z) at the section z

ε_{ec0} is the strain of the point $(0,0,z)$ at the section z

ϕ_x is the projected bending curvature on plan X0Z

ϕ_y is the projected bending curvature on plan Y0Z

5. *Time Dependent Models*:

Use ACI-129-92R Models for NSC analysis, and CEB-FIP 90 Models for HSC. For concrete strength changing versus time under sustained loads, use CEB-FIP model.

3.3.2 Iteration Controlled Derivative Equations

Re-organizing Eqs. (3.4) (3.5) & (3.6):

$$N_z[\sigma_z(x,y)]=P \tag{3.17}$$

$$M_x[\sigma_z(x,y)]= P.\ u(z)+M_{0x}- R_{0x}.z \tag{3.18}$$

$$M_y[\sigma_z(x,y)]= P.\ v(z)+M_{0y}- R_{0y}.z \tag{3.19}$$

The internal forces can be represented by stresses from the balance of the internal stresses:

$$N_z[\sigma_z(x,y)]= \iint_D \sigma_z(x,y)dxdy + \sum_{j=1}^{N_s} A_{sj}\sigma_{sj}(x_j,y_j) \tag{3.20}$$

$$M_x[\sigma_z(x,y)]= \iint_D (\frac{h}{2}-x)\sigma_z(x,y)dxdy + \sum_{j=1}^{N_s} A_{sj}\sigma_{sj}(x_j,y_j)(\frac{h}{2}-x_j) \tag{3.21}$$

$$M_y[\sigma_z(x,y)]= \iint_D (\frac{b}{2}-y)\sigma_z(x,y)dxdy + \sum_{j=1}^{N_s} A_{sj}\sigma_{sj}(x_j,y_j)(\frac{b}{2}-y_j) \tag{3.22}$$

where,

D refers to the domain of concrete compression.

A_{sj} denotes the reinforcement area at j point

x_j, y_j denote the global coordinates at j point

Stresses can be represented further by strains from the basic concrete and steel constitutive equations:

$$\sigma_z(x,y)=f_c(\varepsilon) \tag{3.23}$$

$$\sigma_{sj}(x_j,y_j)=f_s(\varepsilon) \tag{3.24}$$

Substitute (3.17), (3.18), (3.19), (3.23), and (3.24) into (3.20), (3.21), and (3.22), and then re-organize:

$$P=\iint_D \sigma_z(x,y)dxdy+\sum_{j=1}^{N_s} A_{sj}\sigma_{sj}(x_j,y_j) \tag{3.25}$$

$$P.u(z)+M_{0x}\text{-}R_{0x}.z=\frac{h}{2}\iint_D \sigma_z(x,y)dxdy-\iint x\sigma_z(x,y)dxdy+\sum_{j=1}^{N_s} A_{sj}\sigma_{sj}(x_j,y_j)(\frac{h}{2}-x_j) \tag{3.26}$$

$$P.v(z)+M_{0y}\text{-}R_{0y}.z=\frac{b}{2}\iint_D \sigma_z(x,y)dxdy-\iint y\sigma_z(x,y)dxdy+\sum_{j=1}^{N_s} A_{sj}\sigma_{sj}(x_j,y_j)(\frac{b}{2}-y_j) \tag{3.27}$$

Introducing:

$$F_1(\varepsilon)=\int f_c(\varepsilon)d\varepsilon \tag{3.28}$$

$$F_2(\varepsilon)=\int f_c(\varepsilon)\varepsilon d\varepsilon \tag{3.29}$$

Since

$$\varepsilon=\varepsilon_{ec0}\text{-}\phi_x.x\text{-}\phi_y.y \tag{3.30}$$

where,

ε_{ec0}, ϕ_x and ϕ_y are constants

Therefore

$$\frac{\partial\varepsilon}{\partial x}=\text{-}\phi_x \tag{3.31}$$

$$\frac{\partial \varepsilon}{\partial y} = -\phi_y \tag{3.32}$$

Derivate both sides of Eq (3.28):

$$\frac{\partial F_1(\varepsilon)}{\partial x} = \frac{\partial F_1(\varepsilon)}{\partial \varepsilon}\frac{\partial \varepsilon}{\partial x} = -f_c(\varepsilon).\ \phi_x \tag{3.33}$$

$$\therefore \qquad f_c(\varepsilon) = -\frac{1}{\phi_x}\frac{\partial F_1(\varepsilon)}{\partial x} \tag{3.34}$$

Thus the first term of right side of Eq (3.25) becomes:

$$\iint_D f_c(\varepsilon)dxdy = -\frac{1}{\phi_x}\iint_D \frac{\partial F_1(\varepsilon)}{\partial x}dxdy \tag{3.35}$$

Notice Green's Integral Formula:

$$\iint_D \frac{\partial Y}{\partial x}dxdy - \iint_D \frac{\partial X}{\partial y}dxdy = \oint_l Xdx + \oint_l Ydy \tag{3.36}$$

In that L represents the line envelop of the region D. And the line integral goes with anti-clock direction.

Let X=0, and Y= $F_1(\varepsilon)$ in Eq.(3.36), substitute Eq.(3.26) & Eq.(3.36) into Eq.(3.35):

$$\iint_D f_c(\varepsilon)dxdy = -\frac{1}{\phi_x}\oint_L F_1(\varepsilon_{ec0} - \phi_x x - \phi_y y)dy \tag{3.37}$$

For rectangular sections, Eq. (3.37) can be changed to:

$$\iint_D f_c(\varepsilon)dxdy = \frac{1}{\phi_x\phi_y}\left[\int_0^b F_1(\varepsilon_{ec0} - \phi_x h - \phi_y y)\, d(\varepsilon_{ec0} - \phi_x.h - \phi_y.y) + \right.$$

$$\left.\int_b^0 F_1(\varepsilon_{ec0} - \phi_y y)\, d(\varepsilon_{ec0} - \phi_y.y)\right] \tag{3.38}$$

Let

$$G_1(\varepsilon) = \int F_1(\varepsilon)d\varepsilon \tag{3.39}$$

Substitute Eq. (3.39) into Eq. (3.38):

$$\iint_D f_c(\varepsilon)dxdy = \frac{1}{\phi_x \phi_y}\,[G_1(\varepsilon_{ec0}\text{-}\phi_y.b\text{-}\phi_x.h)\text{-}\,G_1\,(\varepsilon_{ec0}\text{-}\phi_x.h)\text{-}G_1(\varepsilon_{ec0}\text{-}\phi_y.b)\text{+}G_1\,(\varepsilon_{ec0})] \tag{3.40}$$

Bring results of Eq. (3.40) into Eq. (3.25), therefore:

$$P = \frac{1}{\phi_x \phi_y}\,[G_1(\varepsilon_{ec0}\text{-}\phi_y.b\text{-}\phi_x.h)\text{-}\,G_1\,(\varepsilon_{ec0}\text{-}\phi_x.h)\text{-}G_1(\varepsilon_{ec0}\text{-}\phi_y.b)\text{+}\,G_1(\varepsilon_{ec0})]\text{+}\Sigma A_{sj.}\,\sigma_{sj}\,(x_j,y_j) \tag{3.41}$$

Using the same method, Eq.(3.26) can also be modified to the following:

Derivate both sides of Eq (3.29), i. e.

$$\frac{\partial F_2(\varepsilon)}{\partial x} = f_c(\varepsilon)\varepsilon\frac{\partial \varepsilon}{\partial x} \tag{3.42}$$

Substitute Eq. (3.30) into Eq.(3.42) and reorganize it :

$$x.f_c(\varepsilon) = \frac{1}{\phi_x^2}\frac{\partial F_2(\varepsilon)}{\partial x} + \frac{1}{\phi_x} f_c(\varepsilon).(\varepsilon_{ec0}\text{-}\phi_y.y) \tag{3.43}$$

Bring result of Eq. (3.43) into the second term at right side of Eq. (3.26):

$$\iint_D x f_c(\varepsilon)dxdy = \frac{1}{\phi_x^2}\iint_D \frac{\partial F_2(\varepsilon)}{\partial x}dxdy + \frac{1}{\phi_x}\iint_D f_c(\varepsilon)(\varepsilon_{ec0} - \phi_y y)dxdy \tag{3.44}$$

Applying Green's Formula, the first part at right side of Eq. (3.44) becomes:

$$\frac{1}{\phi_x^2}\iint_D \frac{\partial F_2(\varepsilon)}{\partial x}dxdy = \frac{1}{\phi_x^2}\oint_L F_2(\varepsilon)dy \tag{3.45}$$

Introducing:

$$G_2(\varepsilon) = \int F_2(\varepsilon)d\varepsilon \tag{3.46}$$

the right side of Eq. (3.45) can be changed into:

$$-\frac{1}{\phi_x^2 \phi_y}\,[G_2(\varepsilon_{ec0}\text{-}\phi_y.b\text{-}\phi_x.h)\text{-}G_2(\varepsilon_{ec0}\text{-}\phi_x.h)\text{-}G_2(\varepsilon_{ec0}\text{-}\phi_y.b)\text{+}G_2(\varepsilon_{ec0})] \tag{3.47}$$

while the second part at right side of Eq. (3.44) becomes:

$$\frac{1}{\phi_x}\iint_D f_c(\varepsilon)(\varepsilon_{ec0}-\phi_y y)dxdy=\frac{1}{\phi_x}\int_0^b(\varepsilon_{ec0}-\phi_y y)\left(\int_{q(y)}^{p(y)} f_c(\varepsilon)\,dx\right)dy$$

$$=-\frac{1}{\phi_x^2}\int_0^b(\varepsilon_{ec0}-\phi_y y)\left(\int_{q(y)\phi_x+\varepsilon_{ec0}}^{p(y)\phi_x+b\phi_y+\varepsilon_{ec0}} f_c(\varepsilon)d\varepsilon\right)dy$$

$$=-\frac{1}{\phi_x^2}\int_0^b(\varepsilon_{ec0}-\phi_y y)\,[F_1(\varepsilon_{ec0}\text{-}\phi_y.y\text{-}\phi_x.p(y))-F_1(\varepsilon_{ec0}\text{-}\phi_y.y\text{-}\phi_x.q(y))].dy$$

$$=-\frac{1}{\phi_x^2}\left[\int_0^b(\varepsilon_{ec0}-\phi_y y)\,F_1(\varepsilon_{ec0}\text{-}\phi_y y\text{-}\phi_x p(y))dy+\int_b^0(\varepsilon_{ec0}-\phi_y y)\,F_1(\varepsilon_{ec0}\text{-}\phi_y y\text{-}\phi_x q(y))dy\right]$$

$$=-\frac{1}{\phi_x^2}\oint_L(\varepsilon_{ec0}-\phi_y y)\,F_1(\varepsilon)dy$$

$$=-\frac{1}{\phi_x^2}\left[\oint_L \varepsilon F_1(\varepsilon)dy+\oint_L \phi_x.xF_1(\varepsilon)dy\right] \tag{3.48}$$

Introduce: $$G_3(\varepsilon)=\int F_1(\varepsilon)\,\varepsilon.d\varepsilon \tag{3.49}$$

For rectangular section, right side of Eq. (3.48) becomes:

$$\frac{1}{\phi_x^2\phi_y}\{G_3(\varepsilon_{ec0}\text{-}\phi_y.b\text{-}\phi_x.h)\text{-}G_3(\varepsilon_{ec0}\text{-}\phi_x.h)\text{-}G_3(\varepsilon_{ec0}\text{-}\phi_y.b)+G_3(\varepsilon_{ec0})+\phi_x.h[$$

$$\int_0^b F_1(\varepsilon_{ec0}-\phi_x h-\phi_y y)\,d(\varepsilon_{ec0}\text{-}\phi_x.h\text{-}\phi_y.y)]\ \}$$

$$=\frac{1}{\phi_x^2\phi_y}\{G_3(\varepsilon_{ec0}\text{-}\phi_y.b\text{-}\phi_x.h)\text{-}\ G_3(\varepsilon_{ec0}\text{-}\phi_x.h)\text{-}G_3(\varepsilon_{ec0}\text{-}\phi_y.b)+\ G_3(\varepsilon_{ec0})+$$

$$h\phi_x.[G_1(\varepsilon_{ec0}\text{-}\phi_y.b\text{-}\phi_x.h)\text{-}G_1(\varepsilon_{ec0}\text{-}\phi_x.h)]\} \tag{3.50}$$

Denotes $$GG_i=G_i(\varepsilon_{ec0}\text{-}\phi_y.b\text{-}\phi_x.h)\text{-}\ G_i(\varepsilon_{ec0}\text{-}\phi_x.h)\text{-}G_i(\varepsilon_{ec0}\text{-}\phi_y.b)+G_i(\varepsilon_{ec0}) \tag{3.51}$$

Bring Eq.(3.39), (3.45), (3.50) and (3.51) into (3.26) thus:

Then Eq. (3.26) becomes:

$$P.u(z)+M_{0x}-R_{0x}.z=\frac{1}{2\phi_x\phi_y}hGG_1+\frac{1}{\phi_x^2\phi_y}\{(GG_3-GG_2)+h\phi_x.[G_1(\varepsilon_{ec0}-\phi_y.b-\phi_x.h)-$$

$$G_1(\varepsilon_{ec0}-\phi_x.h)]\}+\Sigma A_{sj}.f_s(\varepsilon).(\frac{h}{2}-x_j) \quad (3.52)$$

and Eq.(3.41) becomes: $$P=\frac{1}{\phi_x\phi_y}.GG_1+\Sigma A_{sj}.\sigma_{sj}(x_j,y_j) \quad (3.53)$$

Bring Eq. (3.53) into Eq (3.52) and re-organize:

$$\phi_x=\frac{(GG_3-GG_2)[P-\Sigma A_{sj}\sigma_{sj}]}{GG_1[P(u(z)-\frac{1}{2}h)+M_{0x}-R_{0x}z+\Sigma A_{sj}\sigma_{sj}\frac{1}{2}h]+h[G_1(\varepsilon_{ec0}-\phi_y b-\phi_x h)-G_1(\varepsilon_{ec0}-\phi_x h)](P-\Sigma A_{sj}\sigma_{sj})} \quad (3.54)$$

Similarly, Eq.(3.27) can be evolved into:

$$\phi_y=\frac{(GG_3-GG_2)[P-\Sigma A_{sj}\sigma_{sj}]}{GG_1[P(v(z)-\frac{1}{2}b)+M_{0y}-R_{0y}z+\Sigma A_{sj}\sigma_{sj}\frac{1}{2}b]+b[G_1(\varepsilon_{ec0}-\phi_y b-\phi_x h)-G_1(\varepsilon_{ec0}-\phi_y b)](P-\Sigma A_{sj}\sigma_{sj})} \quad (3.55)$$

These three equations are the core equations for iterative solutions. The curvatures ϕ_x, ϕ_y, and boundary conditions, the solution of deflection along column length could be obtained. Refers to Appendix D for details.

3.3.3 Time and Strain Adjustment of Creep Method

Assuming t_0 is the age of concrete when instant eccentric axial load is loaded and T is the duration of the sustained load, divide T into n numbers of minor phases, (1, 2, 3, ..., i, ..., n-1,n), and denote t_i as the age of concrete at the end of i phases. Thus, at a age t_i, the

strain of the top fiber in compression stress on a cross section, which, in fact is at a corner point, would be:

$$\varepsilon(t_0,t_i) = \varepsilon(t_0,t_{i-1}) + \Delta\varepsilon_e(t_i) + [\nu(t_0,t_i) - \nu(t_0,t_{i-1})]\varepsilon_e(t_0) + \sum_{j=1}^{i-1}[\nu(t_j,t_i) - \nu(t_j,t_{i-1})]\Delta\varepsilon_e(t_j)$$

$$+\nu(t_{i-1},t_i)\frac{\Delta\varepsilon_e(t_i)}{2} + \varepsilon'_{sh}(t_0,t_i) \qquad (3.56)$$

where,

$\varepsilon(t_0,t_i)$ denotes the total strain at top fiber in end of t_i phase

t_0 is the age of concrete while loaded

$\Delta\varepsilon_e(t_i)$ is the change of elastic strain happened at t_i phase

$\nu(t_j,t_i)$ is the coefficient of concrete creep strain developed from t_j phase to t_i phase

$\varepsilon'_{sh}(t_0,t_i)$ is the effective shrinkage strain developed at end of t_i phase

$$\varepsilon'_{sh}(t_0,t_i) = \varepsilon_{sh}(t_0,t_i)\frac{A_c E_c}{A_c E_c + A_s E_s} \qquad (3.57)$$

$\varepsilon_{sh}(t_0,t_i)$ is the concrete shrinkage without reinforcement from t_0 to t_i

A_c is the cross section concrete area

A_s is the reinforcement total area of cross section

E_c is the concrete elastic modulus

E_s is the reinforcement elastic modulus

Let $\Delta\varepsilon_e(t_0)$ denotes $\varepsilon_e(t_0)$:

$$\varepsilon(t_0,t_i) = \varepsilon(t_0,t_{i-1}) + \Delta\varepsilon_e(t_i) + \sum_{j=0}^{i-1}[\nu(t_j,t_i) - \nu(t_j,t_{i-1})]\Delta\varepsilon_e(t_j) + \nu(t_{i-1},t_i)\frac{\Delta\varepsilon_e(t_i)}{2} +$$

$$\varepsilon'_{sh}(t_0,t_i) \qquad (3.58)$$

Assumptions are unchanged except for $\Delta\varepsilon_e(t_i) \leq 0$, if $\frac{\Delta\varepsilon_e(t_i)}{2} + \Delta\varepsilon_e(t_{i-1}) > 0$; then:

$$\varepsilon(t_0,t_i)=\varepsilon(t_0,t_{i-1})+\Delta\varepsilon_e(t_i)+\sum_{j=0}^{i-2}[\nu(t_j,t_i)-\nu(t_j,t_{i-1})]\Delta\varepsilon_e(t_j)+\nu(t_{i-1},t_i).\ [\frac{\Delta\varepsilon_e(t_i)}{2}+$$

$$\Delta\varepsilon_e(t_{i-1})]+\varepsilon'_{sh}(t_0,t_i) \tag{3.59}$$

else if: $\frac{\Delta\varepsilon_e(t_i)}{2} + \Delta\varepsilon_e(t_{i-1}) + \Delta\varepsilon_e(t_{i-2}) + \ldots + \Delta\varepsilon_e(t_{i-s}) \leq 0$,

while: $\frac{\Delta\varepsilon_e(t_i)}{2} + \Delta\varepsilon_e(t_{i-1}) + \Delta\varepsilon_e(t_{i-2}) + \ldots + \Delta\varepsilon_e(t_{i-s}) + \Delta\varepsilon_e(t_{i-s-1}) > 0$

yet $i\text{-}s\text{-}1 \geq 1$, then:

$$\varepsilon(t_0,t_i) = \varepsilon(t_0,t_{i-1})+\Delta\varepsilon_e(t_i)+\sum_{j=0}^{i-s-2}[\nu(t_j,t_i)-\nu(t_j,t_{i-1})]\Delta\varepsilon_e(t_j)+[\nu(t_{i-s-1},t_i)-\nu(t_{i-s-1},t_{i-1})]$$

$$.[\frac{\Delta\varepsilon_e(t_i)}{2}+\Delta\varepsilon_e(t_{i-1})+\Delta\varepsilon_e(t_{i-2})+\ldots+\Delta\varepsilon_e(t_{i-s-2})+\Delta\varepsilon_e(t_{i-s-1})]+\varepsilon'_{sh}(t_0,t_i) \tag{3.60}$$

else if $i\text{-}s\text{-}1=0$, and $\sum_{j=0}^{i-1}\Delta\varepsilon_e(t_j)+\frac{\Delta\varepsilon_e(t_i)}{2} > 0$, then:

$$\varepsilon(t_0,t_i) = \varepsilon(t_0,t_{i-1})-\Delta\varepsilon_e(t_i)+[\nu(t_0,t_i)-\nu(t_0,t_{i-1})][\sum_{j=0}^{i-1}\Delta\varepsilon_e(t_j)+\frac{\Delta\varepsilon_e(t_i)}{2}]+\varepsilon'_{sh}(t_0,t_i) \tag{3.61}$$

3.3.4 Constant Step of Creep Increasing Technique

For reasons of stability and convergence of iteration process, it is preferred to be able to control the increment step of creep strain constant. Thus:

$$\nu(t_0,t_i)-\nu(t_0,t_{i-1})=C \tag{3.62}$$

$$\nu(t_0,t_i)=C.i \tag{3.63}$$

where,

C denotes constant,

i denotes number of steps

thus we could have $$t_i = v^{-1}(C.i) \tag{3.64}$$

$$\Delta t_i = v^{-1}(C.i) - v^{-1}(C.(i\text{-}1)) \tag{3.65}$$

since $v^{-1}(x)$ is nonlinear and close to log function, thus when $i \Rightarrow \infty$, $\Delta t_i \Rightarrow \infty$.

3.3.5 Main Algorithm Flow Chart

The main flow chart of the algorithm is shown in Figure 3.4. Refer to Appendix F for the information of a detailed algorithm flow chart.

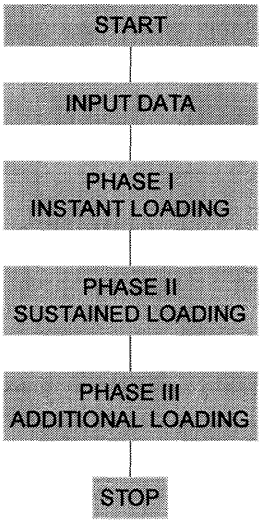

Figure 3.4 Main Flow Chart of the Algorithm

3.4 Convergence and Stability of Solution

To solve the equilibrium equations of force and moment on a section (3.53), (3.54), and (3.55), the vector of solution $\mathbf{R}_{j+1}$ $(\varepsilon_{ec0}, \phi_y, \phi_x)$ of the j+1 round of the iteration can be expressed in the following:

$$\mathbf{R}_{j+1}(\varepsilon_{ec0},\phi_x,\phi_y)=\mathbf{G}_j[\mathbf{R}_j(\varepsilon_{ec0},\phi_x,\phi_y),\mathbf{P}(e_x,e_y,t),\mathbf{U}(u,v)] \tag{3.66}$$

where,

$\mathbf{P}(e_x,e_y,t)$ is the vector of external force on the top of column,

$\mathbf{U}(u,v)$ is the vector of lateral deflection at the center of the section concerned,

$\mathbf{G}_j[\ldots]$ is the vector function of iteration.

The equations for convergence are:

$$\frac{|\varepsilon_{ec0}(j+1)-\varepsilon_{ec0}(j)|}{|\varepsilon_{ec0}(j)|}\leq 10^{-3} \tag{3.67}$$

$$\frac{|\phi_x(j+1)-\phi_x(j)|}{|\phi_x(j)|}\leq 10^{-3} \tag{3.68}$$

$$\frac{|\phi_x(j+1)-\phi_x(j)|}{|\phi_x(j)|}\leq 10^{-3} \tag{3.69}$$

Under each grade of load actions $\mathbf{P}_i(e_x,e_y,t)$, the convergence of the lateral deflection curves controls the second round iteration cycle procedure. The k+1 th round of iteration solution of deflection vector can be expressed as follows:

$$\mathbf{U}_{k+1}(u,v)=\Phi_k[\mathbf{U}_k(u,v),\mathbf{P}_i(e_x,e_y,t)] \tag{3.70}$$

$\Phi_k[\ldots]$ is the vector function of iteration.

The equations for convergence are:

$$\frac{|v(k+1)-v(k)|}{|v(k)|}\leq 3\text{x}10^{-3} \tag{3.71}$$

$$\frac{|u(k+1)-u(k)|}{|u(k)|}\leq 3\text{x}10^{-3} \tag{3.72}$$

3.5 Limitations of Proposed Analytical Model

In this study, there are some limitations to the application of the proposed analytical model due to the following reasons:

1. The constitutive law of concrete used in this model is originally generated from the study of unconfined NSC by Hognested (Wang et al., 1985), and modified by Park et al. (1975) in research of confined NSC plus some specimens of HSC. It is one of many approaches to establish a unified formula for both NSC and HSC in this field. Since there is a big difference in the strain and stress relationships between NSC and HSC, this formula modified by Park et al. (1975) might not work quite well with HSC as it with NSC. Therefore, for the analysis of columns made of HSC, further studies are still needed to study the suitability of Park et al's formula and other constitutive laws of concrete describe HSC.
2. As the ACI 209-92R models have not included the studies of time dependent properties of HSC, thus the CEB-FIP mode code 90 is used here to estimate the creep ultimate creep coefficient for HSC columns. Same efforts are made for considering the creep effects on the concrete with high compressive stress level and the development of strength with time under sustained loads (see Chapter 2.3.2 for more details). Since the models of ACI and CEB-FIP are established separately, it should be very careful when using them in some situations (see Chapter 4.3 for more discussions about the selection of the ultimate creep coefficient value).
3. During the derivation process (Green integral transformation), the concrete is assumed as continues uniformed medium. It is a simplified approach to the practical situation. The practical situation is that the concrete in core is confined by stirrups

while the rest outside the stirrups is unconfined. As the concrete constitutive laws for the two different concrete areas are different, it needs special judgment before an analysis to assume one equivalent concrete constitutive law representing for the entire cross section. An alternative approach is to make Green integral transformation to the two concrete zones with different concrete constitutive laws separately. Then, a new set of derivative equations would need to be set up.

4. In this model, the creep of reinforcement or reinforcement relaxation has been neglected. This is due to the facts that, first, for the normal reinforcement at room temperature the reinforcement of creep or relaxation is much lower as compared with concrete creep (less than 4.5% for high stress leveled ($0.9\sigma_y$) reinforcement relaxation in 1000 hours to 50% creep for concrete during the same time). Second, the development of creep or relaxation of reinforcement is much faster than that of creep (Wang et al., 1985). Third, during most of sustained period the reinforcement stress level in a slender column is not at high level until the column fails. Since low level of stress develops low level of creep or relaxation (Wang et al., 1985), the creep or relaxation of reinforcement could be neglected. As for the situation of using high strength reinforcement and or sustained high stress level in reinforcement such as situation in pre-stressed concrete, the relaxation of reinforcement might need to be considered.
5. The Proposed analytical model experiences convergence difficulty when the lateral displacement of a slender column becomes very large.

CHAPTER 4

TEST DATA VERIFICATION

4.1 Slender Column under Sustained Uni-axial Bending Loads (NSC, HSC)

4.1.1 Test Data from Goyal et al. (NSC)

Goyal et al. (1971) performed a total of 46 slender column specimens, 20 of which were subjected uni-axial bending under sustained loads, while other specimens were short – term loaded. See Figure 4.1, Tables 4.1 & 4.2, for concrete column details, concrete aggregate grading and ultimate loads information.

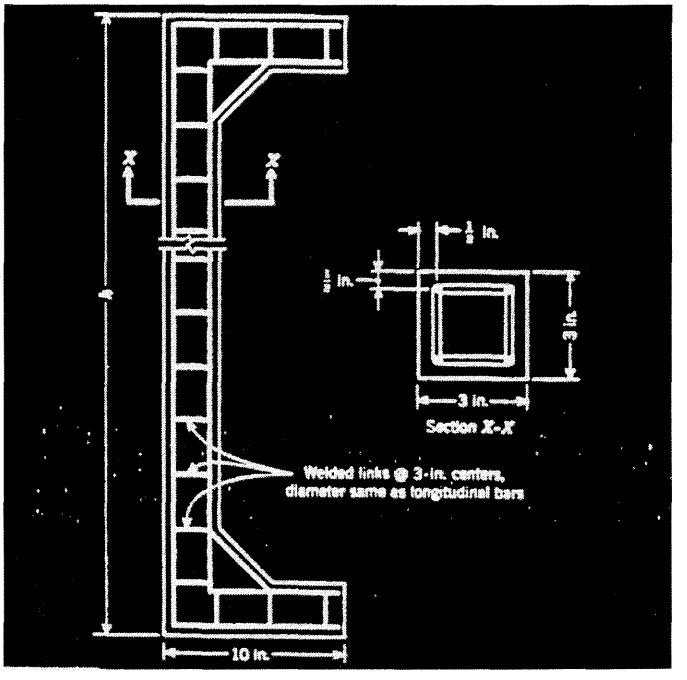

Figure 4.1 Reinforcement Details of Goyal et al. (1971)

The specimens were casted and cured at a temperature of 20±1°C with a relative humidity of 45~60% and tested at 28 days of age.

Table 4.1 Aggregate Grading of Goyal et al.'s Experiment (1971)

Sieve size						
(1)	(2)	(3)	(4)	(5)	(6)	(7)
3/8 in.	3/16 in.	No. 7	No. 14	No. 25	No. 52	No. 100
100[a]	45[a]	33[a]	26[a]	19[a]	8[a]	1[a]

[a] Percentage passing.

Table 4.2 Column Details and Ultimate Loads

Table 4-1 Column Detais and Ultimate Loads

Column Reference	e/h	Klu/h	fc'	fy	Total area of longitudinal reinforcement	Sustained load	Loading duration (days)	Maximum load after sustained loading (test)	Maximum load after sustained loading (analysis)	Maximum load of short term test specimen at 28 days of conc age
(1)	(2)	(3)	(4)	(5)	(6)	(7)	(8)	(9)	(10)	(11)
G (uni)	0.25	24	4,540 psi	51 ksi	0.22 sqi	7.5 kps	208	11.26 kips	11.25 kips	12.19 kips
H (uni)	0.25	24	4,540 psi	51 ksi	0.22 sqi	5.0 kips	208	11.20 kips	11.0 kips	12.19 kips
R (uni)	0.167	36	4,350 psi	45 ksi	0.154 sqi	4.5 kips	208	5.41 kips	5.46 kips	7.26 kips
D-2-A (uni)	0.2	31.2	4,230 psi	56 ksi	0.785 sqi	30 kips	83	30 kips	30 kips	39.2 kips
B-2-A (bi)	0.2/45d	31.2	3,670 psi	56 ksi	0.785 sqi	19.2 kips	728	30.3 kips	25.01 kips	36.2 kips
B-3-B (bi)	0.2/45d	31.2	3,780 psi	56 ksi	0.785 sqi	23 kips	631	23 kips	23 kips	36.8 kips
H201 (uni)	0.2	20	92.3 Mpa	636 Mpa	804 sqmm	1110 KN	203	1367 KN	1409KN	2360 KN *
			13,384 psi	92.2 ksi	1.246 sqi	249.5 kips	203	307.3 kips	316.7 kips	530.5 kips

* Loaded at 203 days of concrete age
G, H, & R tested by Goyal at el.
D-2-A, B-2-A, & B-3-B tested by Drysdal at el.
H201 tested by Claeson at el.

Creep tests were also carried out in the same environmental conditions. The creep test results are shown in Figure 4.2. Where, γ = creep strain/ initial elastic strain, with a maximum value of 2.4 at end of 5000 hours of sustained loading duration.

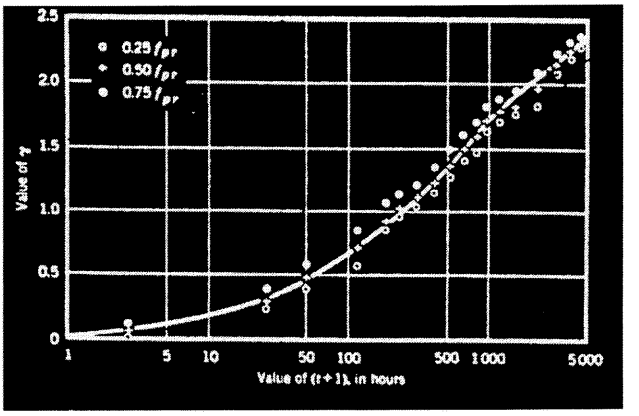

Figure 4.2 Variation of γ with Time at Different Stress Levels (Goyal et al., 1971)

Specimens R, H & G are subjected to ui-axial sustained loading for 5000 Hours (208.333 days) and failed under additional instant load after that. The eccentricity is 0.5 inch at top and bottom. From Table 4.1, the predicted short-term capacity for R is 7.5 kips, for G 12.45 kips and for H 11.92 kips. The constant sustained load for R equals 4.5 kips, for G 7.5 kips and for H 5.0 kips. Thus, the ratio of sustained load/short term load capacity for R, 0.6; for G, 0.6 and for H, 0.42.

Per ACI-209, one has: v_u=1.54; r_{sh}=2.44x10e-4

Per CEB-FIP 90 Model: $\varnothing_0$=3.26; ε_{cs0}=1.15x10e-4;

From the companion creep test (Figure 4.2), the ultimate creep coefficient can be derived as:

$$v_u = \frac{v_t(10 + t^{0.6})}{t^{0.6}} \tag{4.1}$$

Substitute t=208, v_t= 2.40 into Eq.(4.1):

v_u=3.375

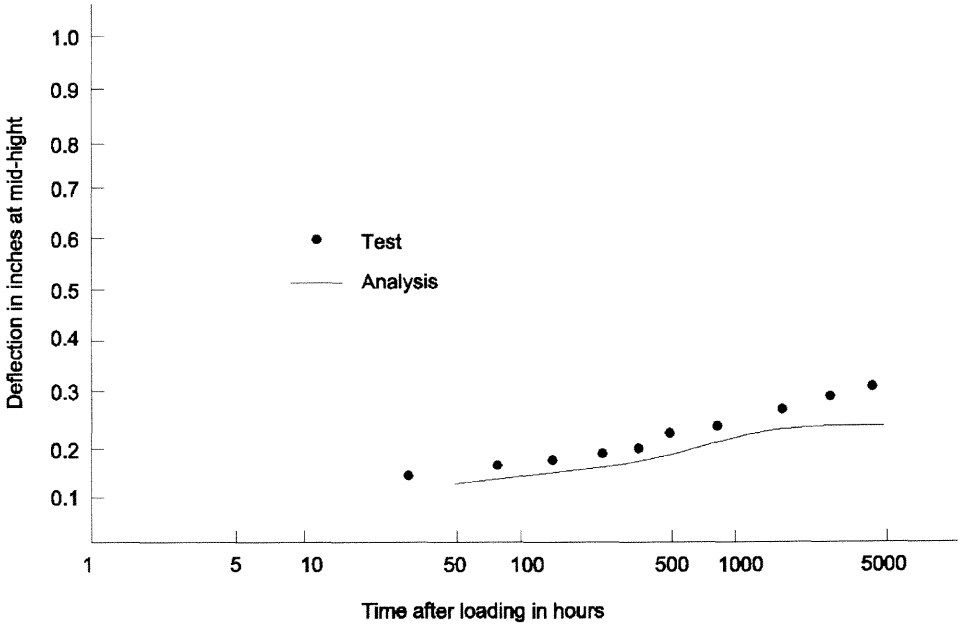

Figure 4.3a Deflection-time Curve of Column H

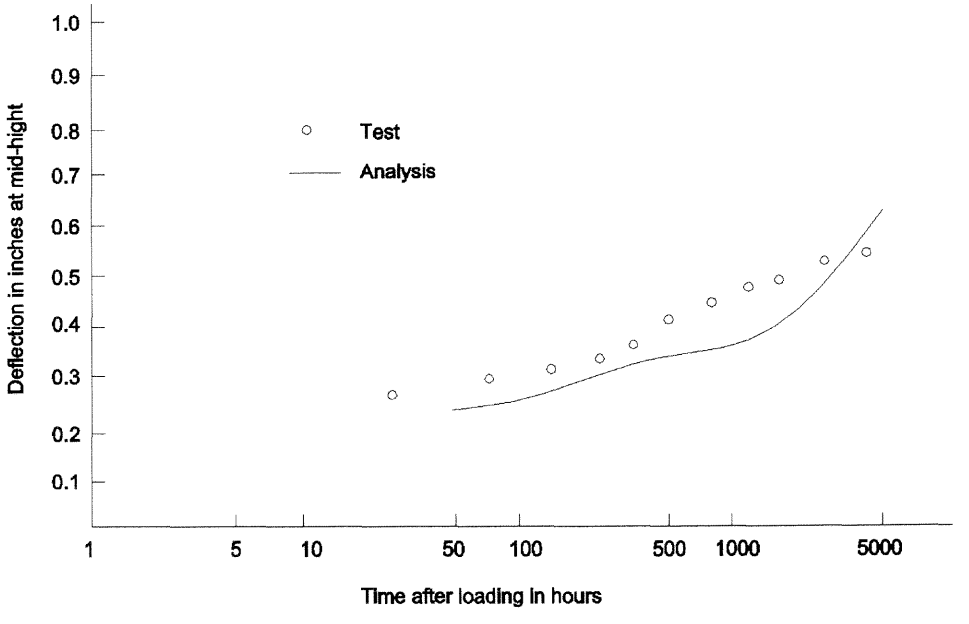

Figure 4.3b Deflection-time Curve of Column G

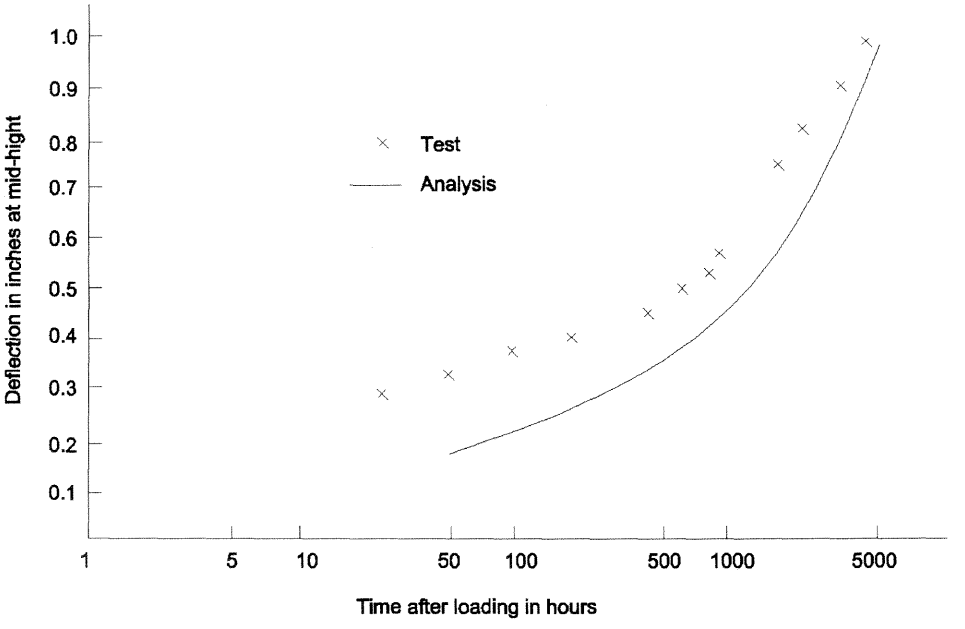

Figure 4.3c Deflection-time Curve of Column R

From Figures 4.3a, b & c, the results of analysis using ACI-209 Model with v_u=3.375, conform with the test data well. Except for deflection values of Column G at 5000 hours, the data of test are always larger than those of analysis. It might imply a modified factor to compensate the differences between test and analysis of all columns.

4.1.2 Test Data from Drysdale et al. (NSC)

Drysdale et al. (1971) completed their experiments of sustained uni-axial and biaxial loads on slender concrete columns in the Department of Civil Engineering, University of Toronto. Of the test, eight specimens were subjected to sustained uni-axial bending loads. See Section 4.2. for more information about the experimental program.

D-2-A is a specimen subjected to uni-axial sustained loading for 83 days until failure. The eccentricity is 1-in at X axis. From Table 4-1, the short-term test capacity is

39.9 kips, the constant sustained load equals 30 kips. Thus, ratio of sustained load/load capacity = 0.75

Per ACI-209, one has: v_u=1.98, r_{sh}=7.02x10e-4

Per CEB-FIP 90 Model: ϕ_u=3.10, ε_{cs0}=6.47x10e-4

Per creep test (see Section 4.2): v_u=3.51

From Figures 4.4a & b, the results of analysis using ACI-209 92 Model with v_u=3.62 agree with the data except the results of deflection curves at 80 days of loading. Since the column fails at 83 days, the difference between test and analysis becomes larger at 80 days of loading.

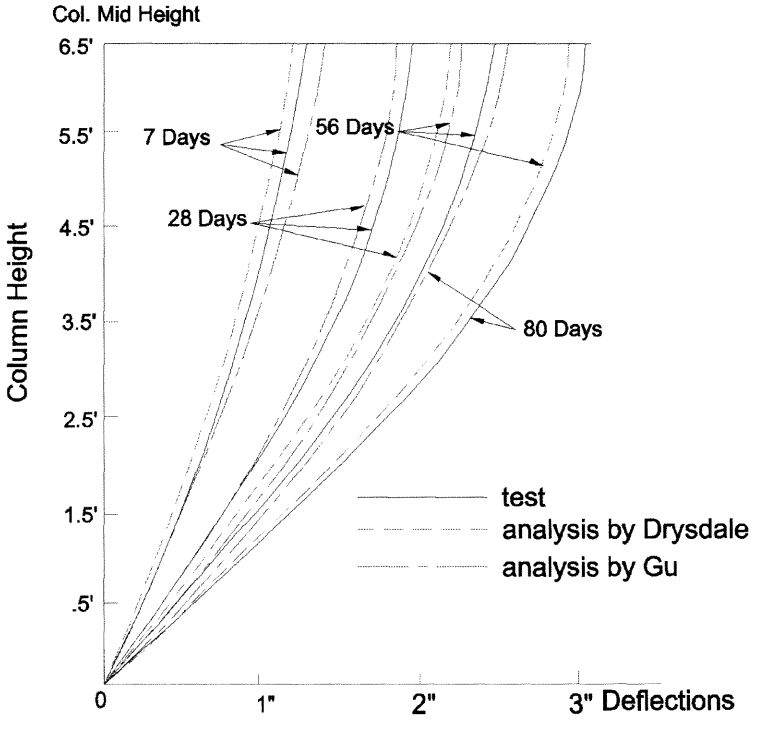

Figure 4.4a Deflection Results of D-2-A

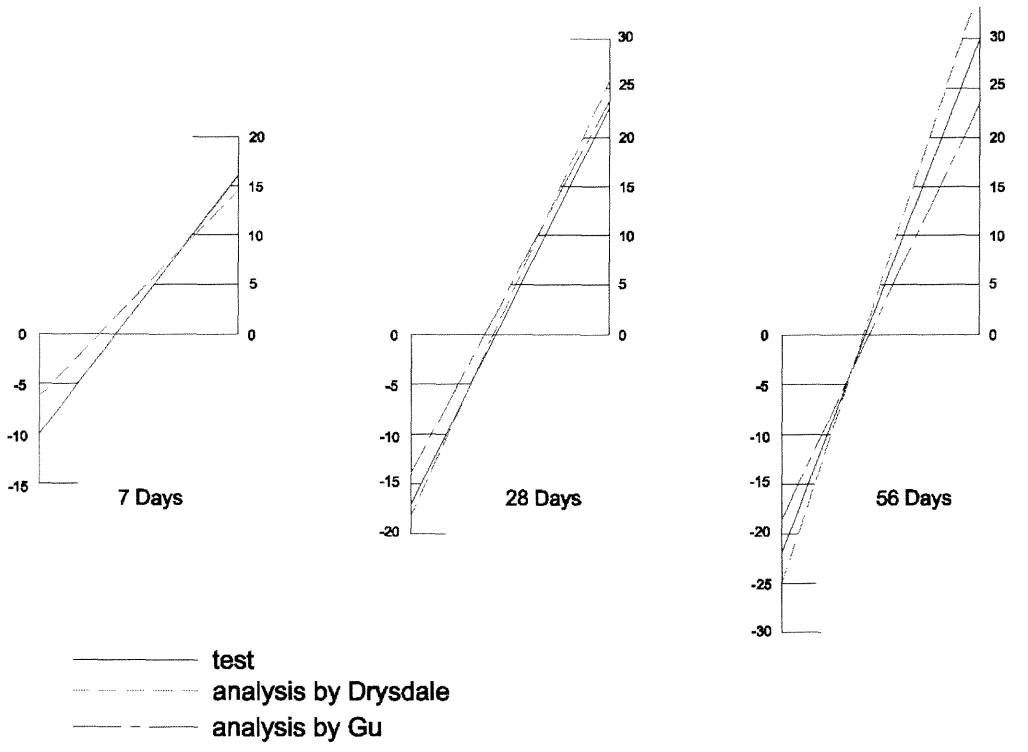

Figure 4.4b Strain Diagrams of D-2-A (strain unit: $1x10^{-4}$)

4.1.3 Test Data from Claeson et al. (HSC)

Claeson and Gylltoft (2000) performed 6 slender columns subjected to uni-axial bending load. One of the specimens was made of HSC and subjected to sustained load. Figures 4.5 and 4.6 present the details of columns and test equipment. In Table 4.4, $f_{c,cyl}$ and $f_{c,cube}$ refer to compressive strengths on compression tests of sizes ø150x300 mm and 150x150x150 mm, respectively and $f_{c,prism}$ refers to compressive strength on compression test of 200x200x800 specimen.

Deformed bars of ø16 used as longitudinal reinforcement, were made of Swedish Type Ks60s with yield strength 636 MPa, hardening strain 36‰, ultimate strength 721 MPa, ultimate strain 142‰, and modulus of elasticity 221 GPa. While those of ø8 used as stirrups, wree made of Swedish Type Ks40s with yield strength 466, hardening strain

22‰, ultimate strength 636 MPa, ultimate strain 87‰, and modulus of elasticity 207 GPa.

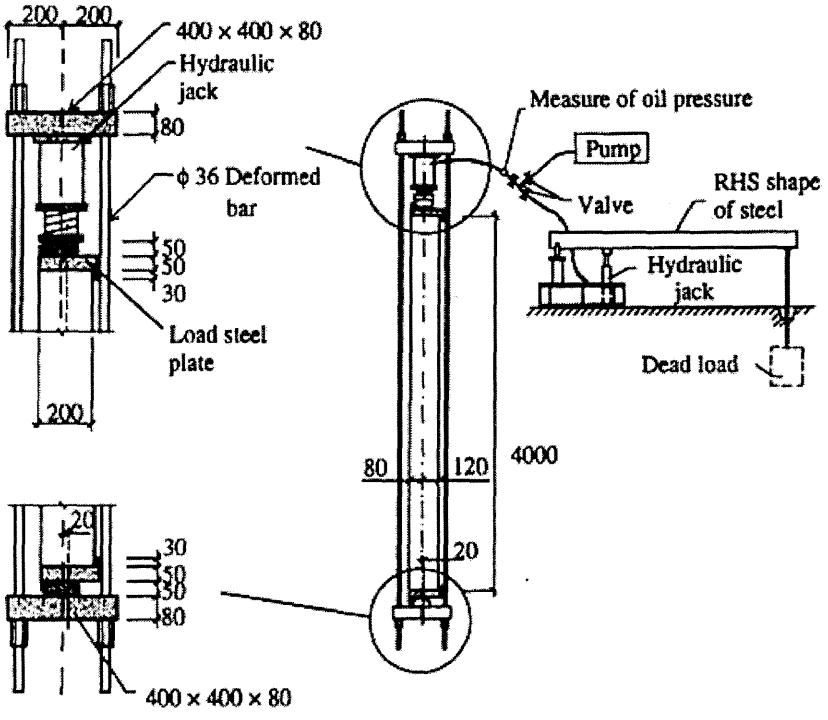

Figure 4.5 Details of Columns and Test Equipment in Claeson et al.'s Experiment (Cleason et al., 2000) (Unit: mm)

Plastic sheeting was used to covere the columns in the first day after pouring. Then the molds were removed and the columns were cured under the lab room conditions (18±2°C) and RH=30% for next 27 days. During sustained loading, the environment conditions were unchanged.

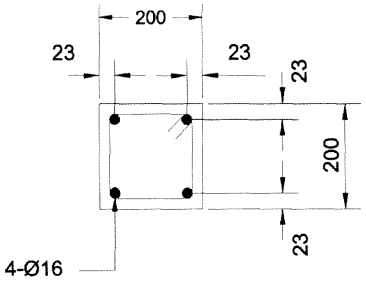

(Unit: mm)

Figure 4.6 Details of Reinforcement in Claeson et al.'s Experiment

Per CEB-FIP 90: $\varnothing_0$=1.90

Per ACI-209: v_u=2.06

Table 4.3 Composite of Concrete Mixtures, kg/m^3 (Claeson et al., 2000)

Concrete	NSC	HSC
Water	189	156
Cement	370	500
Silica fume	—	50
Natural sand	980	954
Crushed stone (gneiss) 8/12	—	799
Crushed stone (gneiss) 8/16	870	—
Superplasticizer (F92)	—	13
Density (28 days)	2403	2500

Table 4.4 Hardened Concrete Properties at Different ages for Each Concrete Strength (Claeson et al., 2000)

Concrete	Age, days	$f_{c,cube}$, MPa	$f_{c,cyl}$, MPa	$f_{t,split}$, MPa	$f_{c,prism}$, MPa	E_c, GPa
HSC	28	111.9	92.3	6.8	—	43[†]
HSC	113	118.8	102.9	7.2	—	—
HSC	203	118.4	107.0	—	83[†]	—

*Strength values are mean average of three specimens unless otherwise noted.
†Average of two specimens.

Since the specimens have been cured for just one day, the creep would be larger than those of the specimens with normal curing process, which are 3 days of steamed curing or 7 days of moist curing. It is difficult to make this adjustment of the ultimate creep coefficient values calculated from ACI or CEB-FIP. From Figure 4.7, it shows, Except the at 23 days of loading, the results of analysis with v_u =2.50 match with the data of test specimen H201 quite well.

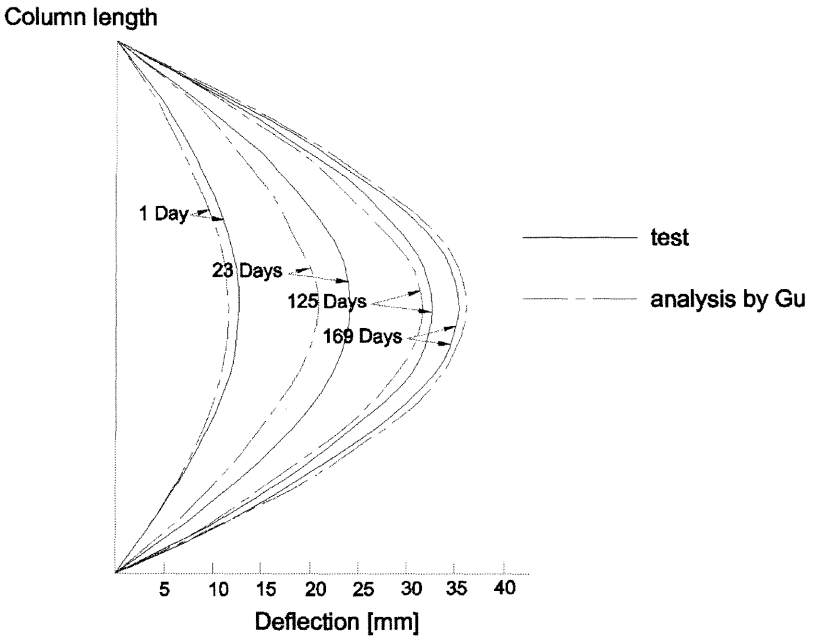

Figure 4.7 Deflection Results of H201

4.2 Slender Columns Under Sustained Bi-axial Bending Loads

4.2.1 Test Specimens

Drysdale et al. (1971) performed an experimental program of sustained biaxial load on slender concrete columns. There were totally 58 test specimens being tested in this program. All specimens were the same in column dimension, reinforcing, concrete strength design, pouring and curing conditions. See Figure 4.8 for the information of test column dimension and reinforcing.

The following factors were influenced in design of the specimens:

1. Make the scale as large as possible to reduce the size effects.
2. Columns were pinned loaded at both ends with the same eccentricities to provide a simple and reliable test method.

3. High slenderness ratio was chosen to enlarge creep effects to the total column deformations.
4. A square cross section with symmetric reinforcing was chosen to make orientation of eccentricity selection as less as possible.

Concrete: A standardized mix for a 28 days compressive strength of 4000 psi was used for all. The mix proportions by weight were: Portland Cement Type I-14%, Water-9.1%, Sand-46.6%, 3/8" in. crushed limestone-30.8%. A slump of 2~3 in. was obtained. All tests were loaded at 28 days age of concrete. Instant load tests were completed the same day while sustained load specimens were subjected under load and along with control prisms and cylinders in a temperature (75±1°F) and humidity (50±2%) controlled tent. Standard 6-in. diameter by 12-in. high cylinders and 5-in. by 5-in. by10-in. prisms were used to determine the concrete stress–strain relationship.

For shrinkage measurement, 16-in. long plain concrete prisms, with 5-in. by 5-in. cross sections containing identical reinforcement, were cast with each group. For creep in concrete, some 32-in. long creep prisms with 5-in. square cross sections were cast with some of the early groups of columns. At age of 28 days, the prisms were subjected under concentric axial load in the same temperature and humidity-controlled tent. Figure 4.9 shows creep test results of this experiment.

Per both ACI and CEB-FIP, the linear creep models are only applied to concrete stress $\leq 0.4 f_c'$. It is noticed that, when $\frac{f_c}{f_c'}$=0.41 at 200 days after loading, the creep strain $\approx 1150 \times 10^{-6}$. Applying Eq. (4.1), one has v_u=3.51.

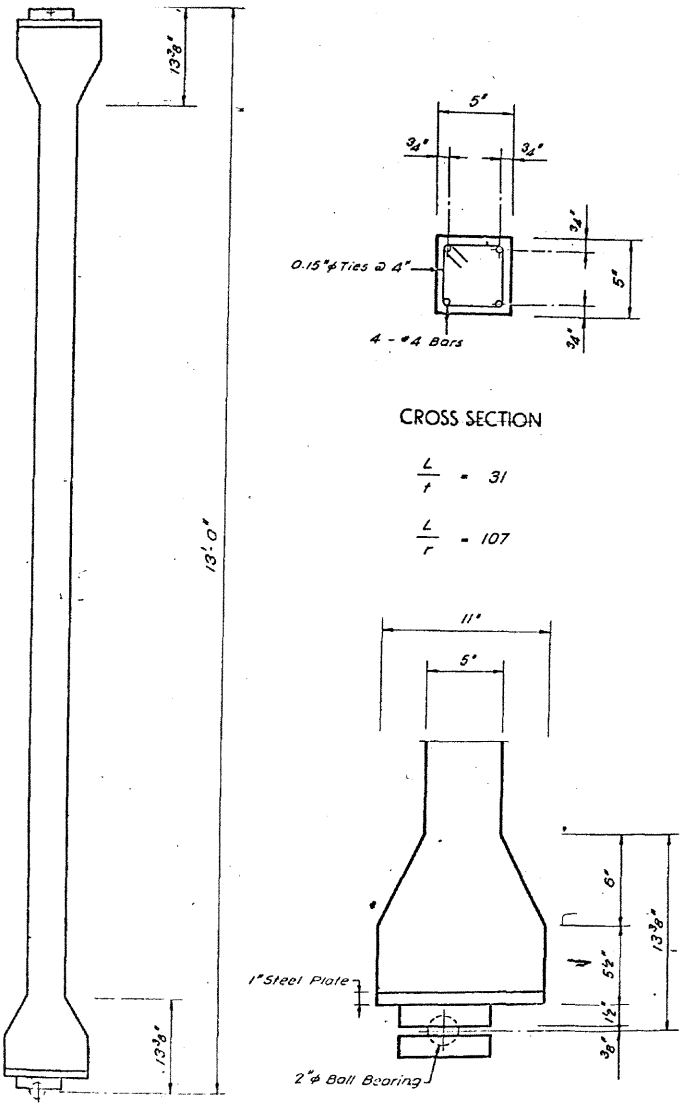

Figure 4.8 Column Details of Specimens in Drysdale et al.'s Experiment (Dysdale, 1967)

4.2.2 Test procedure and Equipment

1. *Loading Sequences*:

The following loading sequences were designed for the experimental tests.

(1) Short term loading to failure at concrete age of 28 days;

(2) Constant sustained loading from 28 days of age to failure;

(3) For those in (2) not failed for 2 years, unloaded sustained loads and replaced instant loading until failure.

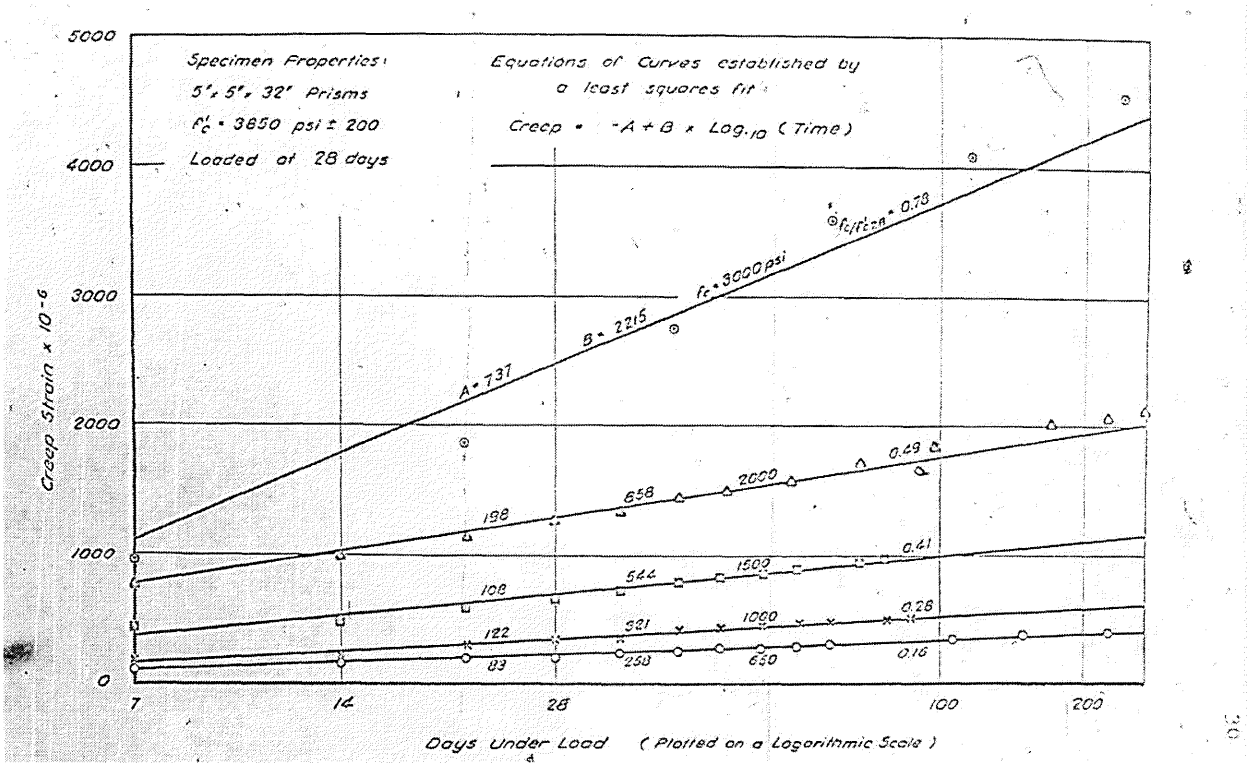

Figure 4.9 Creep Test Results from Drysdale et al.'s Experiment (Drysdale, 1967)

All tests were performed in identical pairs in order to guaranty the quality of test data. The columns are classified by Test series according to the end eccentricities, e.

Series A (data ruined) and B, using e=1.00 in at 45 degree from X axis;

Series C, using e=1.00 in at 22.5 degree from X axis;

Series D, using e=1.00 in along X axis;

Series E, using e=1.50 in at 22.5 degree from X axis;

Series F, using e=0.50 in at 22.5 degree from X axis;

See Table 4.2 for the summary of test and analysis results for column test series.

2. *Strain Measurement*:

Demec mechanical gage (8 in. gage length) points were attached on all sides at five points spaced over the column length. The accuracy of the Demec mechanical strain indicator is 1x10e-5 in/in.

3. *Deflection Measurement*:

A deflection measurement instrument was used with triangulation to determine the position at various levels.

4. *Test Equipment*:

Short-term load test: 1200 kip capacity, hydraulically operated Baldwin Testing Machine. Sustained load test: A specially designed loading platform was used.

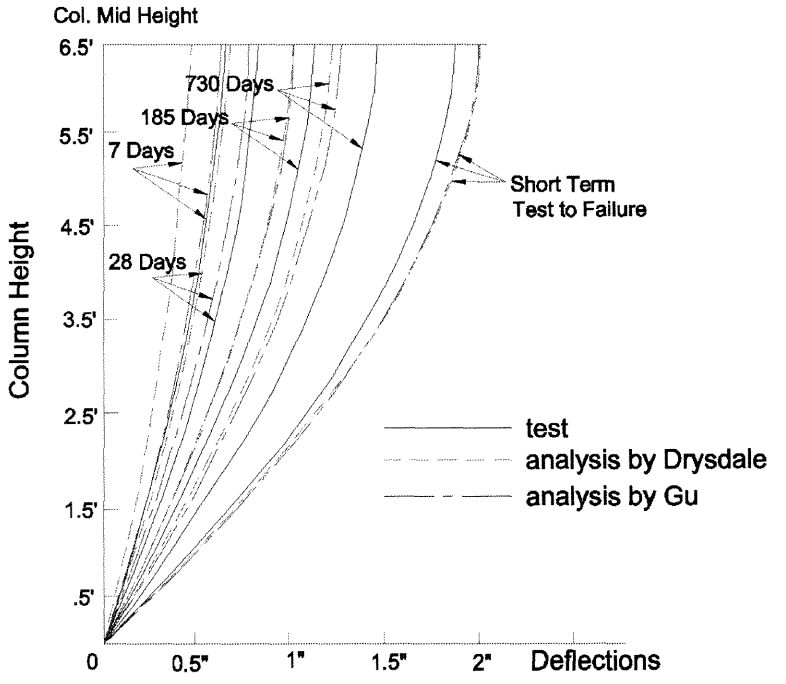

Figure 4.10a Deflection Results of B-2-A

4.2.3 Comparison of Test Results with Numerical Analysis

1. *Test of Specimen B-2-A*:

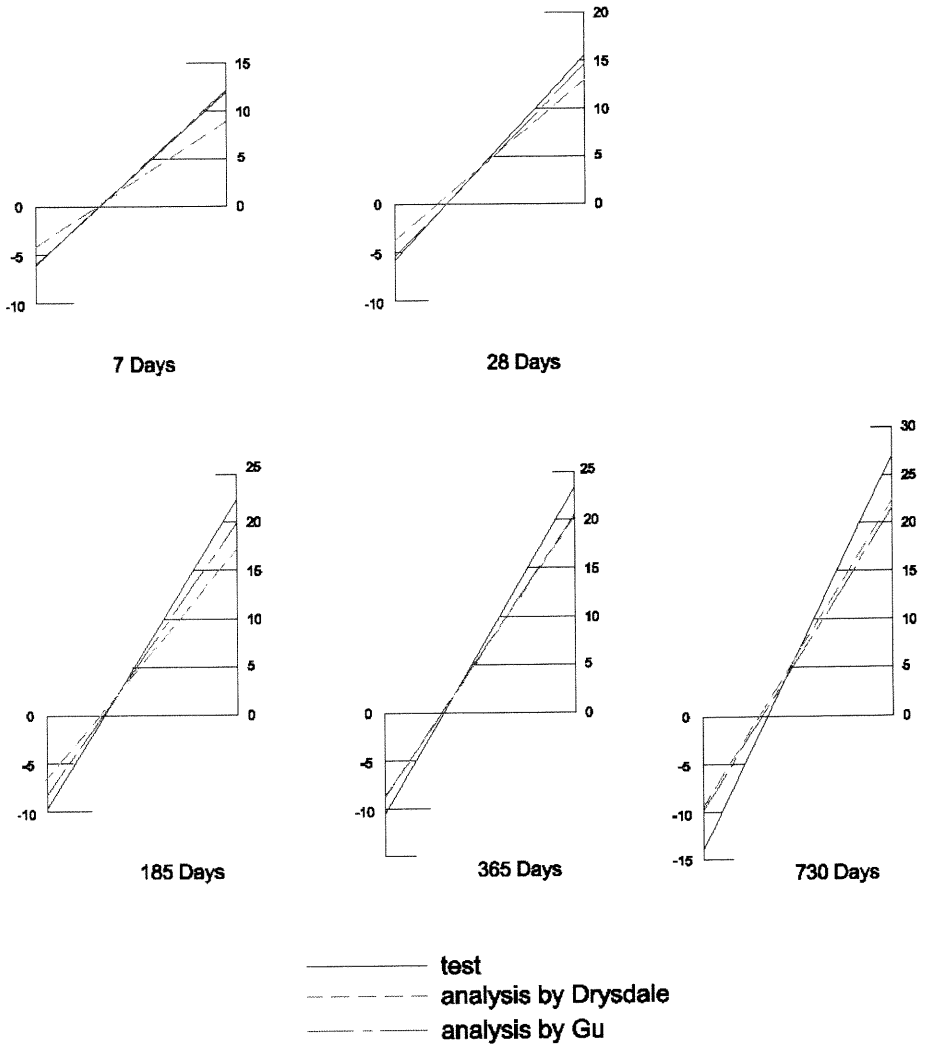

Figure 4.10b Strain Diagrams of B-2-A (strain unit: $1x10^{-4}$)

Column B-2-A was a specimen subjected to biaxial sustained loading for 730 days and failed under an additional instant load. The eccentricity is 1-in at 45 degree from X-axis. From Table 4.2, the predicted short-term capacity is 36.2 kips, the constant sustained load equals 19.2~18.2 kips.

Although ACI-209-92R model is used to perform the sustained load analysis, it is still very important to choose a proper ultimate creep coefficient for the computer analysis program.

Using all original input data for ACI-209-92R Model, one has:

v_u=1.98, r_{sh}=7.02x10e-4;

Per CEB-FIP 90 Model: $ø_0$=3.62, ε_{cs0}=6.47x10e-4.

Per creep test: v_u=3.51

From Figures 4.10a and b, the analysis using ACI-209 Model with v_u=3.51 does not agree with test well when time of loading is over 185 days of loading.

Test of Specimen B-3-B:

Column B-3-B was a specimen subjected to biaxial sustained loading for 631 days and failed under an additional instant load. The eccentricity is 1-in at 45 degree from X axis. From Table 4.2, the predicted short-term capacity is 36.8 kips, the constant sustained load equals 23 kips. Thus, ratio of sustained load/load capacity = 0.625.

Per ACI-209: v_u=1.98, r_{sh}=7.02x10e-4;

Per CEB-FIP 90 Model: $ø_0$=3.33, ε_{cs0}=6.47x10e-4

Per creep test: v_u=3.51

From Figure 4.11 the results of analysis using ACI-209-92R Model with v_u=3.51 agrees with those data of test well.

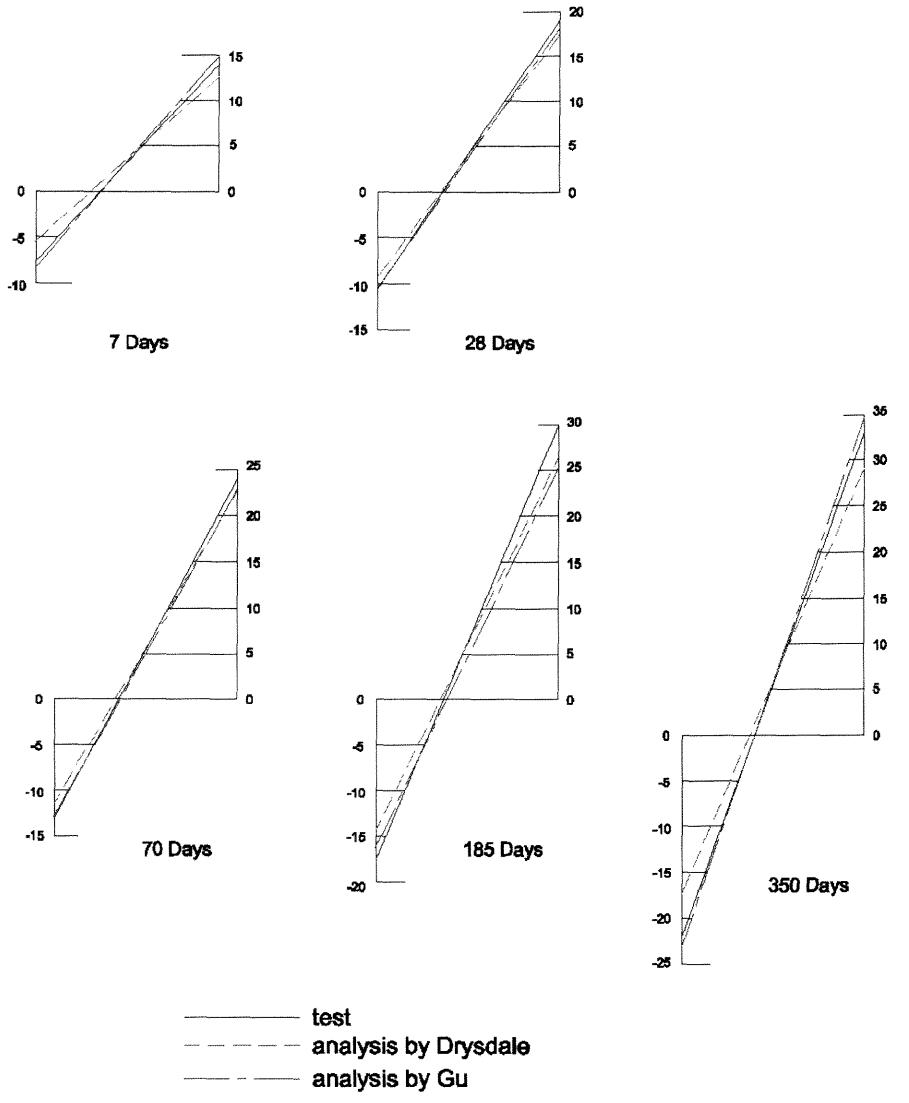

Figure 4.11 Strain Diagrams of B-3-B (strain unit: $1x10^{-4}$)

Figures 4.12 and 4.13 display the maximum concrete elastic strain history at mid-column cross section. The test points in the figures are obtained from the recorded concrete total strains minus the nominal creep strain values recorded from the companion creep tests. The analysis in both figures do not agree with tests as well as other comparisons as shown above, since the creep values are more complicated than what they appear.

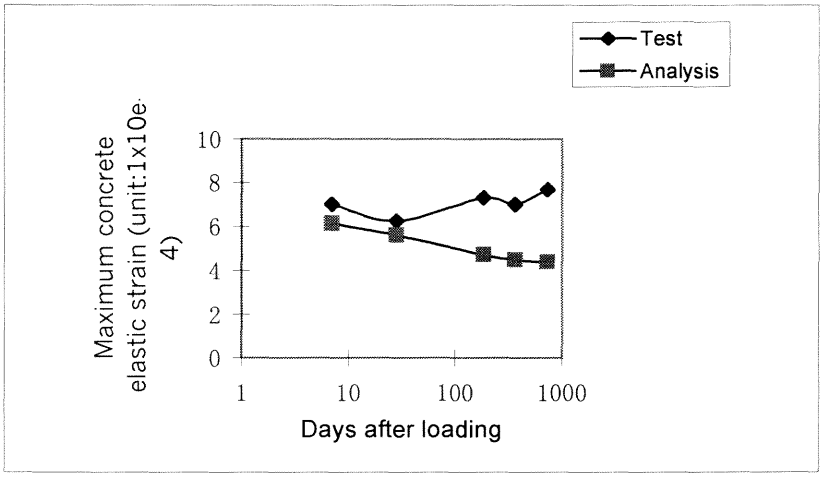

Figure 4.12 Concrete Maximum Elastic Strain History of B-2-A

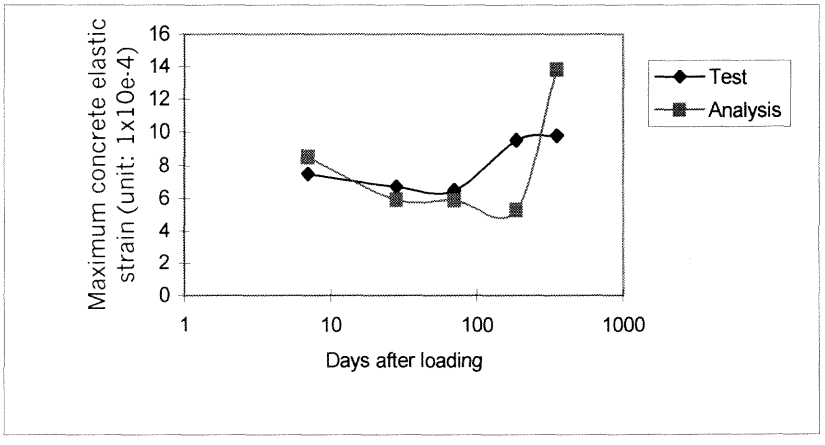

Figure 4.13 Concrete Maximum Elastic Strain History of B-3-B

According to Figures 4.12 and 4.13, both tests and analysis results show that the maximum concrete elastic compressive strain at mid-column cross sections normally experiences a drop process due to the stress redistribution to longitudinal reinforcement

during the sustained loading period. There is a possibility that the elastic strain becomes increased (Figure 4.13) while the total deflection keeps increasing.

4.3 Discussions of Selection of Ultimate Creep Coefficient Values

The most important step for an analysis to become successful is to get the right ultimate creep coefficient value, v_u of ACI 209-92R Models or the notional creep coefficient value, $\varnothing_0$ of CEB-FIP Model Code 1990. They are very critical and sensitive to the theoretical results. In those data verification examples, the test data from the companion creep tests are used for the analysis. Those values are normally close to the numbers from CEB-FIP Model Code 1990 than ACI 209-92R Models. It shows the analysis results due to using the ultimate Creep Coefficients from the experiments are satisfied. The reasons are probably due to:

1. The scales of the experimental specimens are relatively smaller than those used in practical engineering projects. For concrete creep, the smaller the specimen dimension is, the larger the creep would happen. It seems that the ACI specifications are established from the specimens tested with relatively larger scale, thus the ultimate coefficients calculated per ACI-129 92R Model are comparatively smaller. In CEB-FIP Model Code 1990, the scales of specimens tested are smaller, thus the dimension effects are larger. The creep coefficients per CEB-FIP are more suitable for small-scale test specimens. Since the specimens in those slender RC column tests are in small scale. Thus, CEB-FIP Model Code 1990 describes the creep behaviors for those test specimens better than ACI 209-92R Models.

2. Concrete creep is a very complicated phenomenon. The current theories are still not sophisticated enough to describe the comprehensive picture of the phenomenon. In ACI-129-92R models, the effects of the concrete strengths have not been included; the calculation for creep under the high concrete stress is not addressed either, which are both included in CEB-FIP 90. On the other hand, CEB-FIP 90 has failed to include effects of concrete slump and air content that is considered by the ACI-129 92R, which might have an impact on the creep development.

CHAPTER 5

DESIGN RECOMMENDATIONS

5.1 Design Examples: Comparison with Current ACI Design Codes

The purpose of this part is to analyze examples and compare with the current ACI building codes. Under uni-axial bending loads, the effects of slenderness, eccentricities, reinforcement ratio and concrete strength will be discussed. Under biaxial bending loads, the effects of the eccentricity orientation and the influence of length over width ratio of cross section will also be studied. To capture typical engineering situations, the value of the ultimate creep coefficient ν_u is assumed to equal to 2.0 and the sustained duration is selected as 30,455 days (83 years). The analysis model is pinned-ended and equally eccentrical at column top and bottom.

5.1.1 Ultimate Strength of Slender Concrete Column under Uni-axial Bending Loads

Figures 5.1, and 5.2 show the column geometric dimension, material information and P-M strength interaction diagram of a cross section.

1. *Effects of slenderness*

There are five theoretical specimens included in this group. Keep the same cross sectional dimensions, longitudinal reinforcement, and concrete strength for all specimens. At strength boundary of M-P diagram, select five different points on the diagram. Let δ_b= 2 for all specimens.

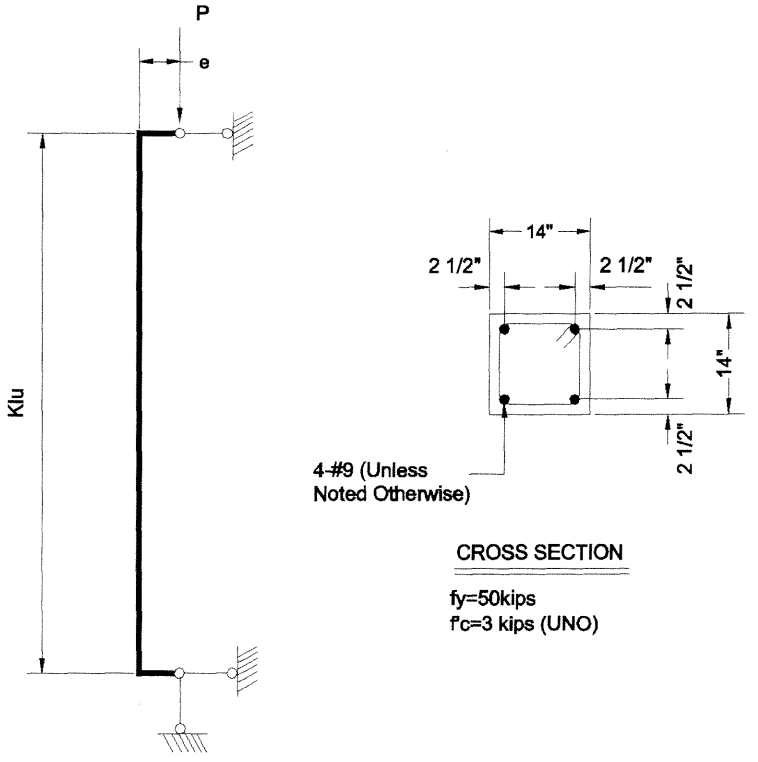

Figure 5.1 Details of Columns in Design Examples

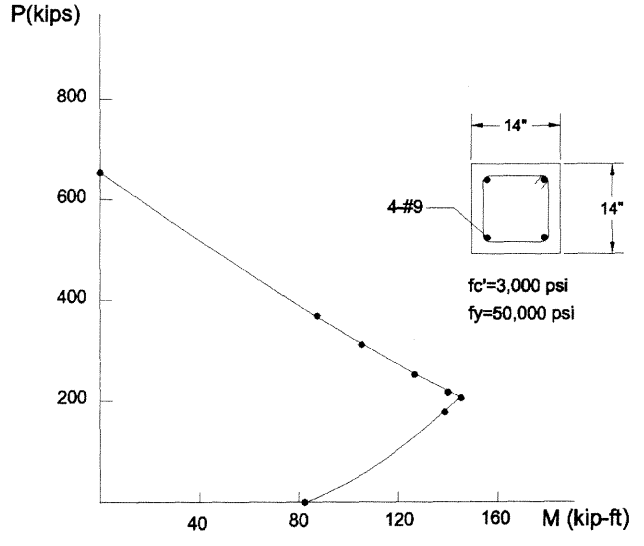

Figure 5.2 Short Column P-M Interaction Diagram

Figure 5.3 shows the results of both computer analysis and ACI-318 99 Building Code. The results show that if columns are relatively shorter, the ultimate strengths under sustained load calculated per ACI code are closer to those from the present computer analysis.

2. Effects of eccentricity

Five other theoretical specimens are included in this group. Keep the same column length, the cross sectional dimensions, longitudinal reinforcement, and concrete strength for all specimens. Select five different (M, P) strength points in the M-P diagram. Thus, all specimens have different loads and eccentricities at the ends of each member.

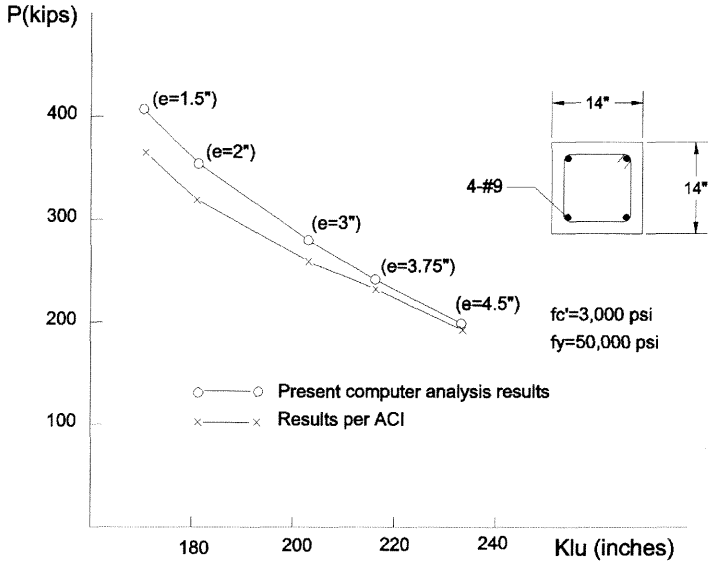

Figure 5.3 Effects of Slenderness

Fig. 5.4 displays the results of analysis from the effects due to eccentricity. It shows that the larger the eccentrically loaded columns is, the less the buckling strength

can be obtained, as per ACI code. This means that the creep influences more to the column loaded with larger eccentricites.

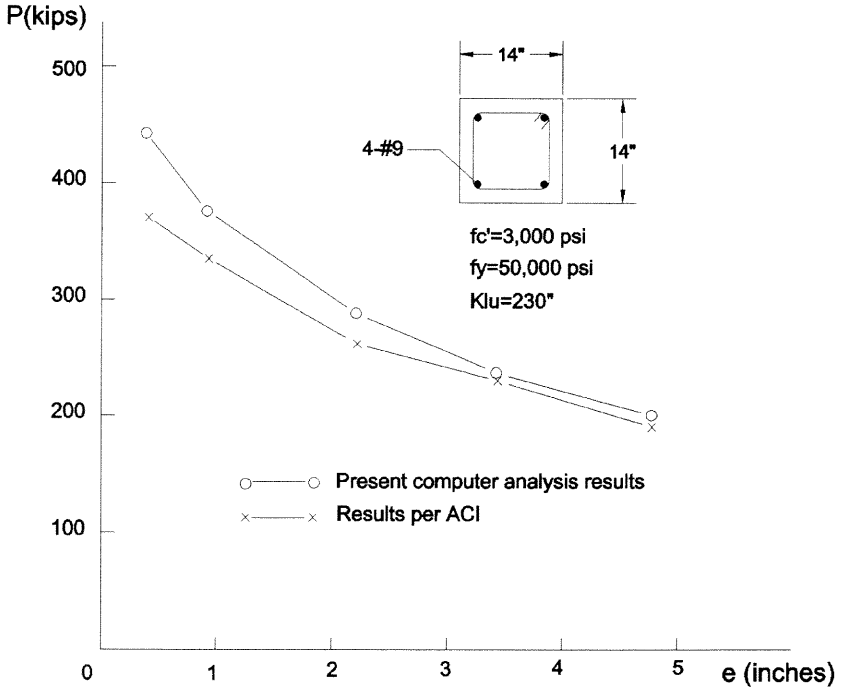

Figure 5.4 Effects of Eccentricities

3. *Effects of reinforcement ratio*

Five theoretical specimens are included in this group. Keep the same length of column, the end eccentricities, the cross sectional dimensions, and concrete strength for all specimens. Select different longitudinal reinforcement ratio for each member.

Figure 5.5 displays the present computer analysis results. It shows that, the lower the longitudinal reinforcement ratios in the columns is, the less buckling strength can be obtained. The results of strength-decreasing rate vs. reinforcement ratio from present analysis are larger than the design method as per ACI building code. This could be explained as: on one hand per ACI building code, when the reinforcement is low enough,

the influence of steel would be neglected by using the concrete stiffness only. On another hand, it reflects the difference between the two methods in accounting for the stiffness of concrete and reinforcement. In ACI building code, the creep reduces the total column stiffness parameter *EI*'s value (see Sections 5.2 and 5.3 for more discussions), while in the present analysis, it only reduces *EI*'s value in the concrete part. Note that the concrete *EI*'s value may be reduced more than that in the ACI building code by using the present computer analysis.

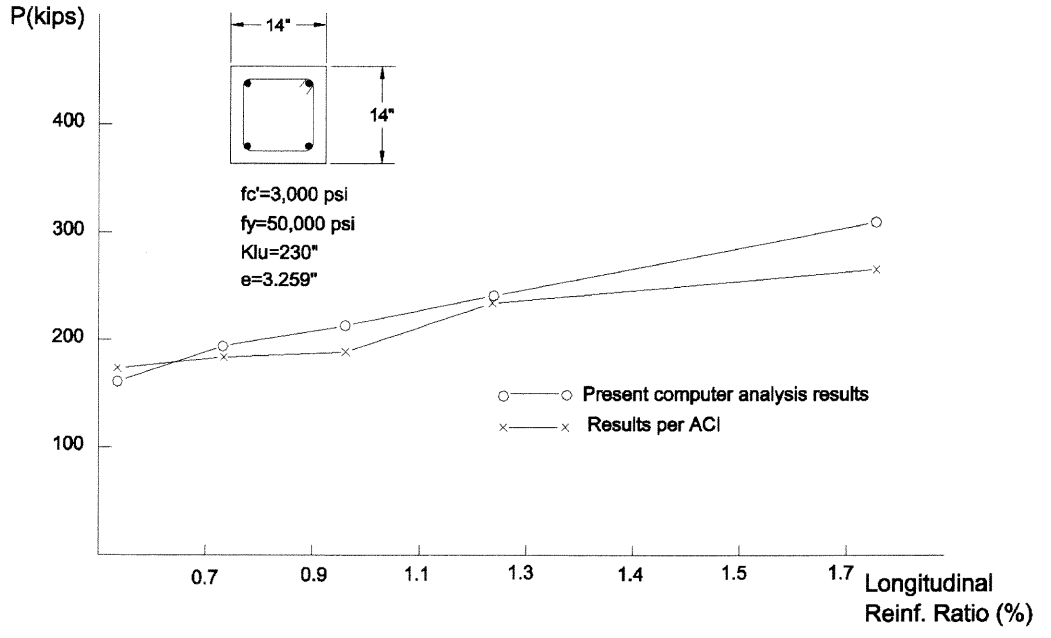

Figure 5.5 Effects of Longitudinal Reinforcement Ratios

4. *Effects of concrete strength*

Five other theoretical specimens are included in this group. Keep the same length of column, the end eccentricities, the cross sectional dimensions, and longitudinal reinforcement for all members. Select different concrete compressive strengths for each column.

Figure 5.6 displays the results of analysis. It shows that, the higher the concrete strength is, the more the load capacities can be obtained. The load capacity increasing rate vs. concrete strength is larger than that designed as per ACI code. This could be explained that, by increasing of concrete strength is equivalent to decreasing the column effective length kL_u. Thus, it increases the Euler capacity of column P_u and reduces the δ_b value.

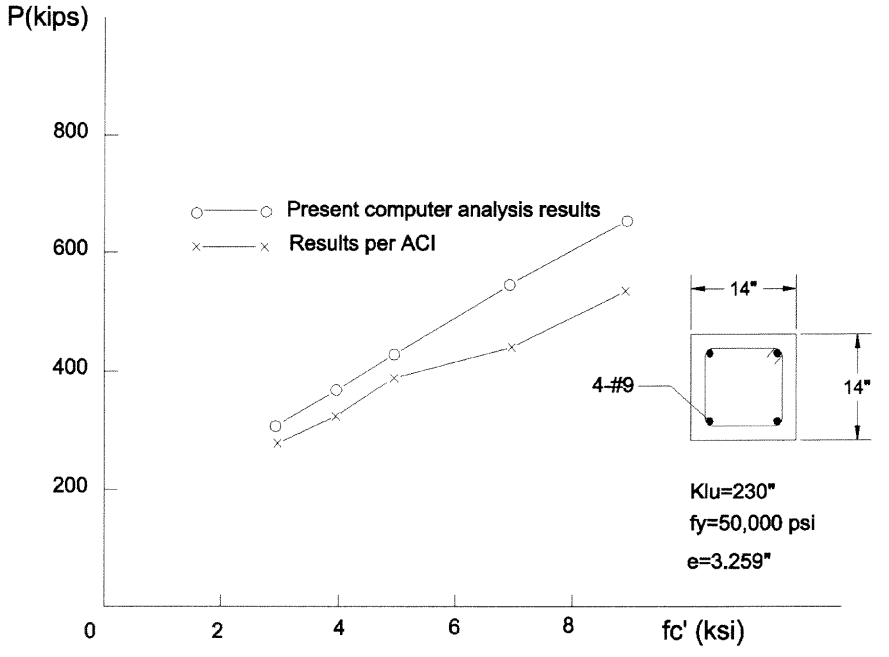

Figure 5.6 Effects of Concrete Compressive Strength

5.1.2 Ultimate Strength of Slender Concrete Column under Bi-axial Bending Loads

1. *Effects of eccentricity orientation of a typical square section column*

Figure 5.7 displays the results of analysis for square NSC columns under bi-axial bending sustained load influenced by different eccentricity orientations. It shows that the load capacities between different orientations are closer than those designed by the

Bresler reciprocal load method, while the variation trends are the same. This could be partly explained that, in Bresler reciprocal load method, bi-axial design method is not consistent with the uni-axial one. Thus, the different capacities between 0 deg. and 11.25 deg. are much larger per Bresler's method than those from the present analysis. Both results show that, the maximum load capacity occurs at 0 degree (the uni-axial case), and the minimum occurs at 45 degree direction.

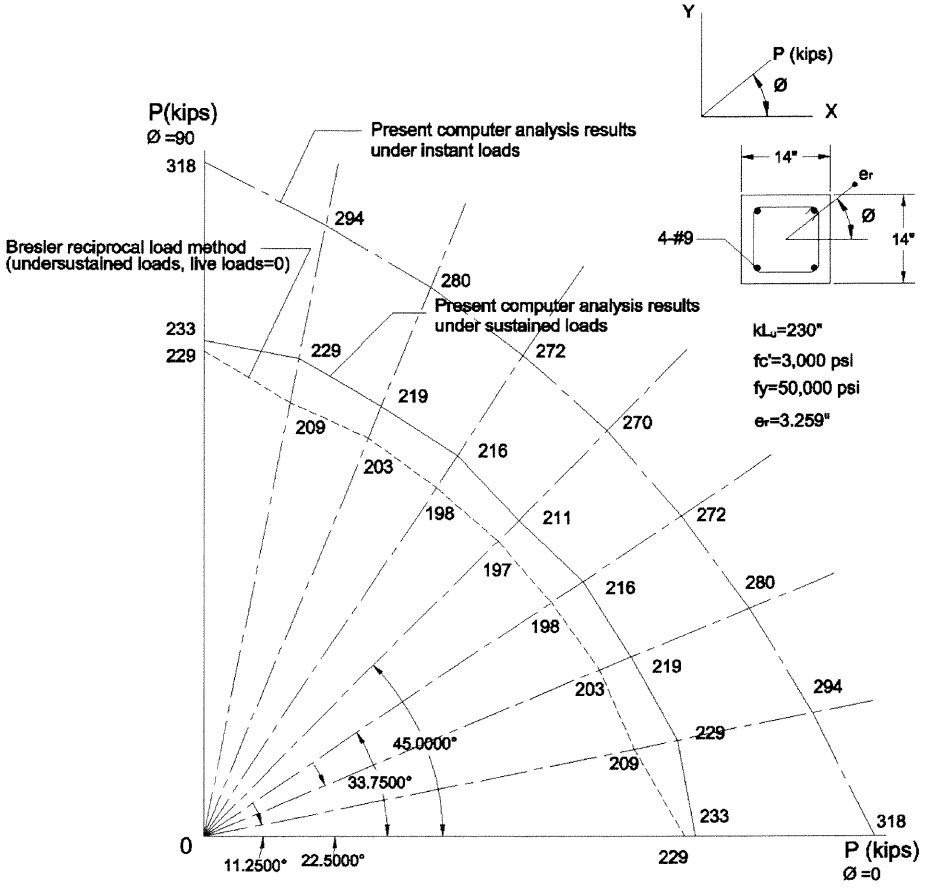

Figure 5.7 Effects of Eccentricity Orientations to Columns with Square Cross Sections

2. *Effects of eccentricity orientation of a typical rectangular section column*

Figure 5.8 displays the results of analysis for rectangular NSC columns under bi-axial bending sustained load influenced by different eccentricity orientations. It shows

that, the variation trends are the same, the maximum load capacity turns out to be at 90 degree (the uni-axial case at strong axis direction), and the minimum is at 0 degree direction. (the uni-axial case at weak axis direction). For biaxial loaded columns, it seems that the Bresler reciprocal load method is conservative as compared to present computer analysis as indicated in Figures 5.7 and 5.8.

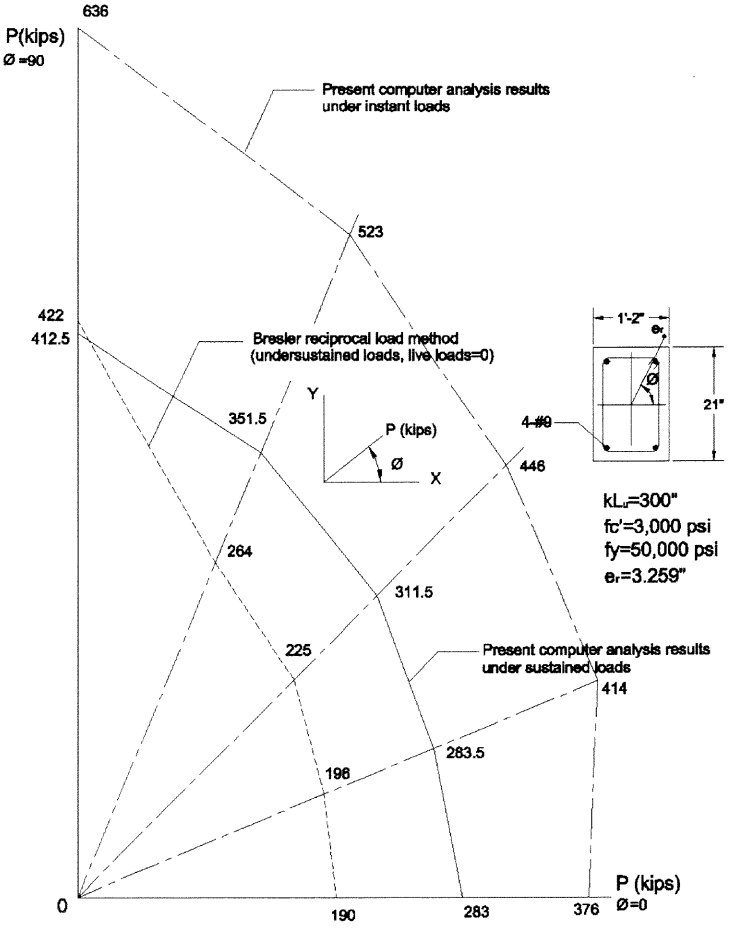

Figure 5.8 Effects of Eccentricity Orientations to Columns with Rectangular Cross Sections

5.2 Mechanism of the RC Column Strength

There are two types of limits in RC column subjected to uni-axial and bi-axial sustained loading: ultimate strength limit and deflection limits.

The ultimate load capacity of a column is reached when its concrete maximum compressive strain reaches concrete crushing strain limit ε_u, which is normally taken as 0.003 for NSC. Theoretically, there is a difference between uni-axial and bi-axial loads. For uni-axial bending, the maximum compressive strain is in a edge line of fibers, while for bi-axial bending, the maximum compressive strain is in a point fiber existed at one of the four corners (rectangular cross section).

For those deflection-controlled analysis, there are two levels of limits:

Service limit: column lateral deflection< $\frac{1}{300}\sim\frac{1}{1000}$L (column length);

Collapse deflection limit: the deflection< $\frac{1}{30}\sim\frac{1}{50}$L.

For pinned-ended columns, the mechanisms of ultimate strength capacity are classified depending on geometry and loading conditions.

1. *Short column under short term (both uni & bi-axially) loading*

According to ACI-318 Building Code (1999), short columns are referred to those columns with which $\frac{kL_u}{r}$<34-12$\frac{M_{1b}}{M_{2b}}$ for braced frame members, or $\frac{kL_u}{r}$< 22 for un-braced frame members. For short columns, lateral deflection of column is neglected. All sections have the same external loading conditions; and the concrete compressive crushing strain limit controls the ultimate strength. For a column under a large eccentric axial load, longitudinal reinforcement in tension zone yields before the maximum concrete compressive strain reaches the crushing limit. For those under small eccentric axial loads, longitudinal reinforcement will not yield in tension zone, while reinforcement

in compression zone normally yields before the maximum concrete strain reaches crushing limit.

For eccentric uni-axial load, the strength can be presented with a strength interaction diagram (P, M). For eccentric bi-axial load, the strength can be presented with a failure surface (P, M_x, M_y). Assume that the eccentricities are constant. Then, the loading path is a straight line in the diagrams starting from origin to the strength line or surface.

2. *Long column under short- term (both uni & bi-axially) loading*

For long columns, the lateral deflections can not be omitted, since P-delta effects create secondary moment. Therefore, at the critical cross section, eccentric axial loads plus secondary moments is the total external forces on the section. The critical section strength capacity controls the failure of the column.

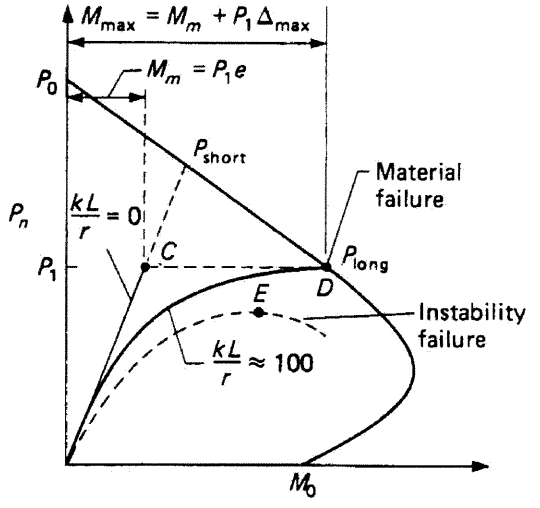

Figure 5.9 Slender Column P-M Interaction Diagram (MacGregor et al., 1970)

If look at the external forces on the critical section, the axial load path in axial load and moment interaction diagrams would become a curve line with derivative

decreasing due to addition of the secondary deflection. In another word, the eccentricities increase faster even than the loads increase. (Refer to Figure 5.9)

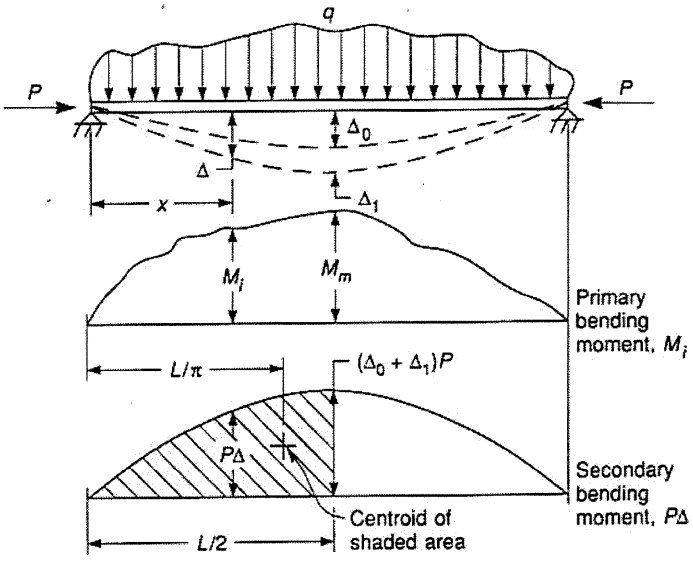

Figure 5.10 Primary and Secondary Moments and Deflections (Wang and Salmon, 1992)

For the column in Figure 5.10 under uni-axial bending, applying Virtual Work Principle, we could obtain the secondary eccentricity value e_{sec} (Wang and Salmon, 1992):

$$e_{sec}=\Delta_1=\Delta_0 \frac{\alpha}{1-\alpha} \tag{5.1}$$

where,

Δ_1 denotes the column secondary deflection in the span

Δ_0 denotes the column primary deflection in the span under an original eccentric load

$$\alpha= \frac{P(kL_u)^2}{\pi^2 EI} = \frac{P}{\frac{\pi^2 EI}{(kL_u)^2}} = \frac{P}{P_c} \tag{5.2}$$

EI denotes the stiffness parameter of a column cross section

kL_u denotes an equivalent pin-end length of column

P_c is the Euler buckling load

For bi-axial bending, the secondary eccentricities equal:

$$e_{xsec}=\Delta_{1x}=\Delta_{0x}\frac{\alpha_x}{1-\alpha_x} \tag{5.3}$$

$$e_{ysec}=\Delta_{1y}=\Delta_{0y}\frac{\alpha_y}{1-\alpha_y} \tag{5.4}$$

$$e_{total\text{-}sec}=\sqrt{e_{x\,\mathrm{sec}}^2+e_{y\,\mathrm{sec}}^2} \tag{5.5}$$

where,

Δ_{1x}, Δ_{1y} denote the column secondary deflections in a span projected to x and y directions separately.

Δ_{0x}, Δ_{0y} denote the primary column deflection in a span projected to x and y directions separately, under original eccentric load.

$$\alpha_x=\frac{P(kL_{ux})^2}{\pi^2 EI_x} \tag{5.6}$$

$$\alpha_y=\frac{P(kL_{uy})^2}{\pi^2 EI_y} \tag{5.7}$$

3. *Short column under long- term (uni & bi-axially) loading*

The short column is assumed being loaded in this way:

Instant loading at the beginning and then followed by sustained constant loading until failure. The lateral deflection is negligible. All cross sections have the same loading conditions, the same creep and shrinkage.

During the sustained loading phase, concrete creep and shrinkage would redistribute concrete compressive stress to reinforcement. Under this situation, creep and

shrinkage create changes of elastic strains and stresses in both concrete and reinforcement. The resultant changes of stresses in concrete are equivalent to adding increments of moment ΔM and axial force ΔN on cross section, which are opposite to the original loading directions. Since axial force is unchanged during the whole sustained loading process, plus the P-Δ effects are negligible, ΔM and ΔN are totally balanced by the stress changes happened in reinforcement. Thus, the maximum concrete compressive strain value would not increase in sustained loading process, unless the reinforcement has yielded already. Which means, the column would never fail if it has not failed in short term. This is also supported from the studies by Russell and Corley (1977), who performed field tests on time-dependent behavior of columns in Water Tower Place. According to those test results (of short columns), it is concluded that, the time – dependent shortening and differential movements do not affect the strength and serviceability of the structure. (Russell and Corley, 1977).

4. *Long column under long-term (uni & bi-axially) loading*

Since it tends to be uniformly developed on a cross section, shrinkage dose not affect the column secondary deflection, but helps transfer the loads from concrete to reinforcement. Thus, increase the column strength.

Geometrically, creep increases the secondary deflection and that threats the column ultimate strength capacity. Nevertheless, in some extent, it also helps concrete compressive stress redistribute just like what happens in short column case, which turns to increase the column strength. Therefore, the effect of creep to the ultimate capacity depends on the resultant of the two folds. Normally, according to test and analysis results, at early phase, the stress redistribution effects are larger than that from increasing

of lateral deflection generated from creep, thus the concrete elastic strain starts to decrease. Creep keeps the lateral deflection increasing, and then the concrete elastic stresses begin to pick up again. The buckling could occur in the following.

Here, reinforcement ratio and initial concrete stress level are the two important factors to affect creep buckling of RC columns. The reinforcement ratio directly influences the degree of stress redistribution, and the initial concrete stress levels also affect the rate of column lateral deflection generated by creep.

5.3 Estimation of Lateral Deflection of Bi-axially Loaded RC Slender Column

It is easy to understand that, under sustained loads, the lateral deflections of RC long columns are larger than those of the columns under the instant loads at the same levels. However, it is difficult to give an accurate result of deflection value through a simple formula. Yet, the following method could be used to estimate the value:

For the column in Figure 5.10 under uni-axial bending, according the Virtual Work Principle we have the secondary deflection result:

$$\Delta_{(t,t_0),1} = \Delta_{(t,t_0),0} \frac{\alpha'}{1-\alpha'} \tag{5.8}$$

$\Delta_{(t,t_0),0}$ represents the primary deflection at time t

$\Delta_{(t,t_0),1}$ represents the secondary deflection at time t

Per ACI-318 Building Code (1999),

$$\Delta_{(t,t_0),0} = (1+\lambda)\Delta_0 \tag{5.9}$$

$$\lambda = k_r . \xi \tag{5.10}$$

$$k_r = \frac{1}{(1+50\rho')} \tag{5.11}$$

where,

λ denotes ACI time-dependent deflection multiplier including creep and shrinkage

k_r denotes compression steel effect factor

ξ denotes time-dependent effect factor

ρ' denotes compressive steel ratio

$$\alpha' = \frac{P(kL_u)^2}{\pi^2 EI'} \tag{5.12}$$

The stiffness parameter EI' will be the larger of:

$$EI' = 0.4\, I_g\, E_{(t,t_0)} \tag{5.13}$$

and,

$$EI' = 0.2\, I_g\, E_{(t,t_0)} + I_{se}E_s \tag{5.14}$$

where,

$E_{(t,t0)}$ denotes the effective elastic modulus of concrete at age t.

$$E_{(t,t_0)} = \frac{E_c}{1+\gamma_t} \tag{5.15}$$

Thus,

$$\Delta_{(t,t_0)\,max} = \Delta_{(t,t_0),0} + \Delta_{(t,t_0),1} = \Delta_0 \frac{1+\lambda}{1-\alpha} = \Delta_0 \frac{1+\frac{\xi}{1+50\rho'}}{1-\frac{P(kL_u)^2}{\pi^2 EI'}} \tag{5.16}$$

Let t > 5years, ξ=2, and ν_t=2.4,

1. In case of low reinforcement ratio: $0.2I_g\, E_{(t,t_0)} > I_{se}E_s$, thus $EI' = 0.4\, I_g\, E_{(t,t_0)}$, and assuming $\rho' \geq 0.15\%$, then Eq (5.16) will become:

$$\Delta_{(t,t_0)\,max} \le \Delta_0 \frac{1+\dfrac{2}{1+0.075}}{1-\dfrac{P(kL_u)^2}{\pi^2 EI}} = \frac{2.86\Delta_0}{1-3.4\dfrac{P(kL_u)^2}{\pi^2 EI}} = \frac{2.86\Delta_0}{1-\dfrac{P(1.84kL_u)^2}{\pi^2 EI}} \tag{5.17}$$

This is a upper boundary value of deflection at column mid-height. It shows that the concrete time dependent effect has an amplification of 186% increase in the first degree deflection and 84% increase of the column equivalent to pinned-ended length for the column Euler buckling capacity. The two effects are multiplied together.

Look at the magnification factor in ACI code, δ, assuming the column is braced and pinned at top and bottom with $M_{1b}=M_{2b}$, thus $C_m=1$. Disregard the safety factors and time-dependent effects, then:

$$\delta_b = \frac{1}{1-\alpha} = \frac{1}{1-\dfrac{P(kL_u)^2}{\pi^2 EI'}} \tag{5.18}$$

From Eq.(5.14), use δ_b' to represent δ_b,

$$\delta_b' = \frac{1+\dfrac{\xi}{1+50\rho'}}{1-\dfrac{P(kL_u)^2}{\pi^2 EI'}} \tag{5.19}$$

substitute ξ=2, ν_t=2.4, and $\rho' \ge 0.15\%$, into Eq.(5.13)-(5.15) and Eq.(5.19), then:

$$\delta_b' \le \frac{2.86}{1-\dfrac{P(1.84kL_u)^2}{\pi^2 EI}} \tag{5.20}$$

from ACI,

$$\delta_b = \frac{1}{1-\dfrac{(1+\beta_d)P(kL_u)^2}{\pi^2 EI}} \tag{5.21}$$

as $0 \le \beta_d \le 1$, thus substitute $\beta_d = 1$ into (5.20), thus:

$$\delta_b \le \frac{1}{1-\frac{P(1.414kL_u)^2}{\pi^2 EI}} < \frac{2.86}{1-\frac{P(1.84kL_u)^2}{\pi^2 EI}} = \delta_b' \tag{5.22}$$

In this case, the upper boundary value of δ_b' is larger than δ_b. The 0.15% value is just for study purpose. ACI building code requires percentage of total longitudinal reinforcement A_{st} must be between 1 and 8%, which means, $\rho' \ge 0.5\%$ is required in practice.

2. In case of high reinforcement ratio, $0.2I_gE_{(t,t0)} < I_{se}E_s$, thus $EI' = 0.2I_gE_{(t,t0)} + I_{se}E_s$ assuming $\rho = \rho' \le 4\%$, $d' = 0.1h$, h = b, and $\frac{E_s}{E_c} = 7$; then per Eq. (2.30b):

$$EI = (0.2I_gE_c + 0.1536\, I_g \text{x} 7E_c)/(1+\beta_d) = 1.275\, \frac{I_gE_c}{1+\beta_d} \tag{5.23}$$

from Eq. (5.14):

$$EI' = 0.2I_gE_c\frac{1}{3.4} + 0.1536 I_g \text{x} 7E_c = 1.1340\, I_gE_c \tag{5.24}$$

thus, $\frac{EI'}{EI} = 0.889(1+\beta_d) \ge 0.889$, it shows with high reinforcement ratio, the column stiffness factor may not decrease much. Keep ξ=2, and ν_t=2.4, then from Eq. (5.18):

$$\Delta_{(t,t_0)max} \ge \frac{(1+\frac{2}{1+2})\Delta_0}{1-\frac{P(kL_u)^2}{1.134\pi^2 E_c I_g}} = \frac{1.667\Delta_0}{1-\frac{P(kL_u)^2}{0.889\pi^2 EI}} \tag{5.25}$$

and from Eq. (5.19),

$$\delta_b' \ge \frac{1.667}{1-\frac{P(kL_u)^2}{0.889\pi^2 EI}} \tag{5.26}$$

substitute $\beta_d = 0$ into (5.20), thus:

$$\delta_b \geq \frac{1}{1-\frac{P(kL_u)^2}{\pi^2 EI}} \tag{5.27}$$

and

$$\frac{1.667}{1-\frac{P(kL_u)^2}{0.889\pi^2 EI}} \geq \frac{1}{1-\frac{P(kL_u)^2}{\pi^2 EI}} \tag{5.28}$$

In this case, the lower boundary value of δ_b' is larger than that per ACI code. It could not be concluded that, $\delta_b' \geq \delta_b$ in all situations, since the comparison of right side in Eq. (5.24) with that in Eq. (5.21) could not give a positive result.

In this case, if 0.2 $I_g E_{(t,t0)}$=$I_{se} E_s$, then,

$\rho = \rho'$ =2.1875‰<minimum ratio of ACI code =5‰,

If $\rho = \rho'$ =0.5‰, with the other conditions unchanged, then:

$$EI = 0.2 I_g E_c + 0.1344\ I_g . E_c = 0.3344 I_g E_c \tag{5.29}$$

$$EI' = 0.2 I_g E_c \frac{1}{3.4} + 0.1344\ I_g . E_c = 0.1933 I_g E_c \tag{5.30}$$

in which $\frac{EI}{EI'} = 57.8\%$

Although it is an approximate approach to estimate the creep effects for slender columns, it clearly shows that, the creep effects act in two ways. First, it increases the primary deflection by introducing time dependent-multiplier factor of λ; second, it increases the second-degree deflection by reducing the concrete modulus. In the ACI approach, the first-degree deflection increasing has not been considered and for the second-degree deflection calculation, the stiffness parameter of column (concrete plus reinforcement) has been reduced by dividing $(1+\beta_d)$.

It is important to point out that theoretically, the definition of β_d, which equals $\frac{\text{factored sustained axial load}}{\text{factored total axial load}}$, might not be able to play as a quantitative creep indicator as it shows in the ACI building code. This is because the real load combinations are too complicated to estimate short-term loads effects on loading age, creep time-developing trend and the little recovery of creep feature when concrete is unloaded. For example, a short-term load at an early age of concrete may develop larger creep than the same amount of permanent load that is to be loaded at later. Further more, if a total loading time of short-term load has occupied about 1/3 of total load duration, just like a typical live loads case does, a short-term load definitely generates some significant amount of creep, sometimes even as large as 80% of the ultimate creep, depending on how it applies. Thus, omitting the effect of short-term load on concrete creep as in the ACI building code seems to be unreasonable.

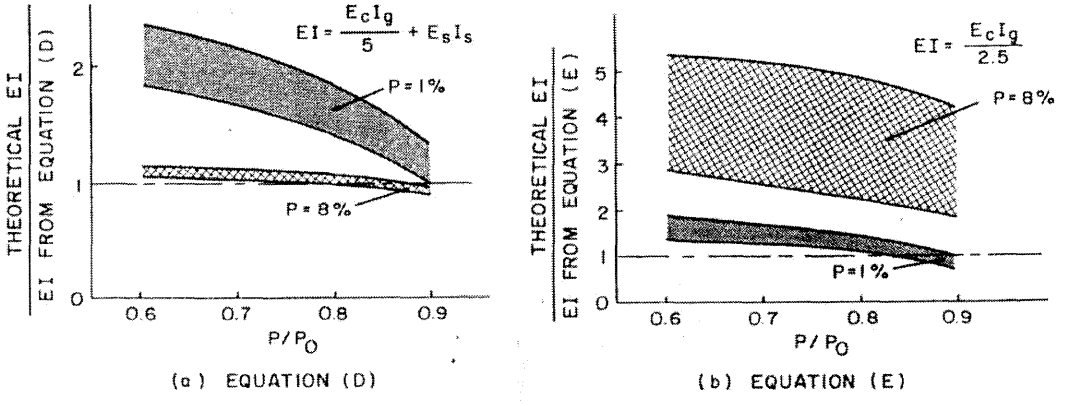

Figure 5.11 Comparison of equations for EI with EI values from Moment-Curvature Diagrams for Short-Duration Loading (MacGregor et al., 1970)

Then why so many engineering practices are still safe by following the ACI approach? Apart from the structural safety factor like internal forces redistribution

among columns, very conservative value has been used for *EI* (Refer to Figure 5.11, in which the theoretical *EI* refers to estimated results from theoretical load-moment-curvature diagrams) by the ACI building code. Also, the ACI code has largely reduced the longitudinal steel reinforcement stiffness during sustained loading period, which in fact should not do so, since the steel reinforcement hardly has any creep effect.

For columns under bi-axial loadings:

$$\Delta_{x\,(t,t_0)\,max}=\frac{1+\dfrac{\xi}{1+50\rho'_x}}{1-\dfrac{P(kL_{ux})^2}{\pi^2 EI'_x}}\Delta_{0x} \tag{5.31}$$

$$\Delta_{y\,(t,t_0)\,\max}=\frac{1+\dfrac{\xi}{1+50\rho'}}{1-\dfrac{P(kL_u)^2}{\pi^2 EI'}}\Delta_{0y} \tag{5.32}$$

$$\delta_{x\,(t,t_0)\,max}=\frac{1+\dfrac{\xi}{1+50\rho'_x}}{1-\dfrac{P(kL_{ux})^2}{\pi^2 EI'_x}} \tag{5.33}$$

$$\delta_{y\,(t,t_0)\,\max}=\frac{1+\dfrac{\xi}{1+50\rho'}}{1-\dfrac{P(kL_u)^2}{\pi^2 EI'}} \tag{5.34}$$

5.4 Recommendations

5.4.1 Engineering Practice

According to the analysis results from this study, it is recommended that:

1. *Increase concrete strength of column*

Concrete strength has very important effects on the strength of the slender columns under sustained loads (refer to section 5.1.1). It is preferred to increase concrete strength of columns in practical engineering design. If possible, use HSC for concrete columns, since HSC has lower creep values than those in NSC.

2. *Avoid large eccentricities*

Large eccentricities create a defect for slender column capacity. Creep is going to enlarge that defect.

3. *Increase longitudinal reinforcement ratio*

The higher the longitudinal reinforcement ratio it is, the less the reduced column stiffness will be in along term. That means the column will gain a higher strength. On another hand, it will also increase the concrete stress redistribution capacity, that is beneficial to its column strength.

5. *Use theoretical analysis tools*

ACI code has provided the specifications for standard design uses. It is not necessary to do theoretical analysis for typical RC columns. But the theoretical analysis is highly valuable for the determination and analysis of internal stresses, strains and deflections of existing slender concrete columns. Thus, it is recommended to conduct a more rigorous theoretical analysis in studying some RC column structures under sustained loads.

5.4.2 Future Research

1. *Experimental study*

More experimental data are needed, especially in the HSC columns under bi-axially under sustained bending loads.

2. *Concrete creep study*

For analyzing slender concrete columns under sustained loading, more research work is needed to develop creep models that are to be more sophisticated to describe the creep phenomenon. The advanced creep models should include the content in a higher stress level, and are more suitable to a larger variation of cross sectional dimensions and creep strain recovery.

3. *Improvement of analysis method*

a). Accuracy of method:

Physical models: improvements of concrete stress-strain relationship, creep models, and creep increment modifications.

Numerical solution: more sophisticated and accurate numerical methods are needed to improve the analysis.

b). Improvement of data process:

There are still some works needed to do for the improvement of the computer program's pre-process and post-process.

CHAPTER 6

CONCLUSIONS

The present research studies the behavior of slender reinforced concrete columns under sustained loads, most studies have concentrated on columns subjected to uni-axial bending loads, while very few researches have focused on bi-axial bending. The latest developed concrete time-dependent property models (creep and shrinkage) have been applied to current theoretical research approaches (Claeson et. al., 2000). However, those models, ACI-209R 92 or CEB-FIP 90, are generated for applications to concrete elements under constant compressive stress conditions. For slender columns subjected to constant sustained loads, concrete elastic strain and creep on a cross section are non-linearly changed with time and affect each other due to the secondary deflection effect, thus a strain history needs to be considered in creep calculation.

Thus, this investigation is to establish a theoretical analysis model and algorithm to simulate the deflection process of slender reinforced concrete columns under bi-axial sustained loads (uni-axial bending is treated as a special case of bi-axial bending). In this study, the ACI-92R time-dependent models are utilized and adjusted with concrete strain history.

In the conventional load-deflection analysis process, with projected transformations, a spatial deflection curve is resolved into a couple of planar curves located separately in two orthogonal plans. Based on the force equilibrium equations of inner force at a column section, a set of three simultaneous non-linear differential equations are derived to establish the relationships between the planar curve functions

with the eccentric load upon the top of column. Using the Green's Integral Formula, the strain and stress nonlinear functions and column section properties can be solely integrated into a few important coefficients of the differential equations. Thus, it makes the approach also suitable for columns with non-rectangular sections and any kinds of constitutive laws of materials.

During the sustained loading process, the established creep computation models, recommended separately by American Concrete Institute (ACI) 209-82 and the Comite' Euro-International du Be'ton (CEB)-FIP 1990 Model Code are used to calculate creep and shrinkage for a member under a constant elastic compression concrete strain for a given period. The presented analysis proposes a computerized method to allow creep increment to be adjusted with increasing of time and variation of strain, the **Time and Strain Adjustment of Creep Method** (**TSACM**), combining the creep calculation formula of constant elastic strains, such as those mentioned above. The creep strain at each cross section can be stored, calculated and adjusted and at each time increment phase, load changes and deflection modifications. It can be concluded that:

1. The present theoretical analysis succeeds in realizing a typical phenomenon in long RC column buckling process under sustained loading conditions.
2. The results of computer analysis of this study are in good agreement with those experimental data available for slender RC (NSC & HSC) columns under both uni-axially and bi-axially sustained bending loads.
3. The algorithm in this computer program is the first to realize an important phenomenon in that the concrete elastic compressive strain in columns normally experiences a drop process due to the stress redistribution to longitudinal

reinforcement when the columns undergo sustained loading. This concrete elastic compressive strain will regain if the total deflection keeps increasing. The phenomenon has been recorded in the previous experiment by Drysdale (1967), without any explanation in his research work. Indeed, this phenomenon has provided a reliable detailed picture of the creep process in long concrete columns.

4. Although at the beginning phase of sustained loading duration, the concrete compressive stresses decreaes, the increments of creep over time still cause the over all deflection to increase and thus increasing the P-delta effects, which in turn cause the column to fail when the maximum concrete compressive strain reaches the ultimate strain value sooner or later.
5. Despite current ACI building code (ACI-318, 1999) has not included calculations on creep, still engineering practice can take actions both in design and construction to control the developments of concrete creep as depicted in Chapter 5 (design recommendations). Based on present design recommendations, one is able to control the direct factors which influence creep and other factors which are indirectly influenced by creep.

APPENDIX A

FACTORS AND COEFFICIENTS OF *ACI 209-R92 MODELS* (1994)

In ACI-209 R92 Models, there are many factors and coefficients need to be calculated before to get the value of the ultimate creep coefficient and the ultimate shrinkage strain.

1. *Correction factors for conditions other than standard concrete compositions*

(1) Loading age

For loading age later than 7 days for moist cured concrete and later than 1-3 days for steam cured concrete, the correction factors are calculated using the following equations:

for moist cured concrete: $\gamma_{la}=1.25\,(t_{la})^{-0.118}$ (A.1)

for steam cured concrete: $\gamma_{la}=1.13\,(t_{la})^{-0.094}$ (A.2)

(2) Initial moist curing factor of shrinkage

For shrinkage of concrete moist cured during a period of time other than 7 days, use γ_{cp} factor in Table 2.5.3 from ACI 209R-92 (ACI Committee 209, 1994).

(3) Ambient relative humidity

For ambient relative humidity greater than 40%, the correction factors are

Creep $\gamma_{\lambda}=1.27-0.0067\lambda$, for $\lambda>40$ (A.3)

Shrinkage $\gamma_{\lambda}=1.4-0.010\lambda$, for $40\leq\lambda\leq80$ (A.4)

$\gamma_{\lambda}=3.00-0.030\lambda$, for $80<\lambda\leq100$ (A.5)

(4) Average thickness of member other than 6 in or volume-surface ratio other than 1.5 inches

Two methods are offered for estimating the effect of member size on v_u and $(\varepsilon_{sh})_u$.

a. Average –thickness method:

For average thickness of member less than 6 inches, use the factors given in Table 2.5.5.1 of ACI 209R-92 (ACI Committee 209, 1994). For average thickness of members greater than 6 in. and up to about 12 to 15 in., use following Equations:

During the first year after loading:

$$\text{Creep } \gamma_h = 1.14 - 0.023h \tag{A.6}$$

$$\text{Shrinkage } \gamma_h = 1.23 - 0.038h \tag{A.7}$$

For ultimate values:

$$\text{Creep } \gamma_h = 1.10 - 0.017h \tag{A.8}$$

$$\text{Shrinkage } \gamma_h = 1.17 - 0.029h \tag{A.9}$$

where h is the average thickness in inches of the part of the member under consideration.

b. Volume-surface ratio method

$$\text{Creep } \gamma_{vs} = \frac{2}{3}\left(1 + 1.13\, e^{-0.54\frac{v}{s}}\right) \tag{A-10}$$

$$\text{Shrinkage } \gamma_{vs} = 1.2\, e^{-0.12\frac{v}{s}} \tag{A.11}$$

where v/s is the volume-surface ratio of the member in inches.

2. *Correction factors for concrete compositions*

(1) Slump effect:

$$\text{Creep } \gamma_s = 0.82 + 0.067s \tag{A.12}$$

$$\text{Shrinkage } \gamma_s = 0.89 + 0.041s \tag{A.13}$$

where s is the observed slump in inches.

(2) Fine aggregate percentage:

$$\text{Creep } \gamma_\psi = 0.88 + 0.0024\psi \tag{A.14}$$

For $\psi \leq 50$ percent:

$$\text{Shrinkage } \gamma_s = 0.30 + 0.014\psi \tag{A.15}$$

For $\psi > 50$ percent:

$$\text{Shrinkage } \gamma_s = 0.90 + 0.002\psi \tag{A.16}$$

where ψ is the ratio of the fine aggregate to total aggregate by weight expressed as percentage.

(3) Cement content

$$\text{Shrinkage } \gamma_c = 0.75 + 0.00036c \tag{A.17}$$

where c is the cement content in pounds per cubic yard.

(4) Air content

$$\text{Creep } \gamma_\alpha = 0.46 + 0.09\alpha \quad (\geq 1.0) \tag{A.18}$$

$$\text{Shrinkage } \gamma_\alpha = 0.95 + 0.008\alpha \tag{A.19}$$

where α is the air content in percent.

APPENDIX B

COEFFICIENTS OF *CEB-FIP MODEL CODE 1990* (1993)

Per CEB-FIP Model Code 1990, the notional creep and shrinkage coefficients may be estimated by the following calculations.

1. Calculation of the notional creep coefficient:

$$\phi_0=\phi_{RH}\beta(f_{cm})\beta(t_0) \tag{B.1}$$

with

$$\phi_{RH}=1+\frac{1-\frac{RH}{RH_0}}{(0.46\frac{h}{h_0})^{\frac{1}{3}}} \tag{B.2}$$

$$\beta(f_{cm})=\frac{5.3}{(\frac{f_{cm}}{f_{cm0}})^{0.5}} \tag{B.3}$$

$$\beta(t_0)=\frac{1}{0.1+(\frac{t_0}{t_1})^{0.2}} \tag{B.4}$$

where,

$$h=\frac{2A_0}{u} \tag{B.5}$$

f_{cm} is the mean compressive strength of concrete at the age of 28 days (MP_a)

$$f_{cm0}=10MP_a \tag{B.6}$$

RH is the relative humidity of the ambient environment (%)

$$RH_0=100\% \tag{B.7}$$

h is the notational size of member (mm), where A_0 is the cross section and u is the perimeter of the member in contact with the atmosphere

$$h_0=100\text{mm} \tag{B.8}$$

$$t_1=1 \text{ day} \tag{B.9}$$

The development of creep with time is given by

$$\beta(t-t_0)=\left(\frac{\frac{t-t_0}{t_1}}{\beta_H+\frac{t-t_0}{t_1}}\right)^{0.5} \tag{B.10}$$

with

$$\beta_H=150\left[1+\left(1.2\frac{RH}{RH_0}\right)^{18}\right]\frac{h}{h_0}+250\leq 1500 \tag{B.11}$$

Effect of cement and curing temperature:

$$t_0=t_{0,T}\left[\frac{9}{2+\left(\frac{t_{0,T}}{t_{1,T}}\right)^{1.2}}+1\right]^{\alpha}\geq 0.5 \text{ days} \tag{B.12}$$

where,

$t_{0,T}$ is the age of concrete at loading (days)

$t_{1,T}=1$ day

α is the power which depends on the type of cement;

α=-1 for slowing hardening cement SL, 0 for normal or rapid hardening cement N and R, and 1 for rapid hardening high strength cements RS.

2. Calculation of the notional shrinkage coefficient:

Per CEB-FIP Model Code 1990, the notional shrinkage coefficient may be estimated by

$$\varepsilon_{cso0}=\varepsilon_s(f_{cm})\beta_{RH} \tag{B.13}$$

with

$$\varepsilon_s(f_{cm})= [160+10\beta_{sc}(9- \frac{f_{cm}}{f_{cm0}})]\text{x}10^{-6} \tag{B.14}$$

where,

β_{sc} is a coefficient which depends on the type of cement; β_{sc}=4 for slowly hardening cement SL, β_{sc}=5 for normal or rapidly hardening cement N or R, and β_{sc}=8 for rapid hardening high strength cements RS,

$$\beta_{RH}=-1.55\beta_{SRH} \quad \text{for } 40\% \leq RH < 99\% \tag{B.15}$$

$$\beta_{RH}=+0.25 \quad \text{for } RH \geq 99\% \tag{B.16}$$

where,

$$\beta_{SRH}=1-(\frac{RH}{RH_0})^3 \tag{B.17}$$

with

RH is the relative humidity of the ambient atmosphere (%)

RH_0 =100%

$$\beta_s(t-t_s)= \{\frac{t-t_s}{t_1[350(\frac{h}{h_0})^2+\frac{(t-t_s)}{t_1}]}\}^{0.5} \tag{B.18}$$

where,

h is defined in Eq.(B.5)

h_0 is defined in Eq.(B.8)

t_1 is defined in Eq.(B.9)

APPENDIX C

ELASTIC ANALYSIS VERIFICATION RESULTS

McGill Column specimen U series U-4 (Wang and Hsu, 1992) is selected to do the test data verification of the elastic analysis. Column U-4 is a NSC specimen under bi-axial instant bending loads. Figure C.1 shows the dimension and reinforcement of the specimen series. Tables C.1, C.2 and C.3 display the test data. The analysis results in those tables are from the study of Wang & Hsu (1992). The results from Gu's analysis for U-4 are:

$P_{analysis}$=13.25 kips, P_{test}=14.3 kips, $P_{analysis}/P_{max}$=0.93

$\delta_{x\text{-}analysis}=\delta_{y\text{-}analysis}$ = 0.28 in, $\delta_{x\text{-}test}=\delta_{x\text{-}test}$= 0.33 in, $\delta_{y\text{-}analysi}/\delta_{x\text{-}test}$= 0.85

Table C.1 Column Specimens (Wang and Hsu,1992)

Column (1)	Size (sq. in.) (2)	Height/ breadth (3)	Number and size of bars (4)	f_y (ksi) (5)	$E_s \times 10^6$ (psi) (6)	f'_c (psi) (7)	e_x (in.) (8)	e_y (in.) (9)
U-1	4 × 4	10	9-D5	73	29.2	3,905	2.5	3.5
U-2	4 × 4	10	9-D5	73	29.2	3,806	3.0	3.5
U-3	4 × 4	10	9-D5	73	29.2	3,894	3.5	3.5
U-4	4 × 4	10	9-D5	73	29.2	3,830	2.0	2.0
U-5	4 × 4	10	9-D5	73	29.2	3,715	0.5	4.0[a]
U-6	4 × 4	10	9-D5	73	29.2	3,895	0.5	7.0

Table C.2 Maximum Moment Results (kips-in) (Wang and Hsu, 1992)

Column (1)	Analysis		Test	
	M_x (2)	M_y (3)	M_x (4)	M_y (5)
U-1	35.90	25.75	34.05	25.84
U-2	32.64	28.09	32.37	26.85
U-3	30.48	30.48	29.29	29.29
U-4	31.83	31.83	30.96	30.96
U-5	47.17	6.22	49.33	6.22
U-6	47.39	3.58	47.74	3.48

Note: All failure modes are tension failure; 1 kip-in. = 1.13 × 10^2 N-m.

Table C.3 Maximum Load Deflection Results (Wang and Hsu, 1992)

Column (1)	Analysis			Test		
	P_{max} (kip) (2)	δ_x (in.) (3)	δ_y (in.) (4)	P_{max} (kip) (5)	δ_x (in.) (6)	δ_y (in.) (7)
U-1	9.35	0.25	0.336	9.6	—	—
U-2	8.57	0.27	0.302	8.7	—	—
U-3	8.04	0.28	0.28	8.0	0.317	0.317
U-4	13.87	0.29	0.29	14.3	0.331	0.331
U-5	10.47	0.08	0.462	10.8	0.071	0.548
U-6	6.19	0.06	0.656	6.24	0.051	0.636

Note: 1 kip = 4,448.2 N; 1 in. = 25.4 mm.

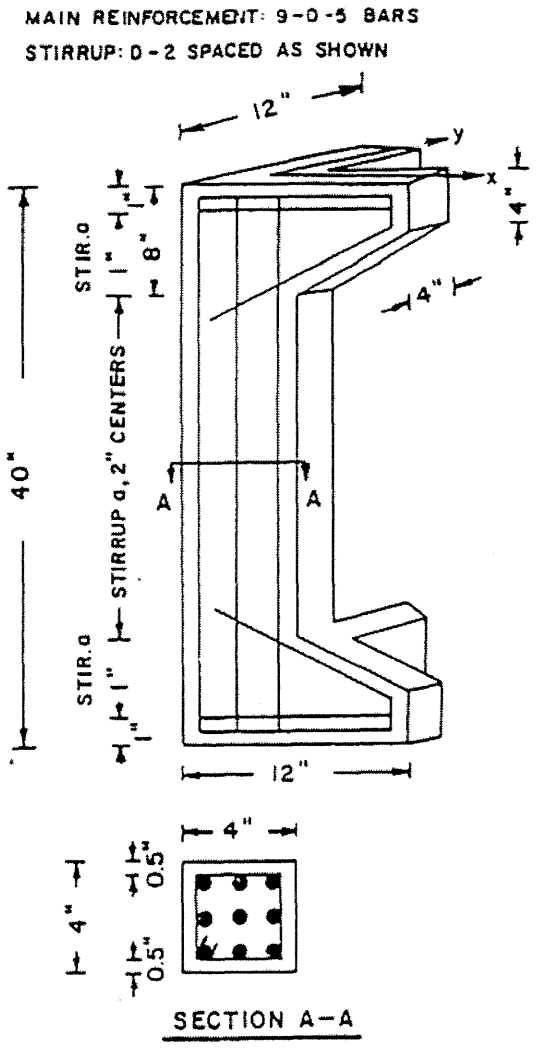

Figure C.1 Column Details (Wang and Hsu, 1992)

APPENDIX D

PROCESS OF DEFLECTION SOLUTION

In this part, a solution to deflection from knowing of the second derivatives is provided. This solution process is based on numerical analysis theories.

Assuming f(x) is a function at $[x_0, x_n]$. If $f'(x), f''(x)$ and $f'''(x)$ exist at phase of $[x_0, x_n]$, then let:

$$\Delta_x = \frac{x_n - x_0}{n} \tag{D.1}$$

then we have $x_1, x_2, \ldots x_{n-1}$ points between x_0 and x_n:

$$x_1 = x_0 + \Delta x \tag{D.2a}$$

$$x_2 = x_1 + \Delta x \tag{D.2b}$$

$$x_3 = x_2 + \Delta x \tag{D.2c}$$

.....

$$x_{n-1} = x_{n-2} + \Delta x \tag{D.2d}$$

$$x_n = x_{n-1} + \Delta x \tag{D.2e}$$

From Taylor's series:

$$f(x_1) = f(x_0) + \Delta x f'(x_0) + \frac{\Delta x^2}{2} f''(x_0) + \frac{\Delta x^3}{3!} f'''(\xi) \tag{D.3a}$$

Let n big enough thus Δx so small that,

$$f(x_1) \approx f(x_0) + \Delta x f'(x_0) + \frac{\Delta x^2}{2} f''(x_0) \tag{D.3b}$$

similarly,

$$f(x_2) \approx f(x_1) + \Delta x f'(x_1) + \frac{\Delta x^2}{2} f''(x_1) \tag{D.3c}$$

.....

$$f(x_n) \approx f(x_{n-1}) + \Delta x f'(x_{n-1}) + \frac{\Delta x^2}{2} f''(x_{n-1}) \quad \text{(D.3d)}$$

Also we can get approximate $f(x_0)$ from value of x_1 point,

$$f(x_0) \approx f(x_1) - \Delta x f'(x_1) + \frac{\Delta x^2}{2} f''(x_1) \quad \text{(D.4a)}$$

$$f(x_2) \approx f(x_3) - \Delta x f'(x_3) + \frac{\Delta x^2}{2} f''(x_3) \quad \text{(D.4b)}$$

.....

$$f(x_{n-1}) \approx f(x_n) - \Delta x f'(x_n) + \frac{\Delta x^2}{2} f''(x_n) \quad \text{(D.4c)}$$

Add Eq.(D.3a) and Eq. (D.4a):

$$f(x_0) + f(x_2) \approx 2f(x_1) + \Delta x^2 f''(x_1) \quad \text{(D.5a)}$$

Thus the first degree of derivative $f'(x)$ is excluded, with this way we can establish a new set of equation including (D.5a):

$$f(x_1) + f(x_3) \approx 2f(x_2) + \Delta x^2 f''(x_2) \quad \text{(D.5b)}$$

$$f(x_2) + f(x_4) \approx 2f(x_3) + \Delta x^2 f''(x_3) \quad \text{(D.5c)}$$

.....

$$f(x_{n-3}) + f(x_{n-1}) \approx 2f(x_{n-2}) + \Delta x^2 f''(x_{n-2}) \quad \text{(D.5d)}$$

$$f(x_{n-2}) + f(x_n) \approx 2f(x_{n-1}) + \Delta x^2 f''(x_{n-1}) \quad \text{(D.5e)}$$

Reorganize Eq. (D.5a) to Eq. (D.5e) a matrix Equation Eq. (D.6) is formed.

$$\begin{pmatrix} -2 & 1 & & & & & & \\ 1 & -2 & 1 & & & & & \\ & 1 & -2 & 1 & & & & \\ & & & \cdots & \cdots & \cdots & & \\ & & & & \cdots & \cdots & \cdots & \\ & & & & 1 & -2 & 1 & \\ & & & & & 1 & -2 & 1 \\ & & & & & & 1 & -2 \end{pmatrix} \begin{bmatrix} f(x_1) \\ f(x_2) \\ f(x_3) \\ \cdots \\ \cdots \\ f(x_{n-3}) \\ f(x_{n-2}) \\ f(x_{n-1}) \end{bmatrix} = \begin{bmatrix} \Delta x^2 f''(x_1) \\ \Delta x^2 f''(x_2) \\ \Delta x^2 f''(x_3) \\ \cdots \\ \cdots \\ \Delta x^2 f''(x_{n-3}) \\ \Delta x^2 f''(x_{n-2}) \\ \Delta x^2 f''(x_{n-1}) \end{bmatrix} \tag{D.6}$$

Let

$$m_1 = \frac{1}{2} \tag{D.7a}$$

$$m_2 = \frac{2}{3} \tag{D.7b}$$

.....

$$m_{n-2} = \frac{n-2}{n-1} \tag{D.7c}$$

$$m_{n-1} = \frac{n-1}{n} \tag{D.7d}$$

and

$$g_1 = m_1 \Delta x^2 f''(x_1) \tag{D.8a}$$

$$g_2 = m_2(g_1 + \Delta x^2 f''(x_2)) \tag{D.8b}$$

.....

$$g_{n-2} = m_{n-2}(g_{n-3} + \Delta x^2 f''(x_{n-2})) \tag{D.8c}$$

$$g_{n-1} = m_{n-1}(g_{n-2} + \Delta x^2 f''(x_{n-1})) \tag{D.8d}$$

The solution of the Eq. (D.19) can be obtained as:

$$f(x_{n-1}) = -g_{n-1} \tag{D.9}$$

$$f(x_{n-2}) = 2f(x_{n-1}) + \Delta x^2 f''(x_{n-1}) \tag{D.10a}$$

$$f(x_{n-3}) = 2f(x_{n-2}) - f(x_{n-1}) + \Delta x^2 f''(x_{n-2}) \tag{D.10b}$$

.....

$$f(x_1) = 2f(x_2) - f(x_3) + \Delta x^2 f''(x_2) \tag{D.10c}$$

Bring in boundary condition, for column pinned at top and bottom, $f(x_0)=f(x_n)=0$, $f''(x_0) = f''(x_n) = -\varphi_0$

APPENDIX E

NOTATIONS OF SOURCE CODE AND FUNCTIONS OF C PROGRAM

E.1 Notations of the Source Code

The notations of the variables in this analysis program composed with Standard C Language are listed below:

1. Input Data

Geometry Information

b: width of the section (y dir.)

h: height of the section (x dir.)

len: length of the col. (z dir.)

ng: number of segments

Ini[3]: geometry initial of the section

Material Information

tas: total area of steel

nas: total number of rebars

As[20]: area of reinforcement @ different points

Xs[20]: x co-ordinate of As[20]

Ys[20]: y co-ordinate of As[20]

fcp: fc′ compressive strength of concrete, measured at 28 days after casting

ecu: ultimate strain of concrete under compression

ec0: strain at maximum strength

emc: elastic modulous of concrete in compression

ems: elastic modulous of steel

fyt: yield point of steel

cu: ultimate creep coefficient

Loading Control Variables

typ: type of restraint (0,1,2,3) (refer to pin-pin, fix-cant'l, fix-fix, pin-fix)

et[3]: eccentricity @ top of col.

eb[3]: eccentricity @ bott. of col.

ntf: number of short term-sustained loading patern recycles

nts[ntf] number of time increments in each loading time duration

npi[ntf] number of loading increments in each loading time duration

pi[ntf] loading value in each short term loading

tp[ntf] time duration for each sustained period

Error Control Variables

rdwmax: max. relative difference

arwamax: allowed relative maximum bending deflection of the member

awamax: allowed absolute maximum bending deflection of the member

adis: allowed vertical displacement at load point

ardis: allowed relative vertical displacement at load point

ardecm: allowed relative maximum difference between ece0[...] and ece1[...]

adecm: allowed maximum difference between ece0[...] and ece1[...]

2. Intermediate Process Variables

t: time since short term loading

clen: projt. vertical len. of col.

dx: length of segment

z: segment co-ordinate @ z dir.

mt[3]: initial moment at top restraint

mb[3]: initial moment at bottom restraint

rt[3]:reactions @ top

rt: related computation variables @ section

dp: load increment

dt: time increment

pp: vertical loading value at the computing point

dis: vertical displacement at load point

ct: ratio of creep strain to elastic strain

w00s: related intermediate variable of w00[ng]

w01s: related intermediate variable of w00[ng]

w02s: related intermediate variable of w00[ng]

w01[ng]: initial function of first degree of derivative of the projected deflection curve in x dir.

w11[ng]: resulted function first degree of derivative of the projected deflection curve in x dir.

yw00s: related intermediate variable of yw00[ng]

yw01s: related intermediate variable of yw00[ng]

yw02s: related intermediate variable of yw00[ng]

yw01[ng]: initial function of first degree of derivative of the projected deflection curve in y dir.

yw11[ng]: resulted function of first degree of derivative of the projected deflection curve in y dir.

wela0[ng]: component of w02[ng] resulted from elastic deformation (x dir.)

x02s:related computation variables @ section

ywela0[ng]: component of yw02[ng] resulted from elastic deformation (y dir.)

y02s:related computation variables @ section

ece1as: related computation variables @ section

wela0[ng]: component of w02[ng] resulted from elastic deformation (x dir.)

wela[ng]: component of w12[ng] resulted from elastic deformation (x dir.)

x12s: related computation variables @ section

ywela0[ng]: component of yw02[ng] resulted from elastic deformation (y dir.)

ywela[ng]: component of yw12[ng] resulted from elastic deformation (y dir.)

y12s:related computation variables @ section

ywcrp0[ng]: component of yw02[ng] resulted from creep deformation (y dir.)

ywcrp[ng]: component of yw12[ng] resulted from creep deformation (y dir.)

yw02c: related computation variables @ section

ecrp0[ng]: component of ece0[ng] resulted from creep deformation

ecrp[ng]: component of ece1[ng] resulted from creep deformation

ece0c: related computation variables @ section

wcrp0[ng]: component of w02[ng] resulted from creep deformation (x dir.)

wcrp[ng]: component of w12[ng] resulted from creep deformation (x dir.)

w02c: related computation variables @ section

r00[ng]: initial deflection function resulted from linear elastic analysis

r02[ng]: initial curvature function resulted from linear elastic analysis

finc: resultant of conc. Stress

mcx: moment component contribute by conc. (x dir.)

mcy: moment component contribute by conc. (y dir.)

dx12[ng][nts[ntf]]: increment of w12[ng] @ n section & t time;

dy12[ng][nts[ntf]]: increment of yw12[ng] @ n section & t time;

depsi[ng][nts[ntf]]: increment of ece1asr[ng] @ n section & t time;

stime[nts[ntf]]:initial time value @ n time increment phase

3. Out Put Data

w00[ng]: initial function of projected deflection curve in x dir.

w02[ng]: initial second degree of derivative of the projected deflection function in x dir.

yw00[ng]: initial function of projected deflection curve in y dir.

yw02[ng]: initial second degree of derivative of the projected deflection function in y dir.

w10[ng]: resulted function of projected deflection curve in x dir.

w12[ng]: resulted second degree of derivative of the projected deflection function in x dir.

yw10[ng]: resulted function of projected deflection curve in y dir.

yw12[ng]: resulted second degree of derivative of the projected deflection function in y dir.

ece0[ng]: initial edge concrete fiber strain

ece1[ng]: computed edge concrete fiber strain

ecelasr0[ng]: component of ece0[ng] resulted from elastic deformation

ecelasr[ng]: component of ece1[ng] resulted from elastic deformation

E.2 Functions of the Program

The notations of the functions in this analysis program composed with Standard C Language are listed below:

fs(): sub-function for disp();

yfs(): sub-function for disp();

def():solve deflection array w10[];

A1(), A2(), B1(), B2(), D1(), D2(): integral functions of Concrete Stress-Strain rlationship;

G1(), G2(), G3(), G1X(), G1Y(): transferred coefficient integral functions;

df(): summation of reinf. forces;

dMx(): summation of reinf. moments over y axis;

dMy():summation of reinf. moments over x axis;

stress(): solve concrete stress; (for checking purpose)

sigc(): force resultant of concrete stresses; (for checking purpose)

Mc(): moment resultant of concrete stresses; (for checking purpose)

F0x():checking function;

disp(): to calculate dis; (usless)

f(): function to be solved;

xpoint():xpoint function;

root(): roots of f();

ss(): solving function for f();

solve():solving function for the equilibrium Eqs. under instant loads ;

we0,1,2,3():elastic solution function for the column;(0, 1, 2, & 3 ref. to diff. support condition)

solvc():solving function for the equilibrium Eqs. under sustained loads;

main(): input & output, main frame flow.

E.3 Detailed Algorithm Flow Chart

The main flow chart of the algorithm is shown in Chapter 3.3.5. In this part, a more detailed flow chart is created to display the structure of the algorithm. The total statements of the program is 2190.

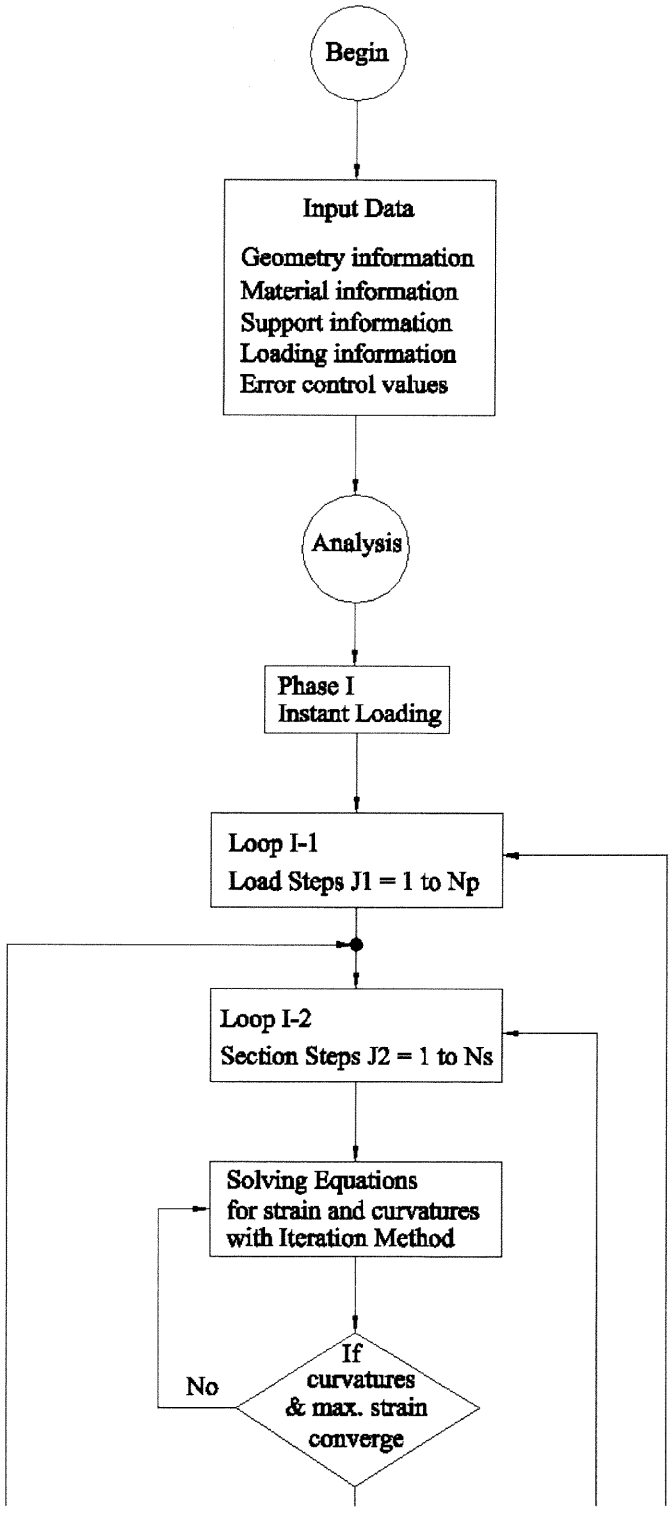

Figure E.1a Detailed Algorithm Flow Chart I

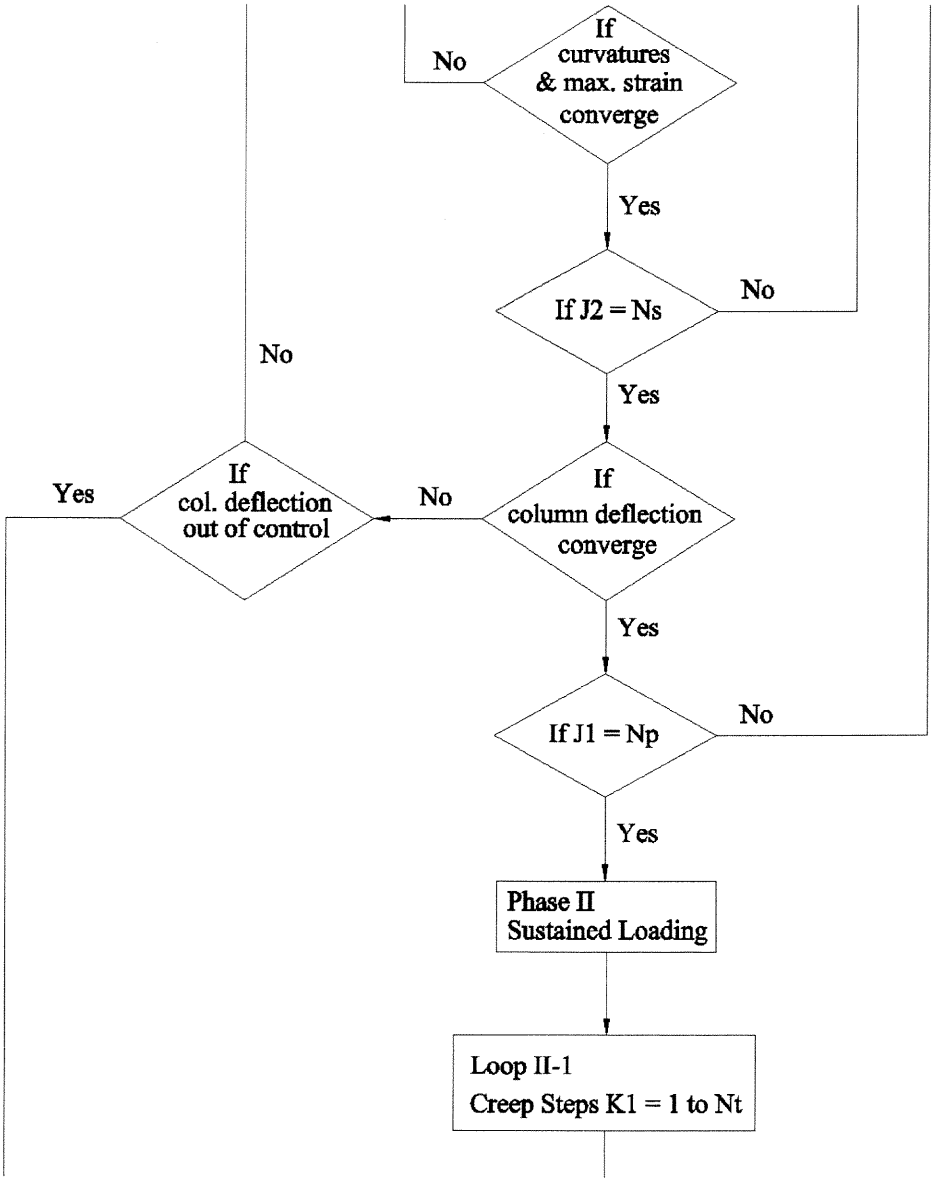

Figure E.1b Detailed Algorithm Flow Chart II

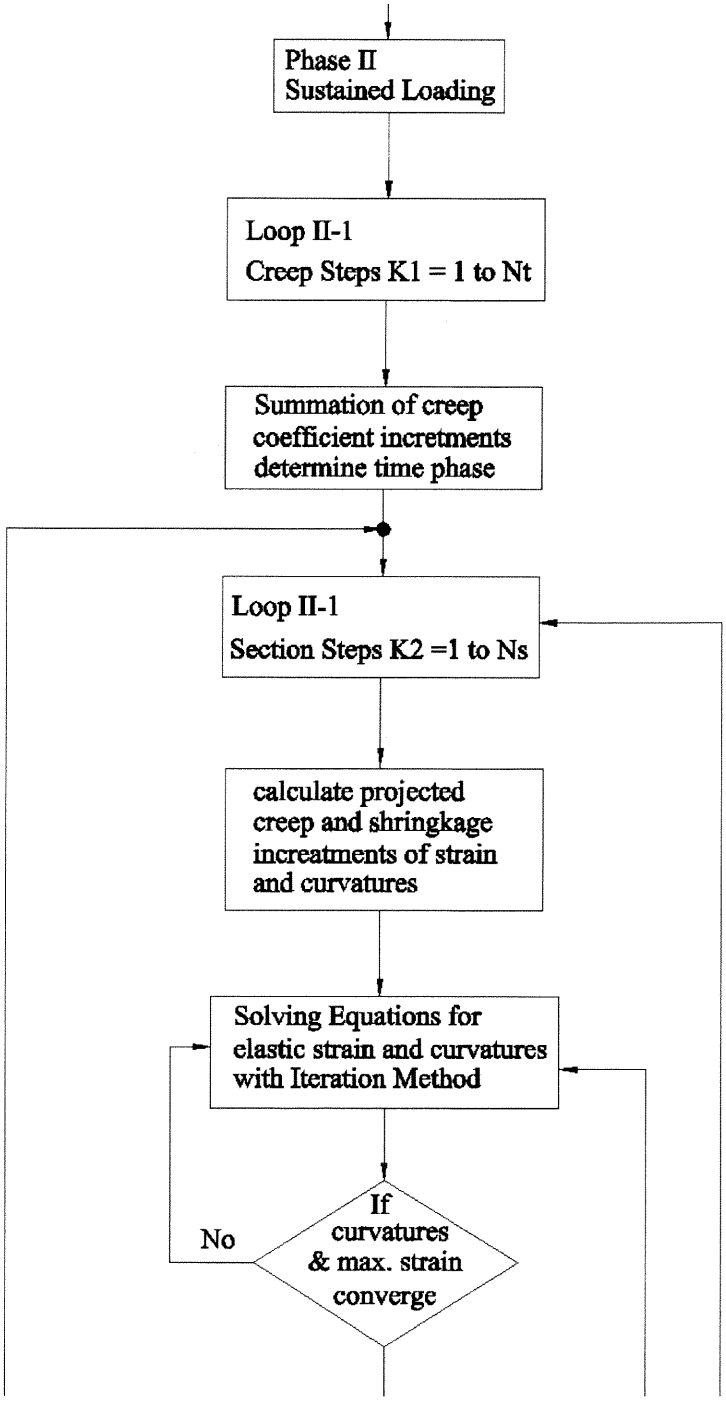

Figure E.1c Detailed Algorithm Flow Chart III

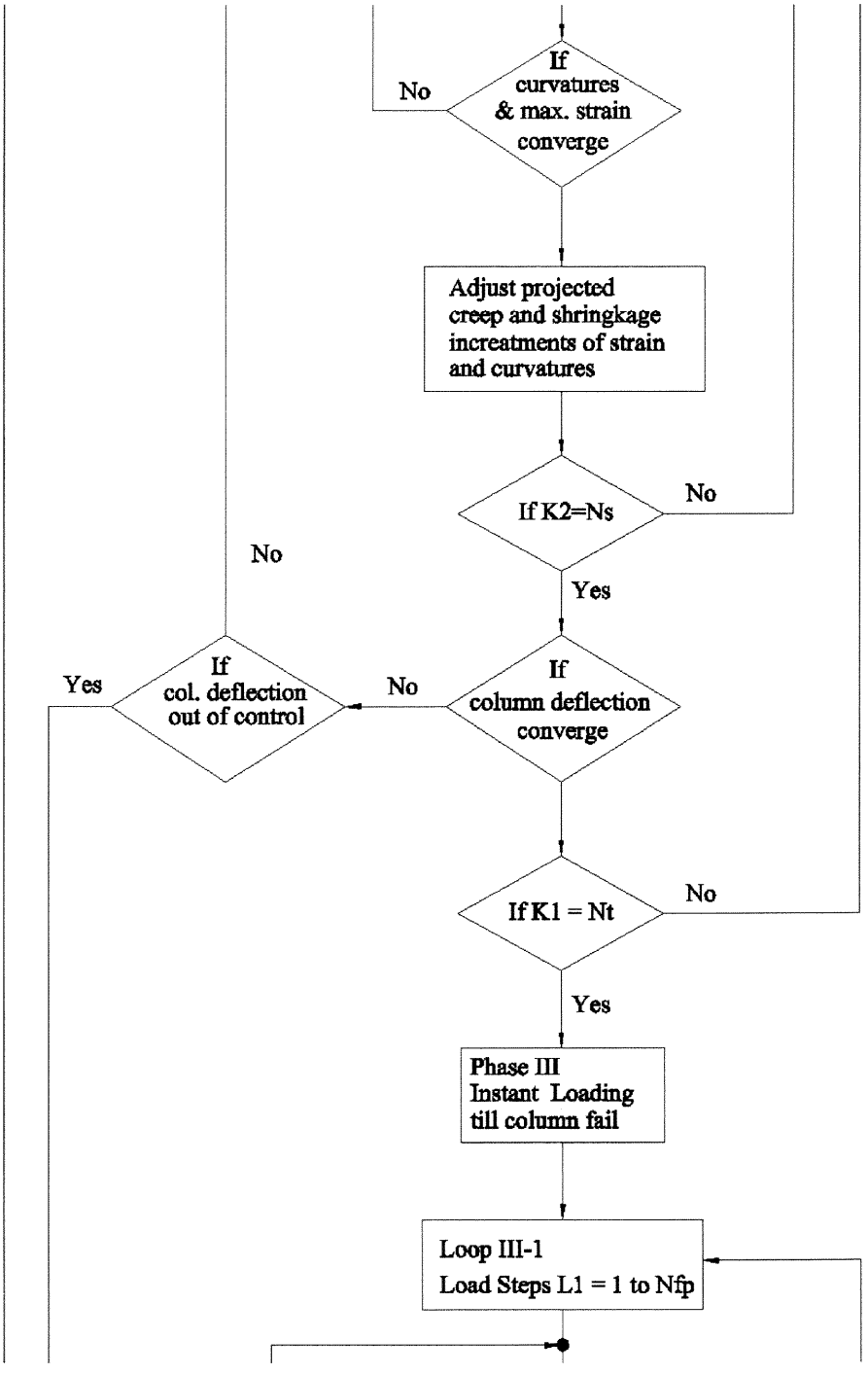

Figure E.1d Detailed Algorithm Flow Chart IV

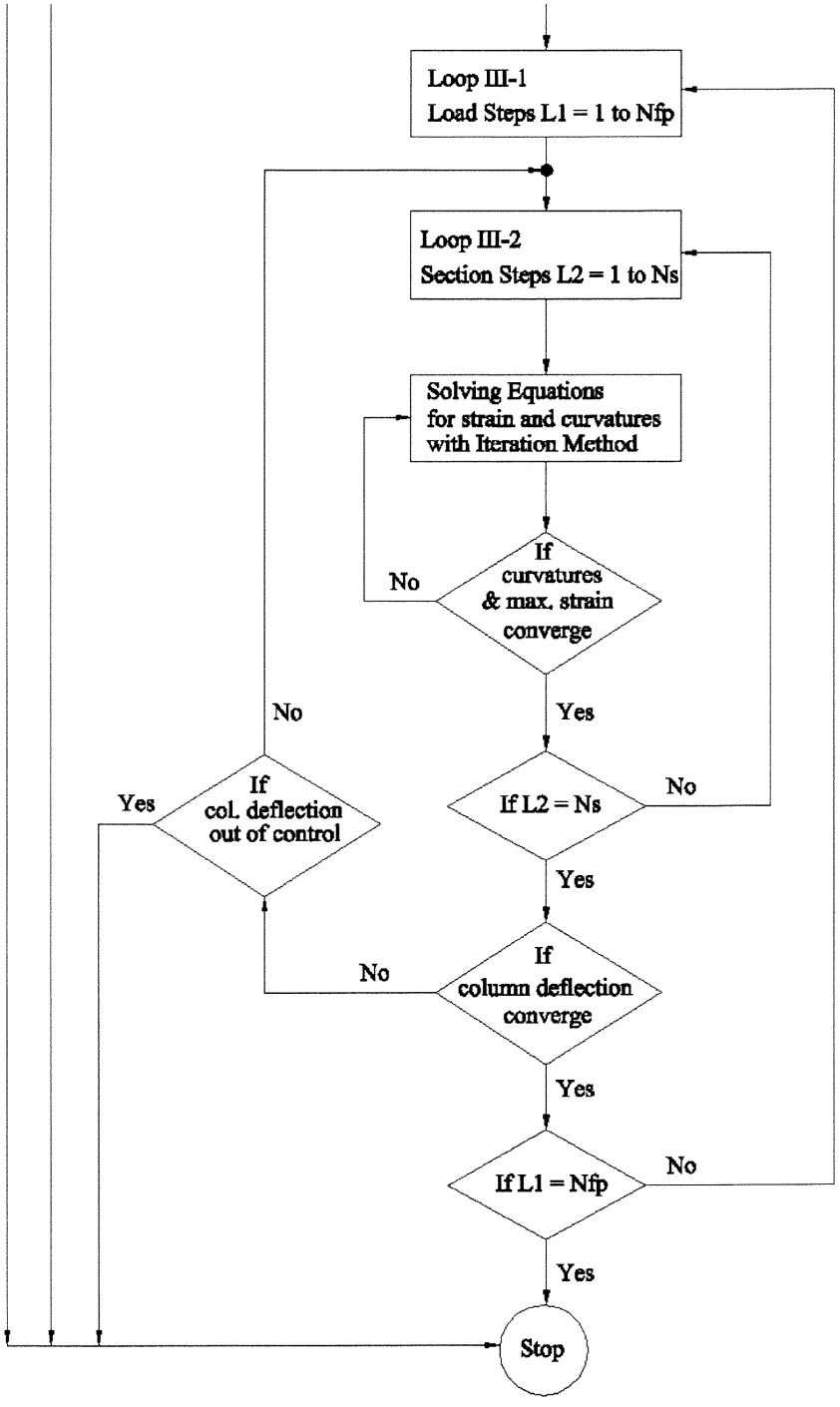

Figure E.1e Detailed Algorithm Flow Chart V

REFERENCES

ACI Committee 209 (1994), "Prediction of creep, Shrinkage, and Temperature effects in concrete structures," *ACI 209R-92*, American Concrete Institute, Detroit, MI, (2nd Printing) April, pp. 1-47.

ACI Committee 318 (1963), *Building Code Requirements for Structural Concrete (ACI 318-63)*, American Concrete Institute, Farmington Hills, MI., pp. 1-144.

ACI Committee 318 (1971), *Building Code Requirements for Structural Concrete (ACI 318-71)*, American Concrete Institute, Farmington Hills, MI., pp. 1-78.

ACI Committee 318 (1999), *Building Code Requirements for Structural Concrete (ACI 318-99) and Commentary (ACI 318-R-99)*, American Concrete Institute, Farmington Hills, MI., pp. 1-391.

Attard, M. M. and Setunge, S. (1996), "Stress-Strain Relationship of Confined and Unconfined Concrete," *ACI Material Journal*, September-Octorber, pp. 432-442.

Bazant, Z. P. (1972), " Prediction of Concrete Creep Effects using Age-Adjusted Effective Modulus Method," *ACI Journal*, Vol. 69, April, pp. 212-217.

Bazant, Z. P., Hauggaard, A. B., Baweja, S. and Ulm, F.-J. (1997), "Mirocro-Solidification Theory for Concrete Creep. I: Aging and Drying Effects," Journal of Engineering Mechanics, November, pp. 1188-1194.

Bazant, Z. P., Hauggaard, A. B., Baweja, S. and Ulm, F.-J. (1997), "Mirocro-Solidification Theory for Concrete Creep. II: Algorithm and Verification," Journal of Engineering Mechanics, November, pp. 1195-1201.

Branson, D. E. and Christiason, M. L. (1971), "Time-dependent Concrete Properties Related to Design-Strength and Elastic Properties, Creep and Shrinkage," *Symposium on Creep, Shrinkage, and Temperature Effects*, SP-27, ACI Publications, Detroit, MI., pp. 257-277.

Bresler, B. and Selna, L. (1964), "Analysis of Time Dependent Behavior of Reinforced Concrete Structures," *Symposium on Creep of Concrete*, SP-9, ACI Publications March, pp. 115-128.

CEB-FIP (1993), *CEB-FIP Model Code 1990: Design Code Comite Euro-International Du Buton,* ASCE (Editor & Publisher) January, pp. 1-462.

Chang, W. F. and Ferguson, P. M. (1963), "Long Hinged Reinforced Concrete Columns," *Journal of ACI*, January, Title No. 60-1, January, pp. 1-25.

Claeson, C. and Gylltoft, K. (2000), "Slender Concrete Columns Subjected to Sustained and Short-Term Eccentric Loading," *ACI Structural Journal* January-February, pp. 45-52.

Distefano, J. N. (1965), "Creep Buckling of Slender Columns," Journal of Structural Division, Proceedings of ASCE, ST 3, June, pp. 127-150.

Drysdale, G. R. (1967), "The Behavior of Slender Reinforced Concrete Columns Subjected to Sustained Biaxial Bending" PhD thesis, University of Toronto, Toronto, Canada, pp. 1-224.

Drysdale, G. R. and Huggins, W. M. (1971), "Sustained Biaxial Load on Slender Concrete Columns," *Proceedings of ASCE ST.* May, pp. 1423-1442.

Gardner, N. J. and Zhao, J. W. (1993), "Creep and Shrinkage Revisited," ACI Material Journal, May-June, pp. 236-246.

Gilbert, R. I. and Mickleborough, N. C. (1993), "Creep Effects in Slender Reinforced and Prestressed Concrete Columns," *Computer Analysis of the Effects of Creep, Shrinkage, and Temperature Changes on Concrete Structures*, SP129, ACI Publications, Detroit, MI, pp. 77-100.

Green, R. (1966), "Behavior of Unrestrained Reinforced Concrete Columns under Sustained Loads," Ph.D Dissertation, The University of Texas, Austin.

Green, R. and Breen, J. E. (1969), "Eccentrically Loaded Concrete Columns Under Sustained Load," ACI Journal, Title No. 66-73, November, pp. 863-874.

Goyal, B. B. and Jackson, N. (1971), "Slender Concrete Column under Sustained Load," *Journal of Structural Division*, Proceedings of ASCE, ST11, November, pp. 8544-2749.

Han, N. (1996), "Time-dependent Behavior of High Strength Concrete," PhD dissertation, Deft University of Technology, The Netherlands, pp. 1-314.

Hong, H. P. (2001), "Strength of Slender Reinforced Concrete Columns under Biaxial Bending," *ACI Journal of Structural Journal*, July, pp. 758-762.

Hsu, C.-T. T., Hsu, L. S. M. and Tsao, W.-H. (1995), "Biaxially loaded slender high-strength reinforced concrete columns with and without steel fibres," *Magazine of Concrete Research*, Vol. 47, No. 173, December, pp. 299-310.

Illston, J. M., Dinwoodie, J. M. and Smith, A. A. (1979), *Concrete, Timber and Metals*, Van Nostrand Rheinhold, pp. 1-239.

Iravani, S. and MacGregor, J. G. (1998), "Sustained Load Strength and Short Strain Behavior of High-Strength Concrete," *ACI Material Journal*, September-October, pp. 636-647.

Kent, D. C. and Park, R. (1971), "Flexural Members with Confined Concrete," *Proceedings of ASCE*, ST.7 July

MacGregor, J. G., Breen, J. E. and Pfrang, E. O. (1970), "Design of Slender Concrete Columns," *ACI Journal*, Title No. 67-2, January, pp. 6-28.

Martin, I., MacGregor, J. G., Pfrang, E. O. and Breen, J. E. (1966), "Critical Review of the Design of Reinforced Concrete Columns," *Symposium on Reinforced Concrete Columns*, SP-13, ACI Publications, March, Detroit, MI. pp. 13-53.

Manual R. F. and MacGregor J. G. (1967), "Analysis of Restrained Reinforced Concrete Columns Under Sustained Load," *ACI Journal*, Title No. 64-2, January, pp. 12-23

Mauch, S. P. (1966), "Effect of Creep and Shrinkage on the Capacity of Concrete Columns," *Symposium on Reinforced Concrete Columns,* SP-13, ACI Publications, Detroit, MI, pp. 299-324.

Neville, A. M., Dilger, W. H. and Brooks, J. J. (1983), "Creep of Plain and Structural Concrete", *Construction Press*, London and New York, pp. 1-361.

Park, R. and Paulay, T. (1975), *Reinforced Concrete Structures*, John Wiley & Sons, July pp. 1- 800.

Russell, H. G. and Corley, W. G. (1977), "Time-Dependent Behavior of Columns in Water Tower Place", *Research and Development Bulletin* (RD052.01B), Portand Cement Association

Samra, R. M. (1995), "New Analysis For Creep Behavior in Concrete Columns," *ACI Journal of Structural Engineering*, March, pp. 399-407.

Samra, R. M. (1989), "Creep Model for Reinforced Concrete Columns," *ACI Journal of Structural Journal*, January-Feburay, pp. 77-82.

Schildt, H. (1995), *C: The Complete Reference*, 3rd edition, Osborne McGraw-Hill, Berkeley, CA. pp. 1- 838.

Shen, J. H. (1992), Lineare und nichtlineare Theorie des Kriechens und Relaxation von Beton unter *Druckbeanspruchung, Deutscher Ausschuss fur Stahlbeton*, Heft 432, Berlin.

Teaching and Research Division of Mathematics of Tsinghua University (1978), *Advanced Mathematics*, Basics Part II (in Chinese), People's Educational Press, Peking, P.R. of China, (7th printing), September, pp. 475-869.

Viest, I. M., Elstner, R. C. and Hognestad, E. (1956), "Sustained Load Strength of Eccentrically Loaded Short Reinforced Concrete Columns," *ACI Journal Proceedings*, V.52, March, pp. 727-755.

Wang C.-K. and Salmon G. C. Salmon (1992), *Reinforced Concrete Design*, 5th edition, Harper Collins Publishers Inc.

Wang C.-Z. et al. (1985), *Reinforced Concrete Structure Theories*, (in Chinese), Chinese Construction Industry Press, Peking, P. R. of China, pp. 1-470.

Wang, G. G. and Hsu, C.-T. T. (1992), "Complete Biaxial Load-Deformation Behavior of RC Columns," *Journal of Structural Engineering*, ASCE, ST. Vol. 118, No.9, September, pp. 2590-2609.

Wittmann, F. H. (1982), "Creep and Shrinkage Mechanism," *Creep and Shringkage in Concrete Structures*, edited by Bazant, Z. P. and Wittmann, F.H., John Wiley & Sons, pp. 129-161.

Walraven, J. C. and Shen, J. H. (1993), "Non-linear Creep: A General Constitutive Model," Creep and Shrinkage of Concrete, *Proceedings of the Fifth International RILEM Symposium*, Barcelona, pp. 213-218.

Xie, J., Elwi, A. E. and MacGregor, J. G. (1977), "Performance of High-Strength Concrete Tied Columns-A Parametric Study," *ACI Structural Journal*, March-April, pp. 91-102.